# COMPUTATIONAL STUDIES
# OF ELECTRONICALLY DIABATIC MOLECULAR COLLISIONS

By

JOEL MARTIN COHEN

A DISSERTATION PRESENTED TO THE GRADUATE SCHOOL
OF THE UNIVERSITY OF FLORIDA IN
PARTIAL FULFILLMENT OF THE REQUIREMENTS
FOR THE DEGREE DOCTOR OF PHILOSOPHY

UNIVERSITY OF FLORIDA

1990

# ACKNOWLEDGEMENTS

A very special vote of thanks goes to my father, without whose support none of this could have happened, and to my mother for encouraging my studies.

I wish to acknowledge my supervisor, Dr. David Micha, and thank him for his understanding these past few months.

Dr. Erik Deumens deserves credit for managing the computer

I would like to thank my office-mates for being such good company.

# TABLE OF CONTENTS

Page

ACKNOWLEDGEMENTS ..... ii

ABSTRACT. ..... v

CHAPTERS

I INTRODUCTION ..... 1

II INTRODUCTION TO THE EIKONAL METHOD ..... 10

- 2-1 The Schrodinger Equation for Nuclear Motion ..... 10
- 2-2 The Flux Related Method ..... 13

III ELASTIC COLLISIONS IN THREE DIMENSIONS ..... 17

- 3-1. Elastic Collisions and Eikonal Functions. ..... 17
- 3-2. Eikonal Functions and Transition Integral for Elastic Collisions. ..... 20
- 3-3. The Jacobian Transformation ..... 30
- 3-4. Computational Aspects ..... 34
- 3-5. Sample Calculations ..... 40

IV ELECTRONICALLY INELASTIC SCATTERING IN ONE VARIABLE ..... 47

- 4-1. Converting from a Diabatic Potential to an Adiabatic Potential ..... 47
- 4-2. Equations in the Diabatic Representation ..... 50
- 4-3. Equations in the Adiabatic Representation ..... 57
- 4-4. The Model Potentials ..... 69

V COMPUTATIONAL ASPECTS--ADDITIONAL DETAILS OF THE CALCULATION ..... 85

- 5-1. Introduction ..... 89
- 5-2. The Derivatives of $\gamma$ ..... 90
- 5-3. Derivatives of the Adiabatic Potential Elements ..... 96
- 5-4. Reasonable Behavior--Classical Trajectories and Effective Potentials ..... 97
- 5-5. Exact Calculations--Using LOGDERIV ..... 101
- 5-6. Eikonal Calculations--Using DE ..... 104

VI NUMERICAL RESULTS 134

6-1. Introduction 134
6-2. EXACT and SCE/EP Transition Probabilities 135
6-3. The Averaged Effective Potential 161
6-4. SCE/AEP Transition Probabilities and Summary 180

VII CONCLUSION 197

APPENDICES

A KEY TO PROGRAM NAMES 204

B EIKONAL PROGRAM 205

BIBLIOGRAPHY 211

BIOGRAPHICAL SKETCH 215

Abstract of Thesis Presented to the Graduate School
of the University of Florida in Partial Fulfillment of the
Requirements for the Degree of Doctor of Philosophy

COMPUTATIONAL STUDIES
OF ELECTRONICALLY DIABATIC MOLECULAR COLLISIONS

By

Joel Martin Cohen

December 1990

Chairman: Dr. David Micha
Major Department: Chemistry

Electronically diabatic transitions arise from a breakdown of the Born-Oppenheimer approximation. Motion of the nuclei during these breakdowns can drive the system through changes in electronic configuration. Unfortunately, since exact solutions do not exist for systems with more than a few degrees of freedom, approximate methods are needed. The eikonal method developed in this thesis is a likely choice because of its ability to incorporate any number of potential energy surfaces in its calculations. The formalism has, in fact, been developed and applied on a number of occasions in the diabatic representation. The present work extended that formalism to the adiabatic representation, and compared application of both sets of equations to the same model systems. These included pairs of noncrossing potentials, crossing potentials in repulsive regions, and crossing potentials in attractive regions.

Adiabatic equations were formed by applying a unitary transformation to the diabatic equations. The resulting expressions contained additional terms and could not be

simplified by a phase change to the same extent as in the diabatic case. The adiabatic effective potential contained a momentum variable, P, that could not be eliminated. Special measures were required to form trajectories using this momentum-dependent potential. P also appeared in the denominator of the coefficient equations, giving rise to singularities in the turning point region. Non-Hermitian terms in the time-dependent equations made normalization a requirement for probability conservation. Extensive calculations were performed of transition probabilities versus collision energies. Since both kinds of calculation gave the same results (as they should), the less complicated and computationally faster diabatic equations are preferred. It is, nonetheless, important to have the adiabatic equations working well. Not only can dynamicists learn from them, but it is likely that situations will arise in which they are useful.

An improvement to the usual electronically inelastic eikonal calculation was also proposed and tested. It imposes microreversibility by combining the effective potential for the collision starting in the lower state and the effective potential for the collision starting in the upper state into an averaged effective potential. The improvement was dramatic. Agreement with exact calculations was remarkable. Because little or no additional computer time was required, it was concluded that eikonal calculations are best performed using an averaged effective potential in the diabatic representation.

# CHAPTER I

# INTRODUCTION

Electronically diabatic transitions arise from a breakdown of the Born-Oppenheimer (Levine, 1983) approximation. The basic situation is that the electrons mass is so small and their velocities so large compared to those of the nuclei that the electronic and nuclear motions are effectively decoupled. Variations in electron velocities lead to situations in which one or more components of the kinetic energy of the electrons goes through zero. For a brief instant the electronic motion is not so much faster than the nuclear motion that they can be regarded as decoupled. Any motion of the nuclei at these moments may drive the system through a change in electronic configuration. Clearly, the higher the kinetic energy of the nuclei, the longer these moments will last, and the more chance there is for a transition to occur. Even low energy molecular collisions, however, may lead to diabatic transitions if the two adiabatic potential energy surfaces approach each other closely enough. Some chemical systems whose potential energy surfaces interact are $M + X$ and $M + X_2$ ($M$ = Li, Na, K, [illegible]. and $X$ = F, Cl, Br, I) (Child, 1979). In such situations, transformations may be applied that produce rigorously equivalent sets of equations in the diabatic and adiabatic representations (Olson and Micha, 1982).

Many alternatives to the exact calculation of diabatically active collisions have been devised. Prominent among these are those that use some sort of semiclassical approximation. Reviews of semiclassical methods include Cross (1989) and Ford and Wheeler (1959). Reviews of diabatic interactions include Bunker (1971), Child (1979), Micha (1975), and Tully, (1978). Semiclassical methods regard the motion of the nuclei as predominantly classical while at the same time maintaining the quantum superposition principle to include the effects of interference and tunneling. Among the semiclassical methods are the WKB approach (Messiah, 1961), the path integral formulation (Feynmann and Hibbs, 1985), and the complex-valued trajectory approach (Miller and George, 1972). The present work is part of an ongoing investigation into the eikonal method as formulated by David Micha in 1983, improved upon in 1986 (Micha and Swaminathan), 1987 (Stoddan; Stodden and Micha), and most recently in 1988 (Cohen; Swaminathan, Stodden, and Micha). While exact calculations for systems with more than a few degrees of freedom are not possible (Herman, 1982), the eikonal method is multidimensional by design and naturally incorporates any number of surfaces in its calculations. Trajectories are constructed that represent the "average" state of the system in the Ehrenfest sense. These trajectories might well be described as near-classical in that they are calculated from Hamilton's equations of motion like the usual classical trajectory, but in a way that relies on quantum coefficients. The method invariably displays three features:

a) the wavefunction used to solve Schroedinger's equation assumes a form that is composed of exponential and pre-exponential factors;

b) the phase of that function is associated with a mechanical action integral;

c) simplification is achieved with a short-wavelength approximation.

This work demonstrates the successful use of functions formed in this way as part of the transition integral for 3-dimensional elastic scattering as well as in the development of flux related transition amplitudes for 1-dimensional inelastic scattering. The opening discussion gives a brief account of the general eikonal formalism. Next is a description of elastic scattering as recently treated by this author (Cohen, 1986). A point of interest is the use of a Jacobian transformation to facilitate evaluation of the pre-exponential factor (Knudson, Delos, and Bloom, 1985; Delos, 1986; Stodden, 1987; Stodden and Micha, 1987). The main body follows with a detailed account of the eikonal method applied to electronically diabatic inelastic collisions. Other possible extensions of the method are also touched upon.

The major part of this work was dedicated to applying and comparing the eikonal approach in the diabatic and adiabatic representations. (Other studies of this type have been done. See, for example, Evans, Cohen, and Lane, 1971, and Sawada and Metiu, 1986.) Since the eikonal method had not previously been used together with the adiabatic representation, the equations were rederived and new computational techniques developed for this purpose.

An improvement to the usual electronically inelastic eikonal calculation was also proposed and tested. Basically, it imposes the condition of microreversibility by combining the effective potential for the collision starting in the lower state and the effective potential for the collision starting in the upper state into an averaged effective potential. This implies, in essence, running the forward and reverse calculations simultaneously.

Chapter II is devoted to the general formalism for the eikonal method.

The first section begins with the general form of the Schroedinger equation and ends with a more specialized form involving nuclear motion. The remainder of the work relies on this form.

The next section starts with the eikonal form of the wavefunction, eliminates the exponential factor from the nuclear motion equation, and, by identifying the phase as the action integral, relates the nuclear motion equation to Hamilton's equations of motion. An effective potential, related to the quantum coefficients, is formed in the process. A rigorous method for specifying the effective potential is given next. The notion that, due to conservation of flux, the coefficients can be related to the amplitudes for transition probability is also discussed.

Chapter III is about the eikonal method as applied in the transition integral for elastic scattering.

The first section applies the formalism of Chapter II to elastic scattering.

The second section starts with a general expression for the transition integral and develops an expression that can, as a practical matter, be evaluated. A Jacobian transformation allows the region of space actually integrated over to be limited to that spanned by a representative bundle of classical trajectories. The pre-exponential factor is also re-expressed in terms of Jacobians. The transition integral is related to the differential cross section.

The third section gives details on how the Jacobian is evaluated. It also explains how the dimensionality of the calculation can be reduced for an elastic collision with a central potential. Because no torque is applied to the projectile its motion is confined to a plane.

The fourth section discusses computational aspects including decomposition of the various vectors, utilization of the zero-order Bessel function in integrating over azimuthal angle, $\alpha$, and a linearizing technique to stabilize the integration of a rapidly oscillating integrand.

The fifth section displays a few sample calculations.

Chapter IV develops the eikonal equations in the diabatic and adiabatic representations.

The first section shows how a unitary transformation matrix can be applied to a diabatic potential to convert it to an adiabatic potential. Following the conversion, the transformation angle, γ, retains the information that was in the off-diagonal elements of the diabatic potential.

The second section applies and extends the formalism of Chapter II to arrive at the diabatic equations for the flux related probability amplitudes. The expression for the diabatic effective potential is derived. The expression actually used is simplified by the short-wavelength approximation. The specific form of Hamilton's equations are given. The time-dependent differential equations for the coefficients are derived. Of special interest is a phase change that allows for simplification of the time dependent equations.

The third section applies the conversion presented in the first section to arrive at the adiabatic equations for the flux related probability amplitudes. The expression for the adiabatic effective potential is derived. Once again, the expression actually used is simplified by the short-wavelength approximation. An unusual feature of the the adiabatic effective potential is that it contains a term in P, a momentum variable. Such momentum dependent potentials are not unknown (Goldstein, 1981, Section 1-5), but they do complicate construction of the classical trajectories. The specific form of Hamilton's equations for the nuclear motion is given here also. Not only are they different because of the unusual effective potential, but they require inclusion of the spatial derivatives of the coefficients. These are entirely eliminated in the diabatic case. The time-dependent differential equations for the coefficients are also derived in the adiabatic representation, but they contain two different singularities. A very small imaginary increment, $\varepsilon$, is added to the momentum in the denominator to avoid these. Finally, only part of the phase change that allows for simplification of the time-dependent diabatic equations can be used with the time-dependent adiabatic equations.

The fourth section defines and depicts the three model potentials that are used in the calculations. The first one, called NC, has no crossing. The second one, called RC, has a crossing in the repulsive region. The third one, CA, crosses in the attractive region.

Chapter V covers computational aspects of the diabatic, adiabatic, and exact calculations. The exact calculations, performed with the log-derivative method, are included for comparison purposes. Figures appear at the end of the chapter.

The second section gives expressions for the first two derivatives of the transformation angle, $\gamma$, explains how they were checked with numerical derivatives, and shows how the derivatives of $\gamma$ can themselves be used as part of other testing schemes.

The third section contains the expressions for the adiabatic potential elements and their first derivatives. These derivatives are fairly complicated and are checked.

The fourth section explains how an understanding of the reasonable behavior of classical trajectories was used to place together the SCE/EP DIAB and ADIAB programs.[*] It goes on to show that the reasonable behavior of the effective potentials reinforces the notion that the programs are working correctly.

The fifth section gives details on how to use LOGDERIV (the program that does the exact calculations).

The sixth section gives details on how to use the eikonal programs.

Chapter VI gives the numerical results. Most of them are depicted in graphs of transition probability versus energy.

The first section is about the EXACT and SCE/EP DIAB and ADIAB (1->2 and 2->1) calculations. Features of interest are discussed.

The second section explains and demonstrates the use of the averaged effective potential (AEP) to improve the calculations.

---

[*] Self Consistent Eikonal/Effective Potential DIABatic and ADIABatic. See APPENDIX A for a complete list of abbreviations.

The third section gives the SCE/AEF DIAB and ADIAB results along with some tables that compare all of the calculations. Some analysis is given. The SCE calculations are compared to the EXACT ones. The times required for the DIAB and ADIAB calculations are also compared.

Chapter VII is the conclusion. Here we discuss the results, and point out directions for future work.

# CHAPTER II

# INTRODUCTION TO THE EIKONAL METHOD

## 2-1. The Schrodinger Equation for Nuclear Motion

A discussion of the eikonal method may begin by defining a generalized position variable Q, that appears in the total kinetic energy operator K (Micha, 1983),

$$K = \frac{1}{2m}\left(\frac{\hbar}{i}\frac{\partial}{\partial Q}\right)^2 \quad . \tag{2-1}$$

The "squaring" operation is actually a dot product, and m is the mass of each variable, after mass scaling them. States of the whole system may be described in terms of nuclear positions, Q, such that

$$\left\{ \frac{1}{2m}\left(\frac{\hbar}{i}\frac{\partial}{\partial Q}\right)^2 + \bar{H}_Q - E \right\} |\Psi(Q)\rangle = 0 \tag{2-2}$$

where $|\Psi(Q)\rangle$ is the total wavefunction. States of the electrons are given within bracket notation so that electron variables are not explicitly displayed. The ket $|\Psi(Q)\rangle$ represents $\langle X|\Psi(Q)\rangle = \Psi(X, Q)$ where X is the collection of electronic variables. Similarly

$$\langle X|\hat{H}_Q|\Psi(Q)\rangle = H_Q(X, \tfrac{\partial}{\partial Q})\ \Psi(X, Q)$$

describes the effect of the Hamiltonian acting on $\Psi$ $\hat{H}_Q$ operates over the electron variables and contains the electronic kinetic energy and the Coulombic potential energies. E is the total energy of the system.

A basis of electronic states, $|\phi_1\rangle, |\phi_2\rangle, \ldots$, constructed from the electronic states of the collision partners is introduced. These are orthonormalized and placed by state in a row vector, $|\phi_1^0\rangle, |\phi_2^0\rangle, \ldots$. At asymptotically large values of the internuclear separation these vectors satisfy

$$\langle\phi^0|H_Q|\phi^0\rangle = E^0 \quad ;$$

$$\langle\phi^0|\frac{\partial\phi^0}{\partial Q}\rangle = 0 \qquad (2\text{-}3)$$

$E^0$ is a diagonal matrix equal to the sum of the electronic energy matrices of the colliding particles. $\phi^0$ depends on Q parametrically. $|\Psi(Q)\rangle$ is expanded

$$|\Psi(Q)\rangle = |\phi^0(Q)\rangle\ \psi^0(Q) \quad , \qquad (2\text{-}4)$$

where $\psi^0$ is a column vector of wavefunctions. One may define an expression $G^0$ such that

$$\frac{\hbar}{i}\frac{\partial}{\partial Q}\ |\phi^0(Q)\rangle\ \psi^0(Q) = |\phi^0(Q)\rangle \left(\frac{\hbar}{i}\frac{\partial}{\partial Q} + G^0\right) \psi^0(Q) \quad , (2\text{-}5)$$

where

$$G^0 = \langle \phi^0 \, | \frac{\hbar}{i} \frac{\partial \phi^0}{\partial Q} \rangle \; . \tag{2-6}$$

Using Equation (2-5) twice in Equation (2-2) gives

$$\left\{ \frac{1}{2m} \left( \frac{\hbar}{i} \frac{\partial}{\partial Q} + G^0 \right)^2 + V_Q - E \right\} \phi^0(Q) = 0 \; . \tag{2-7}$$

V is the nuclear potential energy matrix. A complete treatment might attempt to derive V from its electronic structure. In what follows an analytical form is usually borrowed from other authors' published articles.

Equation (2-7) can be rewritten as D$\phi$=0, where D is a differential operator. Manipulation of this simplified form allows one to define a flux of probability that will not diverge, and some form of which will satisfy conservation. The presence of $G^0$ in these expressions leads to anti-Hermitian terms that threaten to complicate a flux related description of the dynamics. A unitary transformation is introduced,

$$|\phi\,(Q)\rangle = |\phi^0(Q)\rangle \, L(Q) \; , \tag{2-8}$$

that is chosen to satisfy the imposed relationship G=0. When $|\phi^0(Q)\rangle$ is the adiabatic basis that diagonalizes $V_Q$, this choice for L leads to the strictly diabatic representation (Smith, 1969) The $\phi^0$ are the Born-Oppenheimer wavefunctions taken directly from electronic structure calculations. Without G there is no momentum coupling between different states. The other diabatic representations that follow from other choices for L will not be used in this work. The equation that remains ultimately provides cross-sections and transition probabilities for the system from the positions and moments of the nuclei,

$$\left[ \frac{1}{2m} \left(\frac{\hbar}{i} \frac{\partial}{\partial Q} \right)^2 + V_Q - E \right] \psi(Q) = 0 \; . \qquad (2\text{-}9)$$

## 2-2. The Flux Related Method

The wave function for nuclear motion can certainly be separated into exponential and pre-exponential factors,

$$\psi(Q) = \chi(Q) \exp[iS(Q)/\hbar] \qquad (2\text{-}10)$$

where $\chi$ is a column multiplied by a common exponential factor. Applying

$$\left(\frac{\hbar}{i} \frac{\partial}{\partial Q}\right) \chi \exp(iS/\hbar) = \exp(iS/\hbar) \left(\frac{\hbar}{i} \frac{\partial}{\partial Q} + \frac{\partial S}{\partial Q} \right) \chi \qquad (2\text{-}11)$$

twice in Equation (2-9) gives

$$\left\{ \frac{1}{2m} \left(\frac{\hbar}{i} \frac{\partial}{\partial Q} + \frac{\partial S}{\partial Q} \right)^2 + V_Q - E \right\} \chi(Q) = 0 \; . \qquad (2\text{-}14)$$

The derivative of the undetermined function, $S(Q)$, can be associated with a momentum function:

$$P = \partial S/\partial Q \tag{2-15}$$

which is related to some potential, $v_{qu}(P,Q)$, as yet undetermined, through the Hamiltonian equation

$$H(P,Q) = \frac{P^2}{2m} + v_{qu}(P,Q) \tag{2-16}$$

The Hamiltonian itself is identical to the conserved (constant) energy of the system giving the Hamilton-Jacobi equation

$$\frac{1}{2m}\left(\frac{\partial S}{\partial Q}\right)^2 + v_{qu}\left(\frac{\partial S}{\partial Q}, Q\right) = E \tag{2-17}$$

If $P$ and $Q$ are functions of time, $t$, then $dH/dt = 0$ provided

$$\partial H/\partial P = dQ/dt \quad \text{and} \quad \partial H/\partial Q = -dP/dt \tag{2-18}$$

It is clear from (2-15) that $S(Q)$ can be determined from $P$ and $Q$ via the prescription

$$S(Q) = S(Q_1) + \int_{Q_1}^{Q} \partial Q \cdot P \ , \tag{2-19}$$

where the subscript refers to the initial time.

$Q_1$ and $P_1$ are nuclear positions and moments selected with the collision partners separated by a great enough distance to be considered noninteracting. Specifically, the initial total energy, $E$, and initial internuclear separation, $r_1$, are pre-selected. In the asymptotic region, changes in momentum for the projectile-target coordinate, $p=p(r)$, are considered negligible, $dp/dt=0$ and $dp/dr=0$. Calculating $u_1$ gives $p_1$ through Equation (2-16). Generally (though, as shall be shown, not always) $(dr/dt)_1=p_1/m$.

To specify $\upsilon_{qu}(P,Q)$ take Equation (2-14) in the simplified form $F\chi = 0$.

Left multiply by $\chi^+$,

$$\chi^+ F\chi = 0$$

and add this to its own adjoint,

$$\chi^+ F\chi + (F\chi)^+\chi = 0. \qquad (2\text{-}20)$$

Dividing by $2\chi^+\chi$ gives Equation (2-17) with

$$u_{qu}(\tfrac{\partial S}{\partial Q},\ Q) = \upsilon_{qu}(P,Q) = (\chi^+\chi)^{-1}\ \chi^+\underline{\upsilon}(\tfrac{\partial}{\partial Q},\ Q)\chi \quad .(2\text{-}21)$$

The specific forms of $\upsilon$ for the elastic collision case, as well as for the adiabatic and diabatic representations, will be constructed below. This manner of choosing $\upsilon$ gives trajectories that represent the average state of the system in the sense given by the Ehrenfest theorem.

It remains to determine $\chi_1$ and subsequently $\chi$. Actually, the classical trajectories are constructed from time dependent equations. Since the coefficients are coupled to these through the effective potential, a time dependent function, $A(t)$, that is closely related to $\chi(r)$, is used in its place. The principle for selecting the initial values is easy enough, select the initial state of the system, place all the probability (P) in that state and none in the others. For instance, if 1 represents the lower state and 2 the upper, and the pre-collision molecule is in the lower, the elements of **A** are chosen so that $P_1$(initial)=1.0 and $P_2$(initial)=0.0. Time dependent equations for **A** are basically transformed r dependent equations for **χ**. As demonstrated below the diabatic equations are simpler because terms can be eliminated through changes in phase. The adiabatic equations contain singularities that prevent this kind of handling, so they remain generally problematic and unwieldy. Complete derivations will be presented separately for the two representations.

# CHAPTER III

## ELASTIC COLLISIONS IN THREE DIMENSIONS

### 3-1. Elastic Collisions and Eikonal Functions

This chapter will show how the eikonal approach can be applied to the transition integral used in computing cross sections for elastic collisions (Messiah, 1962; Micha, 1983; Pauly, 1979). The discussion is simplified by the fact that neither the target nor the projectile have internal motions. They do, however, move in real (3-dimensional) space. The kinetic energy operator (see Equation (2-1)), in Cartesian coordinates, is represented as follows:

$$K = -\frac{\hbar^2}{2m}\nabla^2 \quad , \tag{3-1}$$

where

$$\nabla^2 = \frac{\partial^2}{\partial x^2} + \frac{\partial^2}{\partial y^2} + \frac{\partial^2}{\partial z^2} \tag{3-2}$$

Removing the electronic portion of the wave function gives the elastic analog of Equation (2-9),

$$\left\{-\frac{\hbar^2}{2m}\nabla^2 + V(r) - E\right\}\Psi(r) = 0 \;, \tag{3-3}$$

where $\Psi(r)$ is the radial wave function; $r$ is the vector representing interparticle separation. Assuming a solution of the form

$$\Psi(r) = \chi(r)\, e^{i\,S(r)/\hbar} \;, \tag{3-4}$$

and realizing that

$$\left(\frac{\hbar}{i}\nabla\right)\chi \exp(iS/\hbar) = \exp(iS/\hbar)\left(\frac{\hbar}{i}\nabla + \nabla S\right)\chi \tag{3-5}$$

(where the $r$ has been suppressed), Equation (3-3) may be simplified to

$$\left\{\frac{1}{2m}\left(\frac{\hbar}{i}\nabla + \nabla S\right)^2 + V - E\right\}\chi = 0 \;, \tag{3-6}$$

where the "squaring" of $(\hbar\nabla/i + \nabla S)$ refers to a dot product. Identifying the entire expression operating on $\chi$ as $\mathbf{F}$ allows the total energy for the elastic case to be expressed as in Equation (2-21). First, left multiply Equation (3-6) by $\chi^*$,

$$-\frac{\hbar^2}{2m}\chi^*\nabla^2\chi + \frac{\hbar}{m}\nabla S\,\chi^*\frac{\hbar}{i}\nabla\chi + \frac{(\nabla S)^2}{2m}\chi^*\chi + \frac{\nabla^2 S}{2m}\chi^*\frac{\hbar}{i}\chi$$

$$+V\chi^*\chi - E\chi^*\chi = 0 \;. \tag{3-7}$$

Then, take the adjoint,

$$-\frac{\hbar^2}{2m}(\nabla^2\chi^*)\chi - \frac{\hbar}{m}\nabla S\,(\nabla\chi^*)\,\frac{\hbar}{i}\,\chi + \frac{(\nabla S)^2}{2m}\chi^*\chi - \frac{\nabla^2 S}{2m}\chi^*\,\frac{\hbar}{i}\,\chi$$

$$+V\chi^*\chi - E\chi^*\chi = 0 \qquad (3\text{-}8)$$

Before combining the last two equations, as in Equation (2-20), it is useful to consider S. The nature of S is, as yet, undetermined. Letting it satisfy the momentum equation,

$$p = \nabla S\ , \qquad (3\text{-}9)$$

allows the short-wavelength approximation,

$$|d^2\chi/dr^2| \ll |d\chi/dr\ (p/\hbar)| \ll |\chi\ (p/\hbar)^2|\ , \quad (3\text{-}10)$$

to be applied to Equations (3-7) and (3-8). This eliminates the terms containing $\nabla^2\chi$ and $\nabla\chi$. Adding Equations (3-7) and (3-8) eliminates the terms with $\nabla^2 S$ ($=\nabla.p$) in them. Dividing the result by $2\chi^*\chi$ gives

$$E = \frac{p^2}{2m} + V(r) \qquad (3\text{-}11)$$

Clearly, $p^2/2m$ is the kinetic energy, so V(r) is the effective potential for the elastic case after application of the short-wavelength approximation. Particular choices for V will depend on the demands of problem at hand. Anything from an elaborate table meticulously constructed from experimental data to a simple Lennard-Jones guesstimate can be used. From the last equation comes the Hamiltonian,

$$H(p,r) = \frac{p^2}{2m} + V(r) \qquad (3\text{-}12)$$

where H is constant and equal to E. Both p and r depend parametrically on t (chosen here to represent time) so that trajectories may be constructed using Hamilton's equations of motion,

$$dr/dt = \left(\frac{\partial H}{\partial p}\right)_r = p/m \quad ;$$

$$dp/dt = -\left(\frac{\partial H}{\partial r}\right)_p = -\frac{dV}{dr} \quad . \qquad (3\text{-}13)$$

## 3-2. Eikonal Functions and the Transition Integral for Elastic Collisions

In many cases of practical interest, some of which are included in this work, quantum cross sections and probabilities can be computed from methods that rely on conservation of flux. Unfortunately, when resonances occur, several trajectories with different initial conditions (impact parameters for the elastic case) may contribute to the same result. While the classical cross section is the sum of such contributions, the quantum cross section shows a phase interference which cannot be accounted for by simple addition.

The transition integral is a way of calculating scattering amplitudes that specifically accounts for phase effects. It may be represented

$$T = \langle \Psi_b^{(0)} | V | \Psi_a^{(+)} \rangle \ , \qquad (3\text{-}14)$$

where there is a plane wave associated with some pre-selected final state, b, a scattering wave associated with the initial state of the system, a, and V=V(r) is the potential energy. It is the ability to pre-select the initial and final states that makes this method so appealing. Dynamics calculations can be restricted to collisions with specified product states.

An expression for the transition integral using eikonal wave functions may be derived,

$$T = \int dr \, \exp(\tfrac{i}{\hbar}\, p_b \, r) \; V(r) \; \chi(r) \; \exp[\tfrac{i}{\hbar}\, S(r)] \qquad (3\text{-}15)$$

The first requirement for evaluating T is some way to evaluate $\chi$. Inserting Equation (3-9) in Equation (3-6), and carrying out the operations indicated within the brackets give

$$\left[ -\frac{\hbar^2}{2m} \nabla^2 + \frac{\hbar}{i} \frac{p}{m} \cdot \nabla + \frac{\hbar}{2im} (\nabla \cdot p) \right] \chi = 0 \ . \qquad (3\text{-}16)$$

The appearance of this equation can be greatly simplified with the following relations:

$$-\frac{\hbar^2}{2m}\nabla^2\chi = K_r(\chi)\,\chi \quad , \tag{3-17}$$

$$\frac{\hbar}{2m}(\nabla \cdot p) = U(r) \quad , \tag{3-18}$$

$$\frac{p}{m}\cdot\nabla = dr/dt \cdot d/dr = d/dt \tag{3-19}$$

Using these, Equation (3-16) becomes

$$\left(\frac{\hbar}{i}\frac{\partial}{\partial t} + K_r - i\,U\right)\chi = 0 \tag{3-20}$$

This is a simple first order differential equation whose solution may be expressed as

$$\chi(r) = \exp\left(-\frac{i}{\hbar}\int_{t_1}^{t} dt'\,(K_r - iU)\right) \quad , \tag{3-21}$$

where $t_1$ refers to the initial time.

A high energy, short wavelength, approximation allows $K_r$ to be neglected when it appears next to U, $|K_r| \ll |U|$. This simplifies $\chi$,

$$\chi(r) = \exp\left(\frac{1}{\hbar}\int_{t_1}^{t} dt'\,U\right) \tag{3-22}$$

In practice, even this simplified $\chi$ is difficult to evaluate. An equivalent expression that uses Jacobians has been developed to avoid the problem (Stodden and Miche, 1987). First, U is re-expressed,

$$U(r) = \frac{\hbar}{2m} ( \nabla \cdot p ) = \frac{\hbar}{2} ( \nabla \cdot v ) \qquad (3\text{-}23)$$

v is a three dimensional velocity vector. The transition integral of Equation (3-17) is spatial. For obvious reasons the integration is not carried out over all space. The useful information is contained in the region spanned by a representative bundle of classical trajectories generated by the method of Section 3-1. The initial conditions for these trajectories are chosen to match the actual experimental conditions. The integration follows each classical trajectory as it proceeds until the particles are out of range. The time, t, the impact parameter, b, and the azimuthal angle, α, determine a unique point along the trajectory that is fixed in space. This point, then, can be related to the set of Cartesian coordinates (x, y, and z),

$$x = x(t,b,\alpha)$$

$$y = y(t,b,\alpha)$$

$$z = z(t,b,\alpha)$$

and

$$u(x,y,z) = v(t,b,\alpha) \quad , \qquad (3\text{-}24)$$

where u is the velocity vector in Cartesian coordinates. It is worth noticing that, even though they are determined in two different coordinate systems, $v_x$ is numerically equal to $u_x$. That is, the projection of the velocity vector on the x-axis, a scalar quantity, is the same whether or not that vector is actually given in Cartesian coordinates. In fact,

$$v_x = u_x$$
$$v_y = u_y$$
$$v_z = u_z \qquad (3\text{-}25)$$

Decomposition of $\nabla$ and v (or u) yields

$$\nabla \cdot v = \nabla \cdot u =$$

$$\left(\frac{\partial}{\partial x} i + \frac{\partial}{\partial y} j + \frac{\partial}{\partial z} k\right) \cdot \left(u_x i + u_y j + u_z k\right) =$$

$$\frac{\partial u_x}{\partial x} + \frac{\partial u_y}{\partial y} + \frac{\partial u_z}{\partial z} \qquad (3\text{-}26)$$

where **i**, **j**, and **k** are unit vectors pointing along the x, y, and z axis.

The three derivatives on the right are the terms whose handling is simplified by expressing them in terms of Jacobians. If used in their present form, they would result in improper integrals buried inside other integration loops. This would lead to computer overflow and a host of other mathematical difficulties. Taking the first of the three as an example, we begin by developing and rearranging the following system of linear equations:

$$\partial x/\partial t \frac{\partial u_x}{\partial x} + \partial y/\partial t \frac{\partial u_x}{\partial y} + \partial z/\partial t \frac{\partial u_x}{\partial z} = \frac{\partial v_x}{\partial t} \quad ,$$

$$\partial x/\partial b \frac{\partial u_x}{\partial x} + \partial y/\partial b \frac{\partial u_x}{\partial y} + \partial z/\partial b \frac{\partial u_x}{\partial z} = \frac{\partial v_x}{\partial b} \quad ,$$

$$\partial x/\partial \alpha \frac{\partial u_x}{\partial x} + \partial y/\partial \alpha \frac{\partial u_x}{\partial y} + \partial z/\partial \alpha \frac{\partial u_x}{\partial z} = \frac{\partial v_x}{\partial \alpha} . \qquad (3\text{-}27)$$

This set of equations can be expressed in matrix notation as **AX** = **B**, where

$$\mathbf{A} = \begin{vmatrix} \partial x/\partial t & \partial y/\partial t & \partial z/\partial t \\ \partial x/\partial b & \partial y/\partial b & \partial z/\partial b \\ \partial x/\partial \alpha & \partial y/\partial \alpha & \partial z/\partial \alpha \end{vmatrix} \quad \mathbf{X} = \begin{vmatrix} \partial u_x/\partial x \\ \partial u_x/\partial y \\ \partial u_x/\partial z \end{vmatrix} \quad \mathbf{B} = \begin{vmatrix} \partial v_x/\partial t \\ \partial v_x/\partial b \\ \partial v_x/\partial \alpha \end{vmatrix} \qquad (3\text{-}28)$$

Cramer's Rule, a fundamental of linear algebra, solves for the elements of **X** in the following manner:

$$x_j = \frac{\det(\mathbf{A}_j)}{\det(\mathbf{A})} \qquad (3\text{-}29)$$

This says that the element in the jth row of **X** is equal to the determinant of $\mathbf{A}_j$ divided by the determinant of **A**. $\mathbf{A}_j$ is defined to be a matrix, identical to **A** in every respect except that the jth column has been replaced by **B**. Since $\partial u_x/\partial y$ and $\partial u_x/\partial z$ dropped out in calculating the dot product in Equation (3-26), they are not needed. $\partial u_x/\partial x$ appears in the first row of **X**, so j=1, and

$$\frac{\partial u_x}{\partial x} = \frac{\begin{vmatrix} \partial v_x/\partial t & \partial y/\partial t & \partial z/\partial t \\ \partial v_x/\partial b & \partial y/\partial b & \partial z/\partial b \\ \partial v_x/\partial \alpha & \partial y/\partial \alpha & \partial z/\partial \alpha \end{vmatrix}}{\det(\mathbf{A})} \qquad (3\text{-}30)$$

The Jacobian is the determinant of the derivatives in one coordinate system with respect to the other:

$$J\left(\begin{matrix} x & y & z \\ t & b & \alpha \end{matrix}\right) = \begin{vmatrix} \partial x/\partial t & \partial y/\partial t & \partial z/\partial t \\ \partial x/\partial b & \partial y/\partial b & \partial z/\partial b \\ \partial x/\partial \alpha & \partial y/\partial \alpha & \partial z/\partial \alpha \end{vmatrix} \quad . \qquad (3\text{-}31)$$

The denominator in Equation (3-30) is instantly recognized as the Jacobian. Substituting from the equalities, $v_x = u_x = \partial x/\partial t$,

$$\frac{\partial u_x}{\partial x} = \begin{vmatrix} \frac{\partial^2 x}{\partial t \partial t} & \partial y/\partial t & \partial z/\partial t \\ \frac{\partial^2 x}{\partial t \partial b} & \partial y/\partial b & \partial z/\partial b \\ \frac{\partial^2 x}{\partial t \partial \alpha} & \partial y/\partial \alpha & \partial z/\partial \alpha \end{vmatrix} \quad J^{-1} \quad . \qquad (3\text{-}32)$$

The operations that established $\partial u_x/\partial x$ can be applied to $\partial u_y/\partial y$ and $\partial u_z/\partial z$ to give similar results. $\nabla \cdot v$ is the sum:

$$\nabla \cdot v = \begin{vmatrix} \frac{\partial^2 x}{\partial t \partial t} & \partial y/\partial t & \partial z/\partial t \\ \frac{\partial^2 x}{\partial t \partial b} & \partial y/\partial b & \partial z/\partial b \\ \frac{\partial^2 x}{\partial t \partial \alpha} & \partial y/\partial \alpha & \partial z/\partial \alpha \end{vmatrix} . J^{-1} + \begin{vmatrix} \partial x/\partial t & \frac{\partial^2 y}{\partial t \partial t} & \partial z/\partial t \\ \partial x/\partial b & \frac{\partial^2 y}{\partial t \partial b} & \partial z/\partial b \\ \partial x/\partial \alpha & \frac{\partial^2 y}{\partial t \partial \alpha} & \partial z/\partial \alpha \end{vmatrix} . J^{-1}$$

$$+ \begin{vmatrix} \partial x/\partial t & \partial y/\partial t & \frac{\partial^2 z}{\partial t \partial t} \\ \partial x/\partial b & \partial y/\partial b & \frac{\partial^2 z}{\partial t \partial b} \\ \partial x/\partial \alpha & \partial y/\partial \alpha & \frac{\partial^2 z}{\partial t \partial \alpha} \end{vmatrix} . J^{-1} \qquad (3\text{-}33)$$

But the collection of numerators is precisely $\partial J/\partial t$, so

$$\nabla \cdot v = \frac{1}{J}\frac{\partial J}{\partial t} = \frac{\partial(\ln J)}{\partial t} \quad . \tag{3-34}$$

Putting this into U gives

$$U(r) = \frac{\hbar}{2}\left(\frac{\partial}{\partial t}\right)\ln(J) \tag{3-35}$$

A little manipulation gives

$$\chi(r) = \exp\left(-\frac{1}{2}\int_{t_1}^{t} dt' \left(\frac{\partial}{\partial t'}\right)\ln(J)\right) = (J/J_1)^{-1/2}. \tag{3-36}$$

Since J can be either positive or negative, the square root can be either real or imaginary, positive or negative. To locate the root on the complex plane, J is split,

$$J = |J|\, e^{i\,\arg(J)} \tag{3-37}$$

The function arg(J) is defined to increase by $\pi$ every time J changes sign. $\chi$ is now

$$\begin{aligned}\chi(r) &= (J/J_1)^{-1/2} \\ &= |J/J_1|^{-1/2}\exp[(-i/2)\{\arg(J)-\arg(J_1)\}]\end{aligned} \tag{3-38}$$

The exponent $[\arg(J)-\arg(J_1)]$ merits a little attention. Since J always equals $J_1$ at $t_1$, the exponent's value is zero at the outset of every trajectory. It starts at zero and increments by $-i\pi/2$ every time J changes sign. The entire exponential factor will begin at 1, go to $-i$, $-1$, $i$, and then start back at 1, following changes in the sign of J. In this way, the entire complex plane is repeatedly spanned

Getting back to the transition integral, the various expressions in the integrand, including the Jacobian transformation, are numerically generated in a point-wise fashion along with the trajectories. With this accomplished, integration proceeds over time, impact parameter, and azimuthal angle.

$$\iiint dx\, dy\, dz\, f(x,y,z) =$$

$$\iiint dt\, db\, da \left| J\begin{pmatrix} x & y & z \\ t & b & \alpha \end{pmatrix} \right| f'(t,b,a) \qquad (3\text{-}39)$$

The action is rearranged,

$$S(r) = p_1 \cdot r_1 + \int_{t_1}^{t} dr \cdot p - p_1 \cdot r + \int_{t_1}^{t} dr \cdot (p - p_1) \quad , \qquad (3\text{-}40)$$

where $p_1$ is the momentum at the initial time $(t=t_1)$. By convention it is taken to be entirely along the z axis, that is, there are no x and y components. That makes sense because the initial time is set before the potential has any influence on the projectile.

With $\chi$ expressed in Jacobians and the coordinate system transformed, the transition integral is expressed

$$T = \iiint dt\, db\, d\alpha\, |J_i\, J|^{1/2} \exp[-i/2\{\arg(J)-\arg(J_i)\}]$$

$$\cdot\, V(r) \exp\left[\frac{i}{\hbar}(r.(p_a - p_b) + \int_{t_i}^{t} dr.(p-p_i))\right] , \qquad (3\text{-}41)$$

where $p_a$ is the momentum of the system associated with the initial state, a, and $p_b$ is the momentum of the system associated with the final state, b. Although $p_i$ and $p_a$ are described a little differently, they are in fact the same, $p_i = p_a$. The momentum associated with the initial state is the initial momentum. Not only are they equal but they are single-valued, the initial momentum does not change during a calculation. Since momentum is conserved in an elastic collision, the magnitude of $p_b$ is the same as $p_a$ (or $p_i$). All that changes is the deflection angle θ. Since it is the transition to a pre-selected final state that is being probed by the calculation, $p_b$ is pre-selected. In this case it is sufficient to fix the value of θ. Of the four moments contained in the above expression, $p_a$, $p_b$, $p$, and $p_i$, only one changes, $p$. $p$ is the current momentum of the system conjugate to each point r along the classical trajectory.

This integral has been used to determine the quantum cross section, $\sigma_{qu}$, for a number of cases. A few of them are included in this chapter.

$$\partial\sigma_{qu} / \partial\Omega = \frac{m^2}{4\pi^2\hbar^4} |T|^2 \qquad (3\text{-}42)$$

where $\Omega$ is generally a solid angle, but in the elastic case is just the scattering angle.

## 3-3. The Jacobian Transformation

A great simplification, based on a very simple physical insight, occurred when the region of space required by the transition integral was limited to that spanned by a representative bundle of trajectories. Another such insight also makes things easier. A Jacobian transformation from three-dimensional Cartesian to three-dimensional trajectory coordinates has been indicated (Stodden, 1987). In the case of an elastic collision with a central potential no torque is applied to the projectile. It stays in whatever plane it starts. The calculation may proceed on a single plane and the rest of trajectory space recovered by formally rotating the plane through $\alpha$. Since every function (including J) in the transition integral will have to be evaluated at every point along every trajectory this represents considerable savings.

If the plane of the calculation is designated $(x',z)$ then

$$x' = r\sin(\theta) \text{ and } z = r\cos(\theta), \tag{3-43}$$

where r is the internuclear separation and $\theta$ is the angle r makes with the z axis. Since $\alpha$ is the azimuthal angle the entire $(x',z)$ plane makes with the $(x,z)$ plane when placed in the three-dimensional Cartesian coordinate system,

$$x = x' \cos(\alpha) = r \sin(\theta) \cos(\alpha),$$

$$y = x' \sin(\alpha) = r \sin(\theta) \sin(\alpha),$$

and $$z = z. \qquad (3\text{-}44)$$

A particular choice for trajectory coordinates uses $b^2/2$ in place of b for the three-dimensional case. This causes the three-dimensional sampling to be evenly distributed. Since

$$\frac{\partial}{\partial(b^2/2)} = \frac{1}{b}\frac{\partial}{\partial b} \qquad (3\text{-}45)$$

the Jacobian takes the form

$$J\begin{pmatrix} x & y & z \\ t & b^2/2 & \alpha \end{pmatrix} = \frac{1}{b}\begin{vmatrix} \partial x/\partial t & \partial y/\partial t & \partial z/\partial t \\ \partial x/\partial b & \partial y/\partial b & \partial z/\partial b \\ \partial x/\partial \alpha & \partial y/\partial \alpha & \partial z/\partial \alpha \end{vmatrix} . \qquad (3\text{-}46)$$

Since $z \neq z(\alpha)$, $\partial z/\partial\alpha = 0$. The expanded determinant becomes

$$J = \frac{1}{b}\Big([\partial x/\partial t(-\partial y/\partial \alpha\ \partial z/\partial b)] - [\partial y/\partial t(-\partial x/\partial \alpha\ \partial z/\partial b)]$$

$$+ [\partial z/\partial t\ (\partial x/\partial b\ \partial y/\partial \alpha - \partial x/\partial \alpha\ \partial y/\partial b)]\Big). \qquad (3\text{-}47)$$

Since each trajectory is confined to the $(x',z)$ plane $\partial\alpha/\partial t = 0$. From Equations (3-35),

$$\partial x/\partial t = \partial x'/\partial t \cos(\alpha),$$

$$\partial x/\partial b = \partial x'/\partial b \cos(\alpha),$$

$$\partial x/\partial \alpha = -x' \sin(\alpha),$$

and

$$\partial y/\partial t = \partial x'/\partial t \sin(\alpha),$$

$$\partial y/\partial b = \partial x'/\partial b \sin(\alpha),$$

$$\partial y/\partial \alpha = x' \cos(\alpha). \qquad (3\text{-}48)$$

Using these in Equation (3-38),

$$\begin{aligned} J = \frac{1}{b}\Big(&\{\partial x'/\partial t \cos(\alpha)\ (-x' \cos(\alpha)\ \partial z/\partial b)\} \\ &- \{\partial x'/\partial t \sin(\alpha)\ (x' \sin(\alpha)\ \partial z/\partial b)\} \\ &+ \{\partial z/\partial t\ (\partial x'/\partial b \cos(\alpha)\ x' \cos(\alpha) \\ &+ x' \sin(\alpha)\ \partial x'/\partial b \sin(\alpha))\}\Big] \end{aligned} \qquad (3\text{-}49)$$

Since $\sin^2(\alpha) + \cos^2(\alpha) = 1$,

$$J = \frac{-x'}{b}\left(\partial x'/\partial t\ \partial z/\partial b - \partial x'/\partial b\ \partial z/\partial t\right) \qquad (3\text{-}50)$$

But the expression in $\{\}$ is just $J'\begin{pmatrix} x' & z \\ t & b \end{pmatrix}$, so

$$J\begin{pmatrix} x & y & z \\ t & b^2/2 & \alpha \end{pmatrix} = -\frac{x'}{b}\ J'\begin{pmatrix} x' & z \\ t & b \end{pmatrix} \qquad (3\text{-}51)$$

Instead of evaluating the three-dimensional Jacobian in all three dimensions, a two-dimensional Jacobian is used and simply multiplied by $-x'/b$.

Three of the five factors in J′ are obtained directly from the equations for motion in the (x′,z) plane. The Hamiltonian, with the momentum separated into components, is

$$H = \frac{\left(p_{x'}^2 + p_z^2\right)}{2m} + V(x',z) \quad . \qquad (3\text{-}52)$$

The coupled equations of motion are applied to each coordinate, $\xi$ ($\xi \equiv x'$ or $z$), along with its conjugate momentum, $p_\xi$,

$$\partial\xi/\partial t = (\partial H/\partial p_\xi) = p_\xi/m$$

$$\partial p_\xi/\partial t = -(\partial H/\partial\xi) = -(\partial V/\partial\xi) \tag{3-53}$$

Integrating these expressions with respect to time gives the factors $x'$, $\partial x'/\partial t$, and $\partial z/\partial t$ that appear in $J'$.

With the initial internuclear separation fixed at some reasonably large value, the conjugate pairs of positions and momenta are unique functions of the time and impact parameter of a trajectory,

$$\xi = \xi(t,b) \qquad p_\xi = p_\xi(t,b) \ . \tag{3-54}$$

The derivatives of Equations (3-44) with respect to b are

$$\frac{\partial^2\xi}{\partial t\partial b} = \frac{1}{m}\frac{\partial p_\xi}{\partial b} \quad ,$$

$$\frac{\partial^2 p_\xi}{\partial t\partial b} = -\frac{\partial^2 H}{\partial\xi\partial b} = -\sum_{\eta=x',z}\frac{\partial^2 V}{\partial\xi\partial\eta}\frac{\partial\eta}{\partial b} \tag{3-55}$$

Integrating these expressions  respect to time gives the factors $\partial x'/\partial b$ and $\partial z/\partial b$ that appear in $J'$. $J'$ and $J$ can both be evaluated.

## 3-4 Computational Aspects

The problem of solving for the transition integral is divided into two major tasks: first, the factors that appear in the integrand are evaluated; second, these factors are integrated over time, impact parameter, and azimuthal angle. The information bearing region is delineated in two steps. One, the internuclear separation at which the trajectories commence is the distance required for the interactive potential to be negligible. Two, the maximum impact parameter has been reached when the flight of the projectile is no longer influenced by the target. Since an elastic collision is cylindrically symmetric the third coordinate, $\phi$, passes through 360° in all cases. A statistically significant sample population of trajectories is formed by starting at zero impact parameter, calculating the conjugate positions and momenta for an entire collision, taking small even increments in $b^2/2$ and repeating the process until $b^2_{max}/2$ is reached.

A packaged program, in this case DE, is used to give numerical solutions to the coupled differential equations of motion. DE is a particularly fine predictor-corrector type program written by L. Shampine and K. Gordon (Shampine and Gordon, 1975). It is well known for its reliability in a range of applications. All it requires are the initial function value and derivative (preferably analytical) for each equation to be solved, a parameter that limits the maximum size of the allowable estimated error, and a cutoff value at which the integration is stopped. Classical trajectories are stopped when the particle separation after the collision meets or exceeds the initial separation. In addition to the positions and momenta, DE is used to evaluate a number of other factors in T at each time step along each trajectory. The two that appear in the Jacobian, $\partial x'/\partial b$ and $\partial a/\partial b$, were discussed in Section 3-3. ( See Equation (3-44). ) The other two are components of the action related integral that is part of the exponent in Equation (3-32),

$$\int_{t_1}^{t} dr.(p-p_1) = \int_{t_1}^{t} dt' \left(\frac{p_{x'}^2}{m}\right) + \int_{t_1}^{t} dt' \left(\frac{p_z^2}{m} - p_z v_1\right) . \quad (3-56)$$

Four steps lead from the left to the right hand side of this equation:

1. decompose into three dimensional Cartesian coordinates

2. change to the (x',z) plane using Equations (3-39)

3. the initial motion is chosen to be along the z axis ($p_x$(initial)=0, $p_z$(initial)=$mv_1$)

4. changing variables from dr to dt'.

The derivatives of the integrals on the right, required by DE, are simply their integrands. The momenta in the asymptotic region don't change very fast, so the initial values of the integrals are zero.

The other term in the exponent of Equation (3-32) contains the only explicit reference to the pre-selected final state. The information it contains is critical to the calculation. It also decomposes into two terms,

$$r.(p_a-p_b) = x' \cos(\alpha)[-mv_1 \sin(\theta_b)] + z\, mv_1[1-\cos(\theta_b)]. \tag{3-57}$$

The magnitude of the momentum is conserved in an elastic collision, only the scattering angle, $\theta_b$, varies,

$$\begin{aligned} p_a &= p_b = p = mv_1 , \\ p_{bx} &= p \sin(\theta_b) , \\ p_{bz} &= p \cos(\theta_b) . \end{aligned} \tag{3-58}$$

By a convention that is usual in scattering theory, scattering angles are calculated in the (x,z) plane, $p_{by}=0$. Since everything else is constant with respect to $\alpha$, integration over $\alpha$ reduces to

$$I = \int_0^{2\pi} d\alpha \exp\left\{\frac{i}{\hbar} [x' (-mv_1) \sin(\theta_b) \cos(\alpha)]\right\} . \tag{3-59}$$

Letting

$$c = (i/\hbar)\, x' (-mv_1) \sin(\theta_b) \tag{3-60}$$

gives

$$I(c) = \int_0^{2\pi} d\alpha \, e^{i \, c \, \cos(\alpha)} \qquad (3\text{-}61)$$

Page 360 of Abramowitz and Stegun (1972) gives an integral representation of the n-order Bessel function,

$$J_n(c) = \frac{i^{-n}}{\pi} \int_0^{\pi} d\alpha \, \cos(n\alpha) \, e^{i \, c \, \cos(\alpha)} \quad , \qquad (3\text{-}62)$$

With n equal zero, $\cos(n\alpha)=1$,

$$I(c) = 2\pi \, J_0(c) \qquad (3\text{-}63)$$

Abramowitz and Stegun also supply the polynomial approximation that is used to evaluate $J_0(c)$.

The integral that remains after integrating over $\alpha$ is

$$T = \iint d(b^2/2) \, dt \, |J_1 J|^{1/2} \, I(c)$$

$$\cdot \exp \left\{ \frac{i}{\hbar} \Bigg( \int_{t_1}^{t} dt' \left( \frac{p_x^{2}}{m}' \right) + \int_{t_1}^{t} dt' \left( \frac{p_z^2}{m} - p_z v_1 \right) - \frac{N}{2} \pi \right.$$

$$\left. + \, e \, m v_1 [1 - \cos(\theta_b)] \Bigg) \right\} \qquad (3\text{-}64)$$

where N is the number of times the Jacobian changes sign. The argument of the exponential is generally a large rapidly changing function of time. As a result the exponential itself oscillates with extreme rapidity and cannot be integrated using the usual direct approaches.

The linearizing technique, which may be rendered as numerically precise as the user wishes, is preferable to the stationary phase approximation. The integrand is separated into exponential and pre-exponential cofactors,

$$T = \int dt\, f(t)\, e^{i\,\phi(t)}. \tag{3-65}$$

Over small increments of t, f and $\phi$ are smooth enough to be replaced by the zero and first order terms of their Taylor expansions,

$$f(t) = f_0 + f_1 t$$

$$\phi(t) = \phi_0 + \phi_1 t \quad . \tag{3-66}$$

$f_1$ and $\phi_1$ are the slopes,

$$f_1 = \frac{f(t_f) - f(t_i)}{t_f - t_i}$$

$$\phi_1 = \frac{\phi(t_f) - \phi(t_i)}{t_f - t_i} \quad , \tag{3-67}$$

where i refers to initial t and f to final t. Setting t equal to $t_i$ in Equation (3-57) gives $f_0$ and $\phi_0$,

$$f(t_i) = f_0 + f_1 t_i$$

$$f_0 = f(t_i) - f_1 t_i$$

$$\phi(t_i) = \phi_0 + \phi_1 t_i$$

$$\phi_0 = \phi(t_i) - \phi_1 t_i \tag{3-68}$$

Substituting into Equation (3-56),

$$
\begin{aligned}
T_{fi} &= \int_{t_i}^{t_f} dt\,(f_0 + f_1 t)\, e^{i\phi_0}\, e^{i\phi_1 t} \\
&= e^{i\phi_0} \left\{ \left( f_0 \int_{t_i}^{t_f} dt\, e^{i\phi_1 t} \right) + \left( f_1 \int_{t_i}^{t_f} dt\, t\, e^{i\phi_1 t} \right) \right\} \\
&= e^{i\phi_0} \left\{ \left( \frac{f_0}{i\phi_1} \left[ e^{i\phi_1 t_f} - e^{i\phi_1 t_i} \right] \right) \right. \\
&\quad \left. + \left( \frac{f_1}{\phi_1^2} \int_{\phi_1 t_i}^{\phi_1 t_f} d(\phi_1 t)\, \phi_1 t\, [\cos(\phi_1 t) + i \sin(\phi_1 t)] \right) \right\}
\end{aligned}
\qquad (3\text{-}69)
$$

In the last expression, the variable of integration was changed from t to $\phi_1 t$ and the equality

$$e^{iu} = \cos(u) + i \sin(u) \qquad (3\text{-}70)$$

was employed. The two integrals that result can both be done analytically.

The linearizing technique integrates over f numerically while simultaneously performing local integrations of the exponential analytically. Integration of a rapidly oscillating exponential is transformed into a sequence of locally analytic integrals in the smoothly changing $\phi$.

After temporal integration, the integrand is complex. The final integration over impact parameter is carried out separately for the real and imaginary parts. The trapezoid rule is used with $d(b^2/2)$ approximated by

$$d(b^2/2) = (1/2)(b_{i+1}^2 - b_i^2)$$

$$= (1/2)[(b_i + \Delta b)^2 - b_i^2] = b_i \Delta b + \left(\frac{(\Delta b)^2}{2}\right\}. \quad (3\text{-}71)$$

This ends the brief discussion of how the theory is translated into mathematical expressions that can be evaluated in the practical sense. Each of the building blocks such as the trajectories, the action, the Bessel function, or the Jacobian needs to be thoroughly tested both individually and in various combinations before the entire package can be assembled in complete working order. In many ways producing a working program is as difficult and demanding as the theory itself. The interested reader is referred to "Computational Studies of Molecular Collisions" by this author for more details (Cohen, 1988).

### 3-5 Sample calculations

The following three figures depict sample eikonal calculations for elastic collisions in three dimensions. The first two are for $H_2$+Hg at different total energies. The second one, at a higher energy, loses some of its definition (the oscillations wash out somewhat) but gives a correct overall view. The third one shows Li+Hg. All three were done using a simple Lennard-Jones potential.

Figure 3-1. Quantum Cross Section for $H_2$+Hg at K=1.6.

K is the reduced energy (dimensionless).
The maximum error parameter (input to the eikonal program) was $10^{-6}$.

An eikonal calculation (solid line) compared to a partial wave solution (dashed line) provided by a program called OPTIK (1975). The results from OPTIK are identical to those in Bernstein (1960).

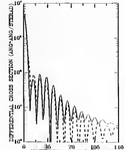
DIFFERENTIAL CROSS SECTION (ANG*ANG/STERAD)
$10^4$
$10^3$
$10^2$
$10^1$
$10^0$
0
35
70
105
140
SCATTERING ANGLE (DEGREES)

Figure 3-2. Quantum Cross Section for $H_2$+Hg at K=2 6.

K is the reduced energy (dimensionless).
The maximum error parameter (input to the eikonal program) was $10^{-6}$.

An eikonal calculation (solid line) compared to a partial wave solution (dashed line) provided by a program called OPTIK (1975).

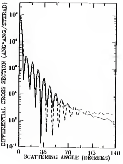
DIFFERENTIAL CROSS SECTION (ANG*ANG/STERAD)
$10^4$
$10^3$
$10^2$
$10^1$
$10^0$
$10^{-1}$
0
35
70
105
140
SCATTERING ANGLE (DEGREES)

Figure 3-3. Quantum Cross Section for Li+Hg at K=2.0

K is the reduced energy (dimensionless).
The maximum error parameter (input to the eikonal program) was $10^{-6}$.

LEFT GRAPH - eikonal calculation

RIGHT GRAPH - partial wave solution provided by OPTIK (1975)

NOTE: The partial wave solution appears smoother because more points were used.

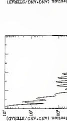
Differential Cross Section (ANG*ANG/STERAD)
10⁴
10³
10²
10¹
10⁰
0
13
25
38
50
Scattering Angle (DEGREES)

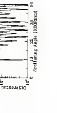
Differential Cross Section (ANG*ANG/STERAD)
10⁴
10³
10²
10¹
10⁰
0
13
25
38
50
Scattering Angle (DEGREES)

# CHAPTER IV

# ELECTRONICALLY INELASTIC SCATTERING IN ONE VARIABLE

## 4-1. Converting from a Diabatic Potential to an Adiabatic Potential

Before launching into the demonstration of how the eikonal method may be applied to inelastic scattering in both the diabatic and adiabatic representations it is useful to know how they interconvert. The present work concentrates on the diabatic to adiabatic conversion. This is of particular interest because the eikonal equations have already been developed and applied in the diabatic representation. The solutions presented here for the adiabatic case are in some degree extensions of these. Due to the general popularity of the diabatic approach in recent years the literature contains a variety of diabatic potentials that can serve as starting points. Readers interested in pursuing the reverse conversion are referred to Olson and Micha (Olson and Micha, 1982). The unitary matrix that transforms a diabatic potential into an adiabatic potential is described in this section. When the equation for nuclear motion, (2-9), is written with a diabatic potential, the same matrix converts the equation itself to the adiabatic representation. This is clarified in Section 4-3.

The diabatic potential in the simple two-state case is expressed as a two-by-two matrix whose diagonal elements contain the surface potentials and whose off-diagonal elements give the potential coupling. The coupling is associated with the probability that an atom or molecule moving on one surface will switch over to the other.

Another aspect of the coupling, that is not part of the potential, is momentum coupling. Diabatic potentials are usually determined in such a way that the momentum coupling can be neglected. Adiabatic potentials present the alternate view, all of the coupling is momentum coupling and none of the coupling is in the potential. By definition, the off-diagonal elements of the adiabatic potential are zero. Conversion from a diabatic potential to an adiabatic potential is effected by applying the unitary transformation matrix, B, containing the transformation angle, γ, to the diabatic potential matrix, $V^d$,

$$B = \begin{pmatrix} \cos\gamma & \sin\gamma \\ -\sin\gamma & \cos\gamma \end{pmatrix} \quad ; \quad B^+B = 1$$

$$V^a = B^+V^d B$$

$$= \begin{pmatrix} \cos\gamma & -\sin\gamma \\ \sin\gamma & \cos\gamma \end{pmatrix} \begin{pmatrix} V^d_{11} & V^d_{12} \\ V^d_{12} & V^d_{22} \end{pmatrix} \begin{pmatrix} \cos\gamma & \sin\gamma \\ -\sin\gamma & \cos\gamma \end{pmatrix}$$

$$= \begin{pmatrix} V_{11}^{a} & 0 \\ 0 & V_{22}^{a} \end{pmatrix} \tag{4-1}$$

The value of $\gamma$ is determined from the values of the diabatic matrix elements and the condition that the off-diagonal (coupling) adiabatic potential matrix elements are zero,

$$V_{12}^{a} = 0 = -V_{11}^{d}\sin(\gamma)\ \cos(\gamma) + V_{12}^{d}\cos^{2}(\gamma)$$

$$-V_{12}^{d}\sin^{2}(\gamma) + V_{22}^{d}\sin(\gamma)\ \cos(\gamma)$$

$$= (V_{22}^{d} - V_{11}^{d})\ \sin(\gamma)\ \cos(\gamma) + V_{12}^{d}[\cos^{2}(\gamma)-\sin^{2}(\gamma)]$$

$$= (V_{22}^{d} - V_{11}^{d})\ \frac{\sin(2\alpha)}{2} + V_{12}^{d}\cos(2\alpha) \qquad ;$$

$$\frac{\tan(2\alpha)}{2} = \frac{-V_{12}^{d}}{V_{22}^{d}-V_{11}^{d}} \qquad ,$$

$$\gamma = \frac{1}{2}\ \mathrm{atan}\left( \frac{2\ V_{12}^{d}}{V_{11}^{d}-V_{22}^{d}} \right) \tag{4-2}$$

When the unitary transformation is applied to Schroedinger's equation for nuclear motion, Equation (2-9), information that was in the diabatic potential coupling is now in B and $\gamma$, which modify terms that contain the momentum, thereby altering the momentum coupling. This will become clearer in Section 4-3. Figures 4-1, 4-3, and 4-5 show examples of diabatic potentials that are transformed to adiabatic potentials.

Figures 4-2, 4-4, and 4-6 show the transformation angles $\gamma$.

## 4-2 Equations in the Diabatic Representation

While more elaborate approaches are certainly possible, (surface scattering, scattering in real space, etc.), the present work basically examines electronically inelastic collisions in terms of a single variable, the interparticle separation R. The development of this section generally follows Riche and Swaminathan (1986). In the diabatic representation,

$$\left[ \frac{1}{2m} \left( \frac{\hbar}{i} \frac{\partial}{\partial R} \right)^2 + V^d(R) - E \right] \psi(R) = 0 \; . \tag{4-3}$$

The eikonal wavefunction is

$$\psi(R) = \chi(R) \exp[i\, S(R)/\hbar] \tag{4-4}$$

Taking the second derivative,

$$\begin{aligned} d^2\psi/dR^2 &= d/dR\left( \frac{d\chi}{dR} e^{\frac{i}{\hbar} S} + \frac{i}{\hbar} \frac{dS}{dR} \chi\, e^{\frac{i}{\hbar} S} \right) \\ &= \frac{d^2\chi}{dR^2} e^{\frac{i}{\hbar} S} + \frac{i}{\hbar}\, 2 \frac{dS}{dR} \frac{d\chi}{dR} e^{\frac{i}{\hbar} S} + \frac{i}{\hbar} \frac{d^2S}{dR^2} \chi\, e^{\frac{i}{\hbar} S} \\ &- \frac{1}{\hbar^2} \left(\frac{dS}{dR}\right)^2 \chi\, e^{\frac{i}{\hbar} S} \quad , \end{aligned} \tag{4-5}$$

and associating dS/dR with the momentum,

$$P = dS/dR \ , \tag{4-6}$$

leads to

$$- \frac{\hbar^2}{2m} \frac{d^2\chi}{dR^2} - i \hbar \frac{P}{m} \frac{d\chi}{dR}$$

$$- i \frac{\hbar}{2m} \frac{dP}{dR} \chi + \frac{P^2}{2m} \chi + V^d \chi - E \chi = 0 \tag{4-7}$$

An equivalent expression for this last equation is obtained by introducing the diagonal matrices $\mathbf{W}(P,R)$ and $\mathbf{K}(R)$. $\mathbf{W}$ is introduced to facilitate a phase change that will simplify the time dependent equations. $\mathbf{W}$ and $\mathbf{K}$ are defined

$$\mathbf{W}(P,R) = V(P,R) + i\mathbf{U}(R) - \mathbf{K}(R) \quad ;$$

$$(\underline{K})_{\gamma'\gamma} = \delta_{\gamma'\gamma} \left( - \frac{\hbar^2}{2m} \right) \frac{d^2\chi_\gamma}{dR^2} \Big/ \chi_\gamma \quad ,$$

$$U(R) = \frac{\hbar}{2m} \frac{d^2S}{dR^2} I = \frac{\hbar}{2m} \frac{dP}{dR} I \tag{4-8}$$

Equation (4-7) becomes

$$\left[ \frac{P}{m} \frac{\hbar}{i} \frac{d}{dR} + V^d(R) - \mathbf{W}(P,R) \right] \chi(R) = 0. \tag{4-9}$$

which is still exact. Applying the short wavelength approximation, Equation (3-10), gives

$$\left( \frac{P}{m} \frac{\hbar}{i} \frac{d}{dR} + v^d(R) - W(R) \right) \chi(R) = 0.$$

$$W(R) = v(R) + iU(R)$$

$$v(R) = (\chi^+\chi)^{-1} \chi^+ v^d \chi \tag{4-10}$$

The exact form of $v^d$ is obtained as described in Section 2-2 and demonstrated, for the elastic case, in Section 3-1. Identify the entire expression operating on $\chi$ in Equation (4-7) as $\mathbf{F}$. Left multiply that equation by $\chi^+$.

$$- \frac{\hbar^2}{2m} \chi^+ \frac{d^2\chi}{dR^2} - i \hbar \frac{P}{m} \chi^+ \frac{d\chi}{dR}$$

$$- i \frac{\hbar}{2m} \frac{dP}{dR} \chi^+\chi + \frac{P^2}{2m} \chi^+\chi + \chi^+ v^d \chi - E \chi^+\chi = 0 , \tag{4-11}$$

and take the adjoint,

$$- \frac{\hbar^2}{2m} \frac{d^2\chi^+}{dR^2} \chi + i \hbar \frac{P}{m} \frac{d\chi^+}{dR} \chi$$

$$+ i \frac{\hbar}{2m} \frac{dP}{dR} \chi^+\chi + \frac{P^2}{2m} \chi^+\chi + \chi^+ v^d \chi - E \chi^+\chi = 0 . \tag{4-12}$$

Adding these last two equations and dividing by $2\chi^+\chi$ gives

$$E = \frac{P^2}{2m} + v^d(R,P) \quad ;$$

$$v^d(R,P) = (\chi^+\chi)^{-1} \left\{ \chi^+ v^d \chi + \frac{i\hbar}{2m} P \left( \frac{\partial\chi^+}{\partial R} \chi - \chi^+ \frac{\partial\chi}{\partial R} \right) \right.$$

$$\left. - \frac{\hbar^2}{2m} \left( \frac{\partial^2\chi^+}{\partial R^2} \chi + \chi^+ \frac{\partial^2\chi}{\partial R^2} \right) \right\} \tag{4-13}$$

Since $R=R(t)$ the function $\chi(R)$ may be expressed as some function of time. The cofactor $A(t)$ that appears in that function is defined to satisfy

$$\chi[R(t)] = \exp\left[i\int_{t_1}^{t} dt'\ W(R(t'))/\hbar\right] A(t) . \qquad (4\text{-}14)$$

Also $V(R) = V[R(t)] = V_t(t)$, so placing Equation (4-14) in Equation (4-10) gives

$$\left\{\frac{\hbar}{i}\frac{d}{dt} + V_t^d(t)\right\} A(t) = 0 \qquad (4\text{-}15)$$

As pointed out in Section 2-2, $A(t_1)=1$ in the initial channel and zero in all the others. Because $V_t^d(t)$ is Hermitian,

$$d(A^+A)/dt = 0$$

and

$$A^+A = 1 \qquad (4\text{-}16)$$

for all times. This corresponds to a conservation of probability. Since A is complex,

$$A = X + iY \ ,$$

$$X = \mathrm{Re}(A) \ , \ Y = \mathrm{Im}(A) \qquad (4\text{-}17)$$

The simple two-state case is

$$dX_1/dt = \frac{1}{\hbar}\,(V^d_{11}Y_1+V^d_{12}Y_2)$$

$$dY_1/dt = -\frac{1}{\hbar}\,(V^d_{11}X_1+V^d_{12}X_2)$$

$$dX_2/dt = \frac{1}{\hbar}\,(V^d_{12}Y_1+V^d_{22}Y_2)$$

$$dY_2/dt = -\frac{1}{\hbar}\,(V^d_{12}X_1+V^d_{22}X_2) \qquad (4\text{-}18)$$

Notice that

$$v^d = (X^+X)^{-1}\, X^+V^dX = (A^+A)^{-1}\, A^+V^dA \qquad (4\text{-}19)$$

so that

$$H(R,P,X_n,Y_n) = \frac{P^2}{2m} + v^d(R,X_n,Y_n)$$

$$dH/dt = 0 = (\partial H/\partial R)\, dR/dt + (\partial H/\partial P)\, dP/dt$$

$$+ (\partial H/\partial X_n)\, dX_n/dt + (\partial H/\partial Y_n)\, dY_n/dt$$

$$dR/dt = \partial H/\partial P = P/m$$

$$dP/dt = -\partial H/\partial R = -\partial v^d/\partial R$$

$$dX_n/dt = \partial H/\partial Y_n = \partial v^d/\partial Y_n$$

$$dY_n/dt = -\partial H/\partial X_n = -\partial v^d/\partial X_n \qquad (4\text{-}20)$$

In fact, the expressions for $dX_n/dt$ and $dY_n/dt$ in Equation (4-20) are identical to those in Equations (4-18). The reader may convince himself this is so by examining the explicit expression for $v^d$ given immediately following. Applying the short-wavelength approximation and Equations (4-19), (4-16) and (4-17).

$$v^d(R) = (X^+X)^{-1}(\ X^+v^dX\ ) = (A^+A)^{-1}\ (\ A^+v^dA\ )$$

$$= (\ A_1^*\ \ A_2^*\ )\ \begin{pmatrix} v_{11}^dA_1 + v_{12}^dA_2 \\ v_{12}^dA_2 + v_{22}^dA_2 \end{pmatrix}$$

$$= A_1^*A_1v_{11}^d + A_1^*A_2v_{12}^d + A_2^*A_1v_{12}^d + A_2^*A_2v_{22}^d$$

$$= (X_1^2 + Y_1^2)\ v_{11}^d + (X_1X_2 + iX_1Y_2 - iY_1X_2 + Y_1Y_2)\ v_{12}^d$$

$$+ (X_2X_1 + iX_2Y_1 - iY_2X_1 + Y_2Y_1)\ v_{12}^d + (X_2^2 + Y_2^2)\ v_{22}^d$$

$$= (X_1^2 + Y_1^2)\ v_{11}^d + 2\ (X_1X_2 + Y_1Y_2)\ v_{12}^d + (X_2^2 + Y_2^2)\ v_{22}^d\ . \tag{4-21}$$

The expression for $-\partial u^d/\partial R$ required to generate the trajectories is given by

$$dP/dt = -\partial u^d(R)/\partial R = -\frac{\partial}{\partial R}\left[(X^+X)^{-1}(\ X^+v^dX\ )\right]$$

$$= -\frac{\partial}{\partial R}\left[(A^+A)^{-1}(\ A^+v^dA\ )\right]$$

$$= (X_1^2+Y_1^2)\ \frac{dv_{11}^d}{dR} + 2\ (X_1X_2+Y_1Y_2)\ \frac{dv_{12}^d}{dR} + (X_2^2+Y_2^2)\ \frac{dv_{22}^d}{dR}\ . \tag{4-22}$$

Notice that this particular expression doesn't contain the derivatives of $X_n$ and $Y_n$, $\partial X_n/\partial R$ and $\partial Y_n/\partial R$. There is a temptation to ascribe this to the short-wavelength approximation, saying terms that (for instance) contain $\partial X/\partial R$ are small compared to terms in X, but it really is not necessary. Because the expressions for dX/dt and dY/dt used here, Equations (4-18), are identical to Equations (4-20) the inclusion of $\partial X_n/\partial R$ and $\partial Y_n/\partial R$ in $\partial u^d/\partial R$ has no net effect:

$$\frac{\partial u^d}{\partial R} = \left(\frac{\partial u^d}{\partial R}\right)_{X,Y} + \sum_{n=1}^{2} \frac{\partial u^d}{\partial X_n}\frac{dX_n}{dR} + \frac{\partial u^d}{\partial Y_n}\frac{dY_n}{dR}$$

$$= \left(\frac{\partial u^d}{\partial R}\right)_{X,Y} + \sum_{n=1}^{2} - \frac{dY_n}{dt}\frac{dX_n}{dR} + \frac{dX_n}{dt}\frac{dY_n}{dR}$$

$$\frac{dX_n}{dR} = \frac{dX_n/dt}{dR/dt} \; ; \; \frac{dY_n}{dR} = \frac{dY_n/dt}{dR/dt}$$

$$\frac{\partial u^d}{\partial R} = \left(\frac{\partial u^d}{\partial R}\right)_{X,Y} + \sum_{n=1}^{2} - \frac{dY_n}{dt}\frac{dX_n/dt}{dR/dt} + \frac{dX_n}{dt}\frac{dY_n/dt}{dR/dt}$$

$$= \left(\frac{\partial u^d}{\partial R}\right)_{X,Y} \qquad (4\text{-}23)$$

Another line of reasoning reinforces this conclusion. In the adiabatic equations described below the expressions for dX/dt and dY/dt are not equivalent to those given by Equations (4-20): $\partial X/\partial R$ and $\partial Y/\partial R$ must be included in $\partial u/\partial R$ in that case in order to get results.

## 4-3. Equations in the Adiabatic Representation

The diabatic equation for nuclear motion, (4-3), is conveniently expressed as

$$( H^d - E ) \psi^d = 0 \quad , \qquad (4\text{-}24)$$

where

$$H^d = \frac{1}{2m} \left( \frac{\hbar}{i} \frac{d}{dR} \right)^2 + V^d \quad . \qquad (4\text{-}25)$$

Transformation to the adiabatic representation is accomplished by left multiplying the entire equation by $B^+$ and inserting the unit matrix in front of $\psi^d$,

$$B^+ ( H^d - E ) \mathbf{1} \psi^d = 0 \quad , \qquad (4\text{-}26)$$

From the definition of B, Equation (4-1), $BB^+ = \mathbf{1}$ so

$$B^+ ( H^d - E ) BB^+ \psi^d = 0 \quad ,$$

and

$$( H^a - E ) \psi^a = 0 \quad , \qquad (4\text{-}27)$$

where

$$H^a = B^+ H^d B \quad \text{and} \quad \psi^a = B^+ \psi^d \qquad (4\text{-}28)$$

Since $V^a = B^+ V^d B$, Equation (4-1), one finds

$$H^a = -\frac{\hbar^2}{2m}\left( B^+ \frac{d^2B}{dR^2} + 2\, B^+ \frac{dB}{dR}\frac{d}{dR} + \frac{d^2}{dR^2} \right) + V^a \quad ;$$

$$\left[ -\frac{\hbar^2}{2m}\left( B^+ \frac{d^2B}{dR^2} + 2\, B^+ \frac{dB}{dR}\frac{d}{dR} + \frac{d^2}{dR^2} \right) + V^a - E \right] \psi^a = 0 \; ,$$

$$(4\text{-}29)$$

From

$$B^+(dB/dR) = \begin{pmatrix} 0 & 1 \\ -1 & 0 \end{pmatrix} \frac{d\gamma}{dR} \qquad ;$$

$$B^+(d^2B/dR^2) = \begin{pmatrix} -1 & 0 \\ 0 & -1 \end{pmatrix} \left(\frac{d\gamma}{dR}\right)^2 + \begin{pmatrix} 0 & 1 \\ -1 & 0 \end{pmatrix} \frac{d^2\gamma}{dR^2} \; , \quad (4\text{-}30)$$

comes

$$-\frac{\hbar^2}{2m}\begin{pmatrix} -1 & 0 \\ 0 & -1 \end{pmatrix} \left(\frac{d\gamma}{dR}\right)^2 \psi^a - \frac{\hbar^2}{2m}\begin{pmatrix} 0 & 1 \\ -1 & 0 \end{pmatrix} \frac{d^2\gamma}{dR^2}\psi^a$$

$$-\frac{\hbar^2}{m}\begin{pmatrix} 0 & 1 \\ -1 & 0 \end{pmatrix} \frac{d\gamma}{dR}\frac{d\psi^a}{dR} - \frac{\hbar^2}{2m}\frac{d^2\psi^a}{dR^2} - E\psi^a + V^a\psi^a = 0. \quad (4\text{-}31)$$

Inserting the first and second derivatives of $\psi$ from Equation (4-5) along with $P = dS/dR$, Equation (4-6), gives (omitting from now on the superscript a),

$$- \frac{\hbar^2}{2m} \frac{d^2\chi}{dR^2} - \frac{\hbar^2}{m} \begin{pmatrix} 0 & 1 \\ -1 & 0 \end{pmatrix} \frac{d\gamma}{dR} \frac{d\chi}{dR} - i \hbar \frac{P}{m} \frac{d\chi}{dR}$$

$$- \frac{\hbar^2}{2m} \begin{pmatrix} -1 & 0 \\ 0 & -1 \end{pmatrix} \left(\frac{d\gamma}{dR}\right)^2 \chi - \frac{\hbar^2}{2m} \begin{pmatrix} 0 & 1 \\ -1 & 0 \end{pmatrix} \frac{d^2\gamma}{dR^2} \chi$$

$$- \frac{i\hbar}{m} P \begin{pmatrix} 0 & 1 \\ -1 & 0 \end{pmatrix} \frac{d\gamma}{dR} \chi$$

$$- i \frac{\hbar}{2m} \frac{dP}{dR} \chi + \frac{P^2}{2m} \chi + V^a \chi - E \chi = 0 \, . \qquad (4\text{-}32)$$

The first steps in making this equation manageable are

a) apply the short-wavelength approximation to eliminate $d^2\chi/dR^2$

b) substitute $v$ for $E - (P^2/2m)$

c) group the cofactors of $d\chi/dR$ and $\chi$ separately

$$\left\{ - \frac{\hbar^2}{m} \begin{pmatrix} 0 & 1 \\ -1 & 0 \end{pmatrix} \frac{d\gamma}{dR} - i \hbar \frac{P}{m} \right\} \frac{d\chi}{dR}$$

$$+ \left\{ - \frac{\hbar^2}{2m} \begin{pmatrix} -1 & 0 \\ 0 & -1 \end{pmatrix} \left(\frac{d\gamma}{dR}\right)^2 - \frac{\hbar^2}{2m} \begin{pmatrix} 0 & 1 \\ -1 & 0 \end{pmatrix} \frac{d^2\gamma}{dR^2}\right.$$

$$\left. - i\hbar \frac{P}{m} \begin{pmatrix} 0 & 1 \\ -1 & 0 \end{pmatrix} \frac{d\gamma}{dR} - i \frac{\hbar}{m} \frac{dP}{dR} - v^a + V^a \right\} \chi = 0. (4\text{-}33)$$

The term $-i$ $(\hbar/m)$ $(dP/dR)$ can be eliminated by a change in phase similar to that shown in Equations (4-8), (4-9), (4-10), (4-14), and (4-15). In principle one ought to be able to eliminate $v^a$ as well. In practice numerical complications arise that prevent this. With the expression multiplying $d\chi/dR$ defined as the C matrix,

$$C = -\frac{\hbar^2}{m}\begin{pmatrix} 0 & i \\ -1 & 0 \end{pmatrix}\frac{d\gamma}{dR} - i\,\hbar\,\frac{P}{m} \quad , \qquad (4\text{-}34)$$

$d\chi/dR$ is

$$\frac{d\chi}{dR} = C^{-1}\left\{\frac{\hbar^2}{2m}\begin{pmatrix} -1 & 0 \\ 0 & -1 \end{pmatrix}\left(\frac{d\gamma}{dR}\right)^2 + \frac{\hbar^2}{2m}\begin{pmatrix} 0 & i \\ -1 & 0 \end{pmatrix}\frac{d^2\gamma}{dR^2}\right.$$

$$\left. + i\,\hbar\,\frac{P}{m}\begin{pmatrix} 0 & 1 \\ -1 & 0 \end{pmatrix}\frac{d\gamma}{dR} + v^a - V^a\right\}\chi \quad . \qquad (4\text{-}35)$$

C can be expressed

$$C = \begin{pmatrix} i\beta & \alpha \\ -\alpha & i\beta \end{pmatrix} \quad , \alpha = -\frac{\hbar^2}{m}\frac{d\gamma}{dR} \; ; \; \beta = -\hbar\frac{P}{m} \quad ,$$

$$C^{-1} = \begin{pmatrix} i\beta & -\alpha \\ \alpha & i\beta \end{pmatrix} / (\alpha^2-\beta^2) = \begin{pmatrix} i\beta & -\alpha \\ \alpha & i\beta \end{pmatrix} q \quad ,$$

$$q = \frac{1}{\alpha^2-\beta^2} \qquad (4\text{-}36)$$

Singularities arise in q (and $d\chi/dR$) near the turning point if, as happens, $|\alpha| = |\beta|$ or at the turning point when $\alpha = \beta = 0$. The condition is handled by adding a very small imaginary number, $\varepsilon$, to P,

$$P \to P + i\varepsilon \Rightarrow \beta \to \beta_\varepsilon = -\hbar\,\frac{P + i\varepsilon}{m} = \mathrm{Re}(\beta_\varepsilon) + i\,\mathrm{Im}(\beta_\varepsilon),$$

$$\mathrm{Re}(\beta_\varepsilon) = -\hbar\frac{P}{m} \quad , \quad \mathrm{Im}(\beta_\varepsilon) = -\hbar\frac{\varepsilon}{m} \qquad (4\text{-}37)$$

This transforms q to an $\varepsilon$ dependent form, $q_\varepsilon$, with a complex denominator. Multiplying by unity (the complex conjugate of the denominator divided by itself) allows $q_\varepsilon$ to be separated into real and imaginary parts.

$$q \to q_\varepsilon = \frac{1}{-[\mathrm{Re}(\beta_\varepsilon) + i\ \mathrm{Im}(\beta_\varepsilon)]^2 + \alpha^2}$$

$$= \frac{1}{-\mathrm{Re}(\beta_\varepsilon)^2 + \mathrm{Im}(\beta_\varepsilon)^2 + \alpha^2 - i2\ \mathrm{Re}(\beta_\varepsilon)\ \mathrm{Im}(\beta_\varepsilon)}$$

$$\times \frac{-\mathrm{Re}(\beta_\varepsilon)^2 + \mathrm{Im}(\beta_\varepsilon)^2 + \alpha^2 + i2\ \mathrm{Re}(\beta_\varepsilon)\ \mathrm{Im}(\beta_\varepsilon)}{-\mathrm{Re}(\beta_\varepsilon)^2 + \mathrm{Im}(\beta_\varepsilon)^2 + \alpha^2 + i2\ \mathrm{Re}(\beta_\varepsilon)\ \mathrm{Im}(\beta_\varepsilon)}$$

$$= \mathrm{Re}(q_\varepsilon) + i\ \mathrm{Im}(q_\varepsilon) \quad ;$$

$$\mathrm{Re}(q_\varepsilon) = \frac{-\mathrm{Re}(\beta_\varepsilon)^2 + \mathrm{Im}(\beta_\varepsilon)^2 + \alpha^2}{[-\mathrm{Re}(\beta_\varepsilon)^2 + \mathrm{Im}(\beta_\varepsilon)^2 + \alpha^2)^2 + 4\ \mathrm{Re}(\beta_\varepsilon)\ \mathrm{Im}(\beta_\varepsilon)} . \quad (4\text{-}38)$$

In fact, the real part of $q_\varepsilon$ satisfies present requirements, it avoids the two singularities and it approaches q as $\varepsilon$ approaches zero,

$$\lim_{\varepsilon \to 0} \mathrm{Re}(q_\varepsilon) = q \quad . \qquad (4\text{-}39)$$

In practice the entire calculation is performed over a range of $\varepsilon$ to determine which values are stable and give meaningful results (see Figures 5-10, 5-11, and 5-12). Adiabatic calculations carried out using only $\mathrm{Re}(q_\varepsilon)$ with $\varepsilon$=0.01 (or in one case $\varepsilon$=0.001) reproduce the results of diabatic calculations (see Chapter VI).

Since $\chi$ is complex let

$$\xi_n = \mathrm{Re}(\chi_n) \; ; \; \eta_n = \mathrm{Im}(\chi_n) \quad . \tag{4-40}$$

The equation for $d\chi/dR$ becomes

$$\frac{d}{dR}\begin{pmatrix}\xi_1+i\eta_1\\ \xi_2+i\eta_2\end{pmatrix} = \begin{pmatrix} i\beta & -\alpha\\ \alpha & i\beta\end{pmatrix} \mathrm{Re}(q_c)\left\{ \frac{\hbar^2}{2m}\begin{pmatrix}-1 & 0\\ 0 & -1\end{pmatrix}\left(\frac{d\gamma}{dR}\right)^2 \right.$$
$$\left. + \frac{\hbar^2}{2m}\begin{pmatrix}0 & 1\\ -1 & 0\end{pmatrix}\frac{d^2\gamma}{dR^2} + i\hbar\frac{P}{m}\begin{pmatrix}0 & 1\\ -1 & 0\end{pmatrix}\frac{d\gamma}{dR} + v^e - v^a \right\}\begin{pmatrix}\xi_1+i\eta_1\\ \xi_2+i\eta_2\end{pmatrix}. \tag{4-41}$$

It is instructive to examine one of the components provided by this equation. As an example, take

$$\frac{d\xi_1}{dR} = \mathrm{Re}(q_c)\left\{ \left( -\alpha\frac{\hbar^2}{2m}\frac{d^2\gamma}{dR^2}\right)\xi_1 \right.$$
$$+ \left( \beta\frac{\hbar^2}{2m}\left(\frac{d\gamma}{dR}\right)^2 - \beta v^e + \beta V^e_{11} + \alpha\hbar\frac{P}{m}\frac{d\gamma}{dR}\right)\eta_1$$
$$+ \left( \alpha\frac{\hbar^2}{2m}\left(\frac{d\gamma}{dR}\right)^2 - \alpha v + \alpha V^e_{22} - \beta\hbar\frac{P}{m}\frac{d\gamma}{dR}\right)\xi_2$$
$$\left. + \left( -\beta\frac{\hbar^2}{2m}\frac{d^2\gamma}{dR^2}\right)\eta_2 \right\} \tag{4-42}$$

The adiabatic equations are not simplified nearly as much by a change in phase when moving into the time domain as the diabatic equations were. The cofactor of $d\chi/dR$ in the diabatic equations was just a number (see Equation (4-9) ) while the cofactor in the adiabatic case is the matrix **C**. Add to this the fact that **C** has two singularities and it becomes impossible to find a genuinely simplifying phase change that provides meaningful results. Although the adiabatic equations that remain are more demanding, the fact that more of the information in the equation for nuclear motion is utilized may (in some cases) turn out to be useful.

The adiabatic effective potential $v^a$ is derived (as in the elastic and diabatic cases) using Equations (2-20) and (2-21). Identify the collection of terms operating on $\chi$ in Equation (4-32) as **F**. Left multiply that equation by $\chi^+$,

$$
\begin{aligned}
&- \frac{\hbar^2}{2m}\, \chi^+ \frac{d^2\chi}{dR^2} - \frac{\hbar^2}{m}\, \chi^+ \begin{pmatrix} 0 & 1 \\ -1 & 0 \end{pmatrix} \frac{d\gamma}{dR} \frac{d\chi}{dR} - i\, \hbar\, \frac{P}{m}\, \chi^+ \frac{d\chi}{dR} \\
&+ \frac{\hbar^2}{2m} \left(\frac{d\gamma}{dR}\right)^2 \chi^+\chi - \frac{\hbar^2}{2m}\, \chi^+ \begin{pmatrix} 0 & 1 \\ -1 & 0 \end{pmatrix} \frac{d^2\gamma}{dR^2}\, \chi \\
&- \frac{i\hbar}{m}\, P\, \chi^+ \begin{pmatrix} 0 & 1 \\ -1 & 0 \end{pmatrix} \frac{d\gamma}{dR}\, \chi \\
&- i\, \frac{\hbar}{2m} \frac{dP}{dR}\, \chi^+\chi + \frac{P^2}{2m}\, \chi^+\chi + \chi^+ v^a \chi - E\, \chi^+\chi = 0 \quad . \qquad (4\text{-}43)
\end{aligned}
$$

Take the adjoint of the result,

$$- \frac{\hbar^2}{2m} \frac{d^2\chi^+}{dR^2} \chi - \frac{\hbar^2}{m} \frac{d\chi^+}{dR} \begin{pmatrix} 0 & -1 \\ 1 & 0 \end{pmatrix} \frac{d\gamma}{dR} \chi + i \hbar \frac{P}{m} \frac{d\chi^+}{dR} \chi$$

$$+ \frac{\hbar^2}{2m} \left(\frac{d\gamma}{dR}\right)^2 \chi^+\chi - \frac{\hbar^2}{2m} \chi^+ \begin{pmatrix} 0 & -1 \\ 1 & 0 \end{pmatrix} \frac{d^2\gamma}{dR^2} \chi$$

$$+ \frac{i\hbar}{m} P \chi^+ \begin{pmatrix} 0 & -1 \\ 1 & 0 \end{pmatrix} \frac{d\gamma}{dR} \chi$$

$$+ i \frac{\hbar}{2m} \frac{dP}{dR} \chi^+\chi + \frac{P^2}{2m} \chi^+\chi + \chi^+ v^a \chi - E \chi^+\chi = 0 \quad . \qquad (4\text{-}44)$$

Add these last two equations and divide by $2\chi^+\chi$ to get

$$E = \frac{P^2}{2m} + u^a(R,P) \quad ;$$

$$v^a(R,P) = (\chi^+\chi)^{-1} \left\{ - \frac{\hbar^2}{2m} \left( \chi^+ \frac{d^2\chi}{dR^2} + \frac{d^2\chi^+}{dR^2} \chi \right) \right.$$

$$+ i \hbar \frac{P}{m} \left[ \frac{d\chi^+}{dR} \chi - \chi^+ \frac{d\chi}{dR} \right]$$

$$+ \frac{\hbar^2}{2m} \left(\frac{d\gamma}{dR}\right)^2 \chi^+\chi + \chi^+ v^a \chi$$

$$\left. + \frac{i\hbar}{m} P \chi^+ \begin{pmatrix} 0 & -1 \\ 1 & 0 \end{pmatrix} \frac{d\gamma}{dR} \chi \right\} \qquad (4\text{-}45)$$

Using the short-wavelength approximation gives

$$u^a(R,P) = (\chi^+\chi)^{-1} \left\{ \frac{\hbar^2}{2m} \left(\frac{d\gamma}{dR}\right)^2 \chi^+\chi + \chi^+ v^a \chi \right.$$

$$\left. + \frac{i\hbar}{m} P \chi^+ \begin{pmatrix} 0 & -1 \\ 1 & 0 \end{pmatrix} \frac{d\gamma}{dR} \chi \right\} \qquad (4\text{-}46)$$

Unlike the diabatic effective potential, the adiabatic effective potential does not (after the short-wavelength approximation is applied) reduce to a function of R, but remains a function of R and P. This has a profound effect on the equations of motion. In the usual case E is identified as H(R,P) and, see Equation (4-20),

$$dR/dt = \partial H/\partial P = P/m \quad . \tag{4-47}$$

When $v=v(R,P)$ however,

$$dR/dt = \partial H/\partial P = P/m + \partial v/\partial P \ . \tag{4-48}$$

The actual position of the system is still given by $\int dt\,(dR/dt)$ so the kinematic momentum is $m(dR/dt) \neq P$. What is P? For this particular set of equations it suffices to define P as dS/dR,

$$P = dS/dR \tag{4-49}$$

It is now convenient to give $v^a$, dR/dt, and dP/dt explicitly:

$$v^a(R,P) = (X^+X)^{-1} \left\{ \frac{\hbar^2}{2m} \left(\frac{d\gamma}{dR}\right)^2 X^+X + X^+v^aX \right.$$

$$\left. + \frac{i\hbar}{m} P\, X^+ \begin{pmatrix} 0 & -i \\ i & 0 \end{pmatrix} \frac{d\gamma}{dR} X \right\}$$

$$= \left(\frac{1}{\xi_1^2 + \eta_1^2 + \xi_2^2 + \eta_2^2}\right) \left\{ \left( \frac{\hbar^2}{2m} \left(\frac{d\gamma}{dR}\right)^2 + V^a_{11} \right) ( \xi_1^2 + \eta_1^2 ) \right.$$

$$+ \left( \frac{\hbar^2}{2m} \left(\frac{d\gamma}{dR}\right)^2 + V^a_{22} \right) ( \xi_2^2 + \eta_2^2 )$$

$$\left. + 2 \frac{\hbar}{m} P \frac{d\gamma}{dR} (\xi_1\eta_2 - \xi_2\eta_1) \right\} \quad , \qquad (4\text{-}50)$$

where we have used that

$$\frac{i\hbar}{m} P X^+ \begin{pmatrix} 0 & -1 \\ 1 & 0 \end{pmatrix} \frac{d\gamma}{dR} X$$

$$= \frac{i\hbar}{m} P \frac{d\gamma}{dR} (-X_1^* X_2 + X_2^* X_1)$$

$$= \frac{i\hbar}{m} P \frac{d\gamma}{dR} (-\xi_1\xi_2 - \eta_1\eta_2 - i\xi_1\eta_2 + i\xi_2\eta_1 + \xi_2\xi_1 + \eta_2\eta_1$$

$$+ i\xi_2\eta_1 - i\xi_1\eta_2)$$

$$= 2 \frac{\hbar}{m} P \frac{d\gamma}{dR} (\xi_1\eta_2 - \xi_2\eta_1) \qquad (4\text{-}51)$$

is real!

Despite the additional term in $dR/dt$, it is still fairly compact,

$$dR/dt = \partial H/\partial P = P/m + \partial U/\partial P$$

$$= (P/m) + 2 \frac{\hbar}{m} \frac{d\gamma}{dR} (\xi_1\eta_2 - \xi_2\eta_1) \quad . \qquad (4\text{-}52)$$

The adiabatic expression for $dP/dt$ contains terms with $d\xi_n/dR$ and $d\eta_n/dR$ that do not cancel each other (see Equations (4-18) and (4-20) and the surrounding text) and it is fairly lengthy,

$$dP/dt = -\partial H/\partial R = -\partial v^a/\partial R$$

$$= \left(\frac{1}{\xi_1^2 + \eta_1^2 + \xi_2^2 + \eta_2^2}\right) \left\{ \left[ \frac{\hbar^2}{m} \frac{d^2\gamma}{dR^2} + \frac{dV^s_{11}}{dR} \right] ( \xi_1^2 + \eta_1^2 ) \right.$$

$$+ \left[ \frac{\hbar^2}{m} \frac{d^2\gamma}{dR^2} + \frac{dV^s_{22}}{dR} \right] ( \xi_2^2 + \eta_2^2 )$$

$$+ 2 \frac{\hbar}{m} P \frac{d^2\gamma}{dR^2} (\xi_1\eta_2 - \xi_2\eta_1)$$

$$+ \left[ \frac{\hbar^2}{2m} \left(\frac{d\gamma}{dR}\right)^2 + V^a_{11} \right] 2 \left( \xi_1 \frac{d\xi_1}{dR} + \eta_1 \frac{d\eta_1}{dR} \right)$$

$$+ \left[ \frac{\hbar^2}{2m} \left(\frac{d\gamma}{dR}\right)^2 + V^a_{22} \right] 2 \left( \xi_2 \frac{d\xi_2}{dR} + \eta_2 \frac{d\eta_2}{dR} \right)$$

$$+ 2 \frac{\hbar}{m} P \frac{d\gamma}{dR} \left(\xi_1 \frac{d\eta_2}{dR} + \frac{d\xi_1}{dR} \eta_2 - \xi_2 \frac{d\eta_1}{dR} - \frac{d\xi_2}{dR} \eta_1\right)$$

$$\left. - v^s\, 2 \left(\xi_1 \frac{d\xi_1}{dR} + \eta_1 \frac{d\eta_1}{dR} - \xi_2 \frac{d\xi_2}{dR} - \eta_2 \frac{d\eta_2}{dR} \right) \right\} \quad (4\text{-}53)$$

Since $X_n = \xi_n + i\eta_n$ it is tempting to neglect terms in $d\xi_n/dR$ and $d\eta_n/dR$ using the short-wavelength approximation. Actual calculations reveal that this is inaccurate. Apparently the short wavelength approximation doesn't apply in this situation

Changing to the t variable, since the adiabatic equations weren't as simplified by changing the phase, the adiabatic analogue of Equation (4-15) is

$$\left( \frac{\hbar}{i} \frac{d}{dt} + \bar{H}^{a}(t) \right) A(t) = 0 \qquad (4\text{-}54)$$

$$\bar{H}^{a} = \frac{\hbar}{i} \frac{dR}{dt} C^{-1} \left\{ \frac{\hbar^2}{2m} \begin{pmatrix} 1 & 0 \\ 0 & 1 \end{pmatrix} \left(\frac{d\gamma}{dR}\right)^2 - \frac{\hbar^2}{2m} \begin{pmatrix} 0 & 1 \\ -1 & 0 \end{pmatrix} \frac{d^2\gamma}{dR^2} \right.$$

$$\left. - i \hbar \frac{p}{m} \begin{pmatrix} 0 & 1 \\ -1 & 0 \end{pmatrix} \frac{d\gamma}{dR} - V^{e} + V^{a} \right\} . \qquad (4\text{-}55)$$

Since $\bar{H}^{a}$ is not Hermitian $A^{+}A$ is not automatically conserved,

$$\frac{d(A^{+}A)}{dt} \neq 0 . \qquad (4\text{-}56)$$

Conservation of probability is achieved through normalization The normalized components, $X_n'$ and $Y_n'$, are

$$X_n' = X_n/(X_1^2+Y_1^2+X_2^2+Y_2^2)^{1/2} \quad ;$$

$$Y_n' = Y_n/(X_1^2+Y_1^2+X_2^2+Y_2^2)^{1/2} \quad , \qquad (4\text{-}57)$$

so the total normalized probability is one,

$$X_1'^2 + Y_1'^2 + X_2'^2 + Y_2'^2 = 1 \qquad (4\text{-}58)$$

It is clear from the material presented in this section that there are a number of drawbacks to applying the adiabatic equations. First, there are the singularities. Attempting to deal with the singularities leads to other complications. Not only is there a more complicated set of equations to actually solve, but there is c to deal with. It must somehow be demonstrated that the selected value of c is reasonable. No matter how this is done it requires additional work. Coefficients that require normalization to conserve probability further complicate matters. The complicated adiabatic equations are clearly less hardy and resilient than the simple symmetric diabatic ones and should almost always be avoided. On the other hand being able to solve the adiabatic equations represents another capability, another tool as it were, in the dynamicists' methodology. Somewhere in the great variety of situations, the adiabatic representation is bound to find appropriate application.

## 4-4. The Model Potentials

Three model matrix potentials were selected to represent the general situation: a noncrossing potential (NC), a potential whose diagonal elements cross in the repulsive region (CR), and a potential whose diagonal elements cross in the attractive region (CA). The noncrossing potential was formed by adding the terms in the upper curve of CR rather than taking their difference. The resulting curves are separated enough to give transition probabilities that could be too small to serve as a useful example. To compensate, the coupling parameter $A_{12}$ was chosen equal to 0.05. The NC potential still remains something of a challenge to the sensitivity of the calculations. An example of a noncrossing potential is $He^+ + H$ (Zygelman et al., 1989). Presumably there are other $A^+ + B$ systems with this same kind of potential. The NC case has been discussed in the literature under the name Demkov's model.

The CR potential itself was taken from Currier and Herman (Currier and Herman, 1985). Ronald McCarroll, in a paper on ion atom collisions (McCarroll, 1980), depicts several potentials that cross in the repulsive region. The $N^{3+} + H$ and $CH^{+4}$ potential energy curves both have such crossings (see Figs. 7-2 and 9-9 in McCarroll's article). Other examples of his cross more or less in the repulsive region.

The CA potential is from Sawada and Metiu (Sawada and Metiu, 1986). This is the type of potential (for simple systems anyway) most frequently reported on in the literature. The entire class of $M + X$ (where M is a metal and X is a halogen) interactions has a characteristic potential that crosses in the attractive region. Similar crossings arise in atom-molecule systems such as $M + X_2$ and $M + NO$, $O_2$, $SF_6$, - - - and many others (Baede, 1975).

Even relatively simple scattering events occasionally require a multitude of surfaces to describe them adequately. The example shown next (Olson and Garrison, 1985) has fewer potential curves than one would like to handle comfortably.

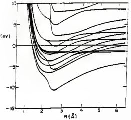

Adiabatic potentials for the sodium atom interacting with the W(110) surface (Olson and Garrison, 1985)

The following tables give all the relevant information for each model potential. In addition to the tables are figures giving diabatic (solid lines) and adiabatic (dashed lines) pictures of each of them. Accompanying the potential figures are graphs of the transformation angles $\gamma$.

TABLE 4-1. NONCROSSING POTENTIAL (NC)

equations:

$$V_{11} = A_{11} \exp(-\alpha_{11} R)$$

$$V_{22} = A_{22} \exp(-\alpha_{22} R) + B_{22} \exp(-\beta_{22} R) + V_{20}$$

$$V_{12} = A_{12} [ 1 - \tanh[ \alpha_{12} ( R - R_{12} )] ]$$

---

parameters:*

$A_{11} = 3.0$ H. ; $A_{12} = .05$ H. ; $A_{22} = 3.0$ H.

$\alpha_{11} = 3.0$ Bohr$^{-1}$ ; $\alpha_{12} = 2.0$ Bohr$^{-1}$ ;

$\alpha_{22} = 3.0$ Bohr$^{-1}$ ; $B_{22} = 1.0$ H.

$R_{12} = 2.0$ Bohr ; $V_{20} = 0.1$ H.

* atomic units (H =Hartree)

TABLE 4-2 POTENTIAL WITH CROSSING IN REPULSIVE REGION (CR)

equations:

$$V_{11} = A_{11} \exp(-\alpha_{11} R)$$

$$V_{22} = A_{22} \exp(-\alpha_{22} R) - B_{22} \exp(-\beta_{22} R) + V_{20}$$

$$V_{12} = A_{12} \{ 1 - \tanh( \alpha_{12} ( R - R_{12} ))\} $$

parameters.*

$A_{11}$ = 3.0 H. ; $A_{12}$ = .01 H. ; $A_{22}$ = 3.0 H.

$\alpha_{11}$ = 3.0 Bohr$^{-1}$ ; $\alpha_{12}$ = 2.0 Bohr$^{-1}$ ;

$\alpha_{22}$ = 3.0 Bohr$^{-1}$ ; $B_{22}$ = 1.0 H.

$R_{12}$ = 2.0 Bohr , $V_{20}$ = 0.1 H.

* atomic units

TABLE 4-3. POTENTIAL WITH CROSSING IN ATTRACTIVE REGION (CA)

equations.

$$V_{11} = U_0 \{ \exp[-2\alpha(R-R_0) + 2 \exp[-\alpha(R-R_0)] \} - (\epsilon/2)$$

$$V_{22} = U_0 \{ \exp[-2\alpha(R-R_0) - 2 \exp[-\alpha(R-R_0)] \} + (\epsilon/2)$$

$$V_{12} = \frac{B\epsilon}{2} \exp[-\alpha^2 (R-R_x)^2 ]$$

parameters:*

$U_0$ = .025 H. ; $\epsilon$ = .005 H. ; $\alpha$ = 0.4 Bohr$^{-1}$

B = 0.3** ; $R_0$ = 5.0 Bohr ; $R_x$ = 12.49 Bohr

* atomic units (H.= Hartree)

** unitless

Figure 4-1. Noncrossing Potential (NC)

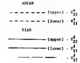

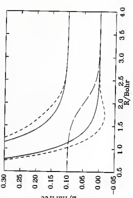
E/Hartree
0.30
0.25
0.20
0.15
0.10
0.05
0.00
−0.05
R/Bohr
0.5
1.0
1.5
2.0
2.5
3.0
3.5
4.0

Figure 4-2. Conversion Angle, $\gamma$, (NC)

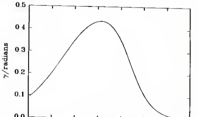
γ/radians
0.0
0.1
0 2
0 3
0 4
0.5
0 0
0.5
1 0
1.5
2 0
2 5
3.0
3 5
R/Bohr

Figure 4-3. Potential with Crossing in Repulsive Region (CR)

ADIAB

- - - - - - - (upper) - $V^a_{22}$

- - - - - - - (lower) - $V^a_{11}$

DIAB

——————— (upper) - $V^d_{22}$

——————— (lower) - $V^d_{11}$

—— —— —— - $V^d_{12}$

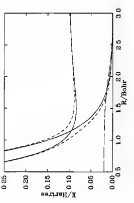
E/Hartree
0.25
0.20
0.15
0.10
0.05
0.00
R/Bohr
0.5
1.0
1.5
2.0
2.5
3.0

Figure 4-4. Conversion Angle, $\gamma$, (CR)

It changes rapidly in the crossing region; otherwise it remains constant

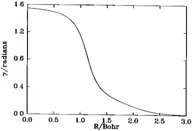
1.6
1.2
0.6
0.4
0.0
$\gamma$/radians
0.0
0.5
1.0
1.5
2.0
2.5
3.0
R/Bohr

Figure 4-5A Potential with Crossing in Attractive Region (CA)

ADIAB

‐ ‐ ‐ ‐ ‐ ‐ ‐ (upper) - $V^a_{22}$

‐ ‐ ‐ ‐ ‐ ‐ ‐ (lower) - $V^a_{11}$

DIAB

———— (upper) - $V^d_{22}$

———— (lower) - $V^d_{11}$

—— —— —— $V^d_{12}$

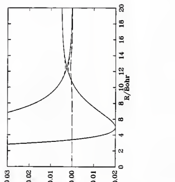
E/Hartree
0.03
0.02
0.01
0.00
−0.01
−0.02
R/Bohr
0
2
4
6
8
10
12
14
16
18
20

Figure 4-58 Potential with Crossing in Attractive Region (CA)

ADIAB

- - - - - - - (upper) - $V_{22}^{a}$

- - - - - - - (lower) - $V_{11}^{a}$

DIAB

———— (upper) - $V_{22}^{d}$

———— (lower) - $V_{11}^{d}$

— — — - $V_{12}^{d}$

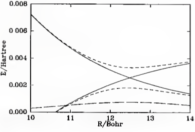
0.008
0.006
0.004
0.002
0.000
E/Hartree
10
11
12
13
14
R/Bohr

Figure 4-6. Conversion Angle, $\gamma$, (CA)

As with CR, it changes rapidly in the crossing region; otherwise it remains constant.

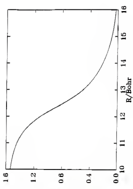
γ/radians
1.6
1.2
0.8
0.4
0.0
10
11
12
13
14
15
16
R/Bohr

# CHAPTER V

## COMPUTATIONAL ASPECTS-- ADDITIONAL DETAILS OF THE CALCULATION

### 5-1. Introduction

This chapter is about software development and implementation. The second and third sections give analytical expressions for the various derivatives required in the SCE programs. There are the first two derivatives of $\gamma$, required by the adiabatic programs. The first two derivatives of the diabatic potential elements are needed to get the derivatives of $\gamma$. The first derivatives of the diabatic and adiabatic potential elements are needed as well for SCE DIAB and SCE ADIAB respectively. An alternative to taking the analytical derivative directly is to spline fit the function and use the coefficients of the spline fit function to form numerical derivatives. This is a natural way to check the analytical derivatives. Another way is to use the derivatives as part of some function that can be integrated numerically by the differential equation solving program (in this case DE). This has the advantage of simultaneously checking the solver itself. Both methods were used.

The fourth section first explains how insights about the behavior of classical trajectories (energy conservation, continuity, etc.) could be used to develop the adiabatic eikonal programs in a piecemeal fashion. Starting with constant coefficients and a simple makeshift effective potential, more complex and realistic expressions were added bit by bit until the formulae developed in Section 4-3 were entirely included in the program and producing reasonable looking trajectories. The fourth section goes on to show that the various effective potentials behaved reasonably, thus reinforcing the validity of the program. Since the diabatic equations, developed at an earlier date, were already known to produce reasonable results, much consideration was given throughout to similarities in behavior demonstrated by the adiabatic equations.

The fifth and sixth sections are devoted to operational details of the exact (LOGDERIV) and eikonal (SCE) programs respectively. They are pretty direct and self-explanatory.

## 5-2. The Derivatives of $\gamma$

In addition to the transformation angle $\gamma$, Equation (4-2), the adiabatic equations for the coefficients require the first and second derivatives of $\gamma$ with respect to the internuclear separation R (see Equation (4-55) ).

Since $\gamma$ is a function of the diabatic potential elements $V_{11}^{d}$, $V_{22}^{d}$, and $V_{12}^{d}$, the first and second derivatives of these elements go into the first and second derivatives of $\gamma$. A simple hierarchy of derivatives can be constructed for the NC potential:

$$V_{11}^{d} = A_{11} \exp( -\alpha_{11} R)$$

$$\frac{dV_{11}^{d}}{dR} = -\alpha_{11} V_{11}^{d}$$

$$\frac{d^2V_{11}^{d}}{dR^2} = \alpha_{11}^{2} V_{11}^{d}$$

$$V_{221}^{d} = A_{22} \exp( -\alpha_{22} R) \; ; \quad V_{222}^{d} = B_{22} \exp( -\beta_{22} R)$$

$$V_{22}^{d} = V_{221}^{d} + V_{222}^{d} + V_{20}$$

$$\frac{dV_{22}^{d}}{dR} = -\alpha_{22} V_{221}^{d} - \beta_{22} V_{222}^{d}$$

$$\frac{d^2V_{22}^{d}}{dR^2} = \alpha_{22}^{2} V_{221}^{d} + \beta_{22}^{2} V_{222}^{d}$$

$$T_{12} = \tanh[ \alpha_{12} (R - R_{12})]$$

$$V_{12}^{d} = A_{12} (1 - T_{12})$$

$$\frac{dV_{12}^{d}}{dR} = -\alpha_{12} A_{12} (1 - T^{2})$$

$$\frac{d^2V_{12}^{d}}{dR^2} = 2 \alpha_{12}^{2} A_{12} T (1 - T^{2}) \quad . \tag{5-1}$$

A convenient expression for the first derivative of $\gamma$ was found in an article by Evans, Cohen, and Lane (1971). Taking the derivative of this gave $d^2\gamma/dR^2$ .

$$\gamma = \frac{1}{2} \tan^{-1}\left(\frac{2V_{12}^d}{V_{22}^d - V_{11}^d}\right)$$

$$U_-^d = \frac{1}{2} (V_{22}^d - V_{11}^d)$$

$$\frac{dU_-^d}{dR} = \frac{1}{2} \left(\frac{dV_{22}^d}{dR} - \frac{dV_{11}^d}{dR}\right)$$

$$\frac{d^2U_-^d}{dR^2} = \frac{1}{2} \left(\frac{d^2V_{22}^d}{dR^2} - \frac{d^2V_{11}^d}{dR^2}\right)$$

$$u^2 = (U_-^d)^2 + (V_{12}^d)^2$$

$$\frac{d(u^2)}{dR} = 2U_-^d \frac{dU_-^d}{dR} + 2V_{12}^d \frac{dV_{12}^d}{dR}$$

$$\frac{d\gamma}{dR} = \frac{1}{2u^2} \left(U_-^d \frac{dV_{12}^d}{dR} - V_{12}^d \frac{dU_-^d}{dR}\right)$$

$$\frac{d^2\gamma}{dR^2} = \frac{d\gamma}{dR} \frac{1}{u^2} \frac{d(u^2)}{dR}$$

$$- \frac{1}{2u^2} \left[\frac{dU_-^d}{dR} \frac{dV_{12}^d}{dR} + U_-^d \frac{d^2V_{12}^d}{dR^2} - \frac{dV_{12}^d}{dR} \frac{dU_-^d}{dR} - V_{12}^d \frac{d^2U_-^d}{dR^2}\right]$$

(5-2)

These expressions are certainly complicated enough to merit some checking and testing. The first step in the testing is accomplished by evaluating the function along with its analytical derivatives over the interesting range of R. The function values, along with the values of R, are input to an International Mathematics and Statistics Library* subroutine, ICSEVU (ICSCCU, 1978), that treats them as data points and forms a cubic-spline fit to the original function. The coefficients of the spline fit function are used to provide numerical derivatives to a high degree of accuracy (IMSL subroutine DCSEVU (DCSEVU, 1981) ). The analytical derivatives are compared to these. The testing follows the hierarchy presented above: first each potential element and its derivatives are tested, then $\gamma$ and its derivatives. Figures 5-1, 5-2, and 5-3 show the final results of this testing for the NC potential. The derivatives were tested for all three potentials until analytical and numerical values were as graphically indistinguishable as in the NC figures. The equations for the CR potential are the same as for the NC except that $B_{22}$ is used in place of $-B_{22}$ and the coupling parameter $A_{12}$ is 0.01 instead of 0.05

Following are the derivatives for the CR potential:

$$T_1 = U_0 \exp[-2\alpha(R - R_0)] \;;\quad T_2 = U_0\, 2 \exp[-\alpha\, (R - R_0)]$$

---

* Information on IMSL software may be obtained at 7500 Bellaire Blvd., Houston TX 77036

$$\frac{dT_1}{dR} = -2\alpha T_1 \qquad , \qquad \frac{dT_2}{dR} = -\alpha T_2$$

$$\frac{d^2T_1}{dR^2} = 4\alpha T_1 \qquad , \qquad \frac{d^2T_2}{dR^2} \alpha^2 T_2$$

$$V^d_{11} = T_1 + T_2 - \frac{\varepsilon}{2}$$

$$\frac{dV^d_{11}}{dR} = \frac{dT_1}{dR} + \frac{dT_2}{dR}$$

$$\frac{dV^2_{11}}{dR^2} = \frac{d^2T_1}{dR^2} + \frac{d^2T_2}{dR^2}$$

$$V^d_{22} = T_1 - T_2 + \frac{\varepsilon}{2}$$

$$\frac{dV^d_{22}}{dR} = \frac{dT_1}{dR} - \frac{dT_2}{dR}$$

$$\frac{dV^2_{22}}{dR^2} = \frac{d^2T_1}{dR^2} - \frac{d^2T_2}{dR^2}$$

$$V^d_{12} = \frac{\beta\varepsilon}{2} \exp[-\alpha^2 (R - R_x)^2]$$

$$\frac{dV^d_{12}}{dR} = -2\alpha^2(R - R_x)\, V^d_{12}$$

$$\frac{d^2V^d_{12}}{dR^2} = -2\alpha^2 (R - R_x) \frac{dV^d_{12}}{dR} - 2\alpha^2 V^d_{12} \qquad (5\text{-}3)$$

The analytical derivatives of $\gamma$ were also used in an entirely different kind of testing. In addition to evaluating $\gamma$ directly, Equation (4-2), there is

$$\gamma = \int dt \, \frac{d\gamma}{dR} \frac{dR}{dt} \tag{5-4}$$

If everything is working as it should the differential equation solver (DE) will integrate dγ/dR dR/dt over time and obtain the same value of γ as gotten from Equation (4-2). If the expressions for either dγ/dR or dR/dt are somehow incorrect or DE is not operating correctly, the γ's will not match. This is a very sophisticated test that can help locate a number of different problems. It is even more powerful when coupled to a test for dγ/dR. dγ/dR is evaluated analytically and also from

$$\frac{d\gamma}{dR} = \int dt \, \frac{d^2\gamma}{dR^2} \frac{dR}{dt} \quad . \tag{5-5}$$

If, for instance, the test for γ succeeded while the test for dγ/dR failed, it would be evident that $d^2\gamma/dR^2$ was incorporated incorrectly into the program. Figure 5-4 shows typical results from this type of testing. Usually graphs would not be necessary, one would simply monitor the numbers along with other intermediate results as the calculation preceeded. This testing does require the solving of two additional differential equations. Once the program tests correctly they are removed to save computer time.

## 5-3. Derivatives of the Adiabatic Potential Elements

From Equation (4-1) come the adiabatic potential elements,

$$V^a_{11} = \cos(\gamma)\ [\ \cos(\gamma)\ V^d_{11} - \sin(\gamma)\ V^d_{12}\ ]$$

$$-\sin(\gamma)\ [\ -\sin(\gamma)\ V^d_{22} + \cos(\gamma)\ V^d_{12}\ ]\quad ;$$

$$V^a_{22} = \sin(\gamma)\ [\ \sin(\gamma)\ V^d_{11} + \cos(\gamma)\ V^d_{12}\ )$$

$$+\cos(\gamma)\ [\ \sin(\gamma)\ V^d_{12} + \cos(\gamma)\ V^d_{22}\ ]\quad . \qquad (5\text{-}6)$$

The time derivative of P, Equation (4-22), requires the first derivatives of these elements with respect to R,

$$\frac{dV^a_{11}}{dR} = -\sin(\gamma)\ \frac{d\gamma}{dR}\ [\ \cos(\gamma)\ V^d_{11} - \sin(\gamma)\ V^d_{12}\ ]$$

$$+\cos(\gamma)\ [\ -\sin(\gamma)\ \frac{d\gamma}{dR}\ V^d_{11} + \cos(\gamma)\ \frac{dV^d_{11}}{dR}$$

$$-\cos(\gamma)\ \frac{d\gamma}{dR}\ V^d_{12} - \sin(\gamma)\ \frac{dV^d_{12}}{dR}\ ]$$

$$-\cos(\gamma)\ \frac{d\gamma}{dR}\ [\ -\sin(\gamma)\ V^d_{22} + \cos(\gamma)\ V^d_{12}\ )$$

$$-\sin(\gamma)\ [\ -\cos(\gamma)\ \frac{d\gamma}{dR}\ V^d_{22} - \sin(\gamma)\ \frac{dV^d_{22}}{dR}$$

$$-\sin(\gamma)\ \frac{d\gamma}{dR}\ V^d_{12} + \cos(\gamma)\ \frac{dV^d_{12}}{dR}\ ]\quad ;$$

$$\frac{dV^{a}_{22}}{dR} = \cos(\gamma)\,\frac{d\gamma}{dR}\,[\,\sin(\gamma)\,V^{d}_{11} + \cos(\gamma)\,V^{d}_{12}\,]$$

$$+\sin(\gamma)\,[\,\cos(\gamma)\,\frac{d\gamma}{dR}\,V^{d}_{11} + \sin(\gamma)\,\frac{dV^{d}_{11}}{dR}$$

$$-\sin(\gamma)\,\frac{d\gamma}{dR}\,V^{d}_{12} + \cos(\gamma)\,\frac{dV^{d}_{12}}{dR}\,)$$

$$-\sin(\gamma)\,\frac{d\gamma}{dR}\,[\,\cos(\gamma)\,V^{d}_{22} + \sin(\gamma)\,V^{d}_{12}\,)$$

$$+\cos(\gamma)\,[\,-\sin(\gamma)\,\frac{d\gamma}{dR}\,V^{d}_{22} + \cos(\gamma)\,\frac{dV^{d}_{22}}{dR}$$

$$+\cos(\gamma)\,\frac{d\gamma}{dR}\,V^{d}_{12} + \sin(\gamma)\,\frac{dV^{d}_{12}}{dR}\,)\quad . \qquad (5\text{-}7)$$

While these expressions are fairly easy to derive, they are also lengthy and were tested by comparison with numerical derivatives as in the first part of the previous section. Figure 5-5 shows the results of these tests.

### 5-4. Reasonable Behavior-- Classical Trajectories and Effective Potentials

In addition to exact tests, a large part of being able to develop and work with programs like these comes from having some idea of what constitutes reasonable behavior. The differential equations for the adiabatic coefficients are extremely complicated and closely intertwined so that any small error in any of them could easily destroy the whole calculation. Trying to get these right while simultaneously developing classical trajectories from momentum-dependent potentials for the first time (for this author) proved to be impossible. The problem was broken into small pieces. As each piece was handled in what appeared to be a reasonable way the next piece was added.

The first step was to calculate trajectories from a simple momentum-dependent effective potential with constant coefficients. As no relation to any physical reality was intended any improvised potential would serve. The actual choice was

$$v = \frac{1}{2} ( V_{11}^{d} + V_{22}^{d} ) + \frac{dv}{dR} P \qquad (5\text{-}8)$$

When this calculation developed to the point where the total energy was conserved and the trajectory was continuous, R didn't increase or decrease haphazardly, the next step was taken. A single simple non-constant coefficient was added. Again, there was no need to be realistic, any simple expression for the coefficient could be used. When this new trajectory demonstrated reasonable behavior a second simple non-constant coefficient was added. Things were gradually built up in this manner until, after a week or so, all the actual (derived) expressions were in place producing what appeared to be reasonable classical trajectories. While there is no reason to reproduce this process here, understanding the approach may be useful to the reader who intends to perform these calculations. Figures 5-6 and 5-7 compare the positions and momenta for a typical trajectory obtained with SCE/AE DIAB and SCE/AE ADIAB The agreement lends credibility to the adiabatic calculations since diabatic calculations are already fairly well understood.

Another clue that the calculations are behaving reasonably can be gotten by examining the effective potentials. The non-averaged effective potential generally (at least in the asymptotic regions) reflects the transition properties of the system Suppose, for example, one were examining a 1->2 transition. As long as the transition probability remained zero the effective potential would remain equal to the ground state potential $V_{11}$. If the transition probability were to become (let us say) 0.2, $P_{21}=0.2$, the effective potential would relocate about two-tenths of the way from $V_{11}$ to $V_{22}$. If one were looking at a 2->1 transition it would locate two-tenths of the way down from the upper surface rather than two-tenths of the way up from the lower. Reasonable behavior for the averaged effective potential is quite different. Due to its symmetric nature one can expect it to remain about half way between the upper and lower surfaces at all times. Its location does not reflect the transition probabilities. These can only be gotten from the amplitudes.

Figure 5-8 shows the three effective potentials for three SCE DIAB calculations at a total energy of 1.75 Hartree. The bottom one is for an SCE/EF 1->2 calculation. Consulting Figure 6-2 reveals that $P_{21}$ (from the 1->2 calculation) at this energy is extremely small. Accordingly, the effective potential stays close to $V_{11}^{d}$. The top curve is for an SCE/EP 2->1 calculation. Consulting Figure 6-2 again reveals that $P_{12}$ (from the 2->1 calculation) at the same energy is close to 0.2, $P_{12}=0.2$. The effective potential in this case goes in at the $V_{22}^{d}$ level but comes out about two-tenths of the way down. Finally, the SCE/AEP DIAB averaged effective potential goes in and comes out precisely half way between the upper and lower surfaces. Figure 5-9 shows the same information for the SCE/AEP ADIAB calculation. (The appropriate transition probabilities may be obtained from Figure 6-3.) The remarkable agreement with the diabatic calculations once again reinforces the credibility of the adiabatic calculations.

On the whole, the effective potentials do behave reasonably for both cases. The only real difference is that the outbound adiabatic averaged effective potential is not generally precisely half way between the two surfaces. This is entirely an effect of passing through the singularity at the turning point. To prove this, increase $\varepsilon$ to the point where the singularity isn't sensed by the equations, and the averaged effective potential will remain at the mean value (even though the coefficients themselves show the normal range of oscillation) Fortunately, because of the way the acceptable values of the coefficients are selected, this erstwhile imperfection has no effect on the calculation.

## 5-5. Exact Calculations--
## Using LOGDERIV

This work uses a number of results for comparison purposes that are produced by calculations from exact methods. These methods do not in general use the time dependent equations. The particular one selected for this project, the log derivative method, is well understood and widely used and will not be explained here. Interested readers are referred to Lawrence Relyea's doctoral dissertation (Relyea, 1980), an article by Johnson (Johnson, 1973), along with the host of other references found in current literature. The program itself, LOGDERIV, was written by Dr. Relyea in 1977. It requires only a few input parameters and is extremely easy to use. The following tables summarize input for the three model potentials (an explanation follows Table 5-1). In fact, a wide variety of forms for the output also require some selection at the input level.

Table 5-1. Input for LOGDERIV - NC and EC Potentials

E =
REDMAS = 1.0 AMU
Y0(I) = 0.0
LMIN = LMAX = 0.0
V1 = V2 = V3 = V5 = V6 = V7 = V8 = V9 = V10 = 0.0
V4 = 2.0 Bohr
EPS(1) = 0.0 Hartree ; EPS(2) = 0.1 Hartree
ELOST(I) = 0.0 Hartree
H(1) = H(2) = 0.001 Bohr
XMIN = -5.0 Bohr ; XMAX = 20.0 Bohr
NCHN = 2
NB = 1 ; NELOST = 1 ; ISFY = 1 ; IVTYPE = 17

E is the total energy. It is left blank here because different ranges were used for different calculations.

REDMAS is the reduced mass of the system.

Y0(I) is the initial value of the *Ith* wave function.

LMIN and LMAX refer to the minimum and maximum values of the angular momentum quantum number, presumed for these calculations to be zero

V1 to V10 are potential parameters. Since the present potentials were added to the existing program these weren't needed. V4 is, however, a characteristic length used by the program itself for locating turning points. Generally the location of a potential minimum is used for V4. This needn't be exact.

EPS(I) gives the asymptotic energy of the Ith potential surface. In the usual case the lower surface is at the zero of energy, EPS(1) = 0.0 hartree. In that case EPS(2) gives the separation of the two surfaces.

ELOST(I) represents the energy lost with the Ith electron. No electrons are lost in these calculations.

H(I) is the stepsize used for the calculation on the Ith surface. The value given, 0.001 bohr, small as it may seem, is the largest value at which the calculations consistently converged. This is important because it increases the computer time required by this method.

XMIN and XMAX represent the minimum and maximum values of the internuclear separation used in the calculation. Probably a little smaller value of XMAX could have been used, but not much.

NCHN is the number of open channels.

NH is not set to one only if several values of the stepsize are used; NELOST is not set to one only if electrons are lost; ISFY is not set to one only if the S-matrix is calculated from the K-matrix rather than directly from the exact solution. Everything else starts at zero except IVTYPE, which didn't apply because new potentials were inserted.

Table 5-2. Input for LOGDERIV - CA Potential

```
E =

REDMAS = 22.991 AMU

Y0(I) = 0.0

LMIN = LMAX = 0.0

V1 = V2 = V3 = V5 = V6 = V7 = V8 = V9 = V10 = 0.0

V4 = 5.0 Bohr

EPS(1) = -0.0025 Hartree   ; EPS(2) = 0.0025 Hartree

ELOST(I) = 0.0 Hartree

H(1) = H(2) = 0.001 Bohr

XMIN = -5.0 Bohr , XMAX = 30.0 Bohr

NCHN = 2

NH = 1 ; NELOST = 1 ; ISFY = 1 ; IVTYPE = 18
```

## 5-6 Eikonal Calculations-- Using DE

The eikonal calculations covered in the present work are for the most part exercises in solving sets of coupled differential equations. As previously stated, the prepackaged program DE is used for this purpose. The advantage in using DE is its ability to vary the size of the step it takes. This saves a considerable amount of computer time. Any of the eikonal programs themselves (SCE/EP DIAB or ADIAB, 1->2 or 2->1, SCE/AEP DIAB or ADIAB, NC, CR, or CA) can be divided, as far as the user is concerned, into three major parts. There is PROGRAM

MAIN, which contains the initial conditions for all the differential equations along with a few operating parameters required by DE, the calling statement to Subroutine DE, and provisions for putting the output into a desired form (graph, table, etc. ). There is Subroutine F that contains the temporal derivatives, analytical in the present case, for each equation to be solved by DE. There is Subroutine DE itself that, with the single exception discussed below (RI), needn't concern the present user. In addition to the inputs to DE one other input, the value of ε, is required for the adiabatic calculations.

Those interested in looking at an eikonal program are referred to APPENDIX B. which contains a fully commented printout of the original portions (not DE) of the code for SCE/AEP DIAB. The discussion that follows is more general.

Tables 5-3 and 5-4 show physically related input. Some explanatory material follows Table 5-3. A discussion of program related input follows Table 5-5. Finally, there is a discussion of ε.

Table 5-3. Input to DE - NC and RC Potentials

E =

RM = 1836.15 au

RI = 15.1 Bohr

VEFFI =

All of the present SCE calculations are written and performed entirely in atomic units. E is the total energy in Hartrees, left blank here (as in the last section) because its range varies with the calculation.

RI is the initial value of the internuclear separation, chosen to be in the asymptotic region of both potential surfaces and well past any crossing (or avoided crossing). RI also furnishes the cutoff value for the calculation. This is unusual in the way DE is handled. In the customary use of DE a maximum cutoff time is passed through the calling statement along with the rest of the input. This value is fixed and cannot respond to the calculation. In the present case this parameter (called TOUT) is set to some large dummy value that can never be reached. A flag, NEND, is set to zero. When the trajectory has gone through the turning point and once again reaches RI a conditional statement automatically changes NEND to one. DE has been altered so that when NEND equals one the calculation is cut off exactly as if TOUT had been reached. Notice that there is no fixed value corresponding to XMIN in LOGDERIV. The turning point of the trajectory serves this purpose naturally.

VEFFI is the initial value of the effective potential. It can take one of three values. If an SCE/EP (1->2) calculation is being performed VEFFI=V11 (V11 is the lower potential surface). If an SCE/EP (2->1) calculation is being performed VEFFI=V22 (V22 is the upper potential surface). If an SCE/AEP calculation is being performed VEFFI=(V11+V22)/2 . The initial momentum, also needed for the calculation, is PMI=SQRT[2 RM(E-VEFFI)]. Notice that the initial total energy E is not always the initial kinetic energy. It depends on which VEFFI is used.

Table 5-4. Input to DE - CA Potential

E =
RM = 42240.0 au
RI = 20.1 Bohr
VEFFI =

In addition to the above, a small number of input parameters are specifically required in the calling statement to DE:

Table 5-5. Input to DE - Program parameters

NEQN = 8 or 10
T = 0.0 au
TOUT = 10000.0 au
RELERR = 1.0E-08
ABSERR = 1.0E-08
IFLAG = 1

NEQN is simply the number of equations to be solved. In an SCE/EP calculation there is an equation for position, an equation for momentum, and four equations for the coefficients. The SCE/AEP calculation has the same items along with four additional coefficients.

T is the initial time. TOUT is the final time (in this case a dummy value).

RELERR and ABSERR are the maximum allowable relative and absolute errors. DE evaluates expressions for these errors at each step. If the resulting values are greater than RELERR or ABSERR the calculation is either terminated or an error condition will be indicated in the output. The results reported in this work have no such problems. A value of 1.0E-06 is the largest acceptable for results that converge consistently. Swaminathan and his coworkers perform calculations of this type with an error of 1.0E-07 (Swaminathan, 1987). Since the adiabatic equations are more demanding 1.0E-08 was chosen to give a little extra margin of safety. All that happens in a practical sense is that DE takes a few extra steps integrating through the turning point region.

IFLAG gives the status of the calculation. IFLAG=1 is the usual condition at the beginning of a new calculation. The user is referred to the documentation for the significance of the other values of IFLAG (Shampine and Gordon, 1975).

Finally, Figures 5-10, 5-11, and 5-12 show the stable region of $\varepsilon$ for a sample trajectory for each model potential. The smaller the value of $\varepsilon$, the more nearly the turning point region is truly singular, and the longer it takes DE to integrate through. Very small values of $\varepsilon$ use up an extraordinary amount of computer time. The object, then, is to find the largest value of $\varepsilon$ in the stable region and use it. The figures show that, at $E=1.75$ Hartree, $\epsilon=0.01$ is a reasonable choice. In fact the effects of $\epsilon$ will vary with $E$. Fortunately it turns out that this choice of $\epsilon$ is reasonable for all the energies examined in this work for the NC and CR potentials. The more reasonable choice for the CA potential at all energies is an order of magnitude smaller, $\epsilon=0.001$.

Figure 5-1. First derivatives of the diabatic potential elements (NC).

All three graphs show the analytical derivative, Equation (5-1), as the solid line. The points (+++) are obtained numerically using IMSL Subroutines (see Section 5-1).

BOTTOM GRAPH – $\frac{\partial V_{12}^{d}}{\partial R}$ vs. R

MIDDLE GRAPH – $\frac{\partial V_{22}^{d}}{\partial R}$ vs. R

TOP GRAPH – $\frac{\partial V_{11}^{d}}{\partial R}$ vs. R

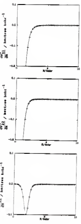

0.1
0.0
-0.1
-0.2
$\frac{dV^d_{11}}{dR}$ / hartree bohr$^{-1}$
0
5
10
R/bohr
0.1
0.0
-0.1
-0.2
$\frac{dV^d_{22}}{dR}$ / hartree bohr$^{-1}$
0
5
10
R/bohr
0.1
0.0
-0.1
$\frac{dV^d_{12}}{dR}$ / hartree bohr$^{-1}$
0
5
10
R/bohr

Figure 5-2. Second derivatives of the diabatic potential elements (NC).

All three graphs show the analytical second derivative, Equation (5-1), as the solid line. The points (+++) are obtained numerically using IMSL Subroutines (see Section 5-1).

BOTTOM GRAPH - $\frac{d^2V^d_{12}}{dR^2}$ vs. R

MIDDLE GRAPH - $\frac{d^2V^d_{22}}{dR^2}$ vs. R

TOP GRAPH - $\frac{d^2V^d_{11}}{dR^2}$ vs R

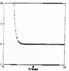
$\frac{d^2V_{22}^d}{dR^2}$ / hartree bohr$^{-2}$
0.2
0.1
0.0
-0.1
0
5
10
R/bohr

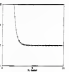
$\frac{d^2V_{11}^d}{dR^2}$ / hartree bohr$^{-2}$
0.2
0.1
0.0
-0.1
0
5
10
R/bohr

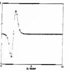
$\frac{d^2V_{12}^d}{dR^2}$ / hartree bohr$^{-2}$
0.2
0.1
-0.1
-0.2
0
5
10
R/bohr

Figure 5-3. The first and second derivatives of Y.

Both graphs show the analytical derivatives, Equation (5-2), as the solid line. The points (+++) are obtained numerically using IMSL Subroutines (see Section 5-1).

LEFT GRAPH – $\frac{dY}{dR}$ vs. R

RIGHT GRAPH – $\frac{d^2Y}{dR^2}$ vs. R

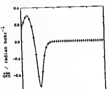
$\frac{d\gamma}{dR}$ / radian bohr$^{-1}$
0.4
0.2
0.0
-0.2
-0.4
-0.6
0
2
4
6
8
10
R/bohr

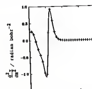
$\frac{d^2\gamma}{dR^2}$ / radian bohr$^{-2}$
1.0
0.5
0.0
-0.5
-1.0
-1.5
0
2
4
6
8
10
R/bohr

Figure 5-4. Testing DE and the derivatives of $\gamma$.

LEFT GRAPH – $\gamma$ vs time

solid line – $\gamma$ obtained directly, Equation (5-2)

points (+++) – $\gamma$ from integral of $d\gamma/dR$, Equation (5-4)

RIGHT GRAPH – $\frac{d\gamma}{dR}$ vs. time

solid line – $d\gamma/dR$ obtained directly, Equation (5-2)

points (+++) – $d\gamma/dR$ from integral of $d^2\gamma/dR^2$, Equation (5-5)

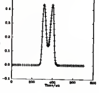
γ/radian
0.5
0.4
0.3
0.2
0.1
0.0
-0.1
0
200
400
600
800
Time/au

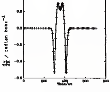
$\frac{d\gamma}{dR}$ / radian bohr$^{-1}$
0.4
0.2
0.0
-0.2
-0.4
-0.6
0
200
400
600
800
Time/au

Figure 5-5. The first derivatives of the adiabatic potential elements (NC).

Both graphs show the analytical derivatives, Equation (5.7), as the solid line. The points (+++) are obtained numerically using IMSL Subroutines (see Sections 5-1 and 5-2).

LEFT GRAPH - $\frac{dV_{11}^{a}}{dR}$ vs. R

RIGHT GRAPH - $\frac{dV_{22}^{a}}{dR}$ vs. R

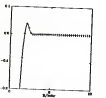
$\frac{dV^a_{11}}{dR}$ / hartree bohr$^{-1}$
0.1
0.0
-0.1
-0.2
0
5
10
R/bohr

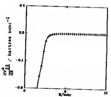
$\frac{dV^a_{22}}{dR}$ / hartree bohr$^{-1}$
0.1
0.0
-0.1
-0.2
0
5
10
R/bohr

Figure 5-6 Classical trajectory comparison- positions
NC Potential. $E = 1.75$ Hartree

R vs. time

solid line - SCE/AEP DIAB

dashed line (- -) - SCE/AEP ADIAB

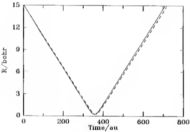
R/bohr
15
12
9
6
3
0
0
200
400
600
800
Time/au

Figure 5-7. Classical trajectory comparison- momenta
NC Potential. E = 1.75 Hartree.

P (momentum) vs time

solid line - SCE/AEP DIAB

dashed line (- -) - SCE/AEP ADIAB

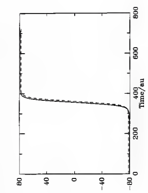
P (momentum) / bohr au$^{-1}$
80
40
0
-40
-80
0
200
400
600
800
Time/au

Figure 5-8 Typical effective potentials: SCE DIAB.
NC Potential. E = 1.75 Hartree.

upper dashed line (- -) - $V^{d}_{22}$

lower dashed line (- -) - $V^{d}_{11}$

upper solid curve - SCE/EP (2->1)

This starts in on $V^{d}_{22}$ and comes out at about 0.08 hartree

middle solid curve - SCE/AEP

This starts halfway between $V^{d}_{22}$ and $V^{d}_{11}$ and stays there

lower solid curve - SCE/EP (1->2)

This starts in on $V^{d}_{11}$ and comes out a hair higher.

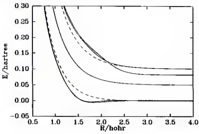
0.30
0.25
0.20
0.15
0.10
0.05
0.00
−0.05
E/hartree
0.5
1.0
1.5
2.0
2.5
3.0
3.5
4.0
R/bohr

Figure 5-9. Typical effective potentials - SCE AD1AB
NC Potential. E = 1.75 Hartree.

upper dashed line (- -) - $V_{22}^{a}$

lower dashed line (- -) - $V_{11}^{a}$

upper solid curve - SCE/EP (2->1)

This starts in on $V_{22}^{a}$ and comes out at about 0.08 hartree.

middle solid curve - SCE/AEP

This starts in halfway between $V_{22}^{a}$ and $V_{11}^{a}$

and comes out a hair higher.

lower solid curve - SCE/EP (1->2)

This starts in on $V_{11}^{a}$ and comes out a hair higher.

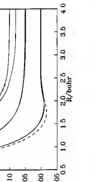
E/hartree
0.30
0.25
0.20
0.15
0.10
0.05
0.00
−0.05
R/bohr
0.5
1.0
1.5
2.0
2.5
3.0
3.5
4.0

Figure 5-10 Stable region of $\varepsilon$.
MC Potential $E = 1.75$ Hartree

$\underline{P_{tr} \text{ vs. } \varepsilon}$

upper and lower dashed lines (- -) highlight stable region

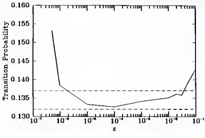
Transition Probability
0.160
0.155
0.150
0.145
0.140
0.135
0.130
$10^{-7}$
$10^{-6}$
$10^{-5}$
$10^{-4}$
$10^{-3}$
$10^{-2}$
$10^{-1}$
$\varepsilon$

Figure 5-11. Stable region of $\varepsilon$.
CR Potential. $E = 1.75$ Hartree.

$\underline{P_{tr} \text{ vs. } \varepsilon}$

upper and lower dashed lines (- -) highlight stable region

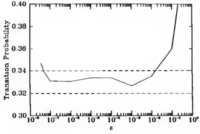
Transition Probability
0.40
0.38
0.36
0.34
0.32
0 30
$10^{-8}$
$10^{-7}$
$10^{-6}$
$10^{-5}$
$10^{-4}$
$10^{-3}$
$10^{-2}$
$10^{-1}$
$10^{0}$
ε

Figure 5-12. Stable region of $\varepsilon$.
CA Potential. E = 1.75 Hartree.

$\underline{P_{tr}\text{ vs. }\varepsilon}$

upper and lower dashed lines (- -) highlight stable region

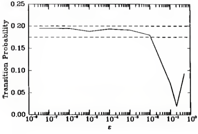
Transition Probability
0.00
0.05
0.10
0.15
0.20
0.25
$10^{-8}$
$10^{-7}$
$10^{-6}$
$10^{-5}$
$10^{-4}$
$10^{-3}$
$10^{-2}$
$10^{-1}$
$10^{0}$
$\varepsilon$

# CHAPTER VI

# NUMERICAL RESULTS

## 6-1. Introduction

This chapter is divided into four sections. The second section contains figures showing transition probability versus energy produced from EXACT and SCE/EP (DIAB and ADIAB, 1->2 and 2->1) calculations for the NC, CR, and CA potentials. Accompanying the graphs are a few observations. The third section develops the concept of the averaged effective potential and shows how it is applied. The motivation for using an average of effective potentials is to include detailed balance (microreversibility) in the calculations. Several figures accompany the explanation. The fourth section shows results (probability vs. energy) for the SCE/AEP, DIAB and ADIAB, calculations for the three model potentials. The figures in this section have two salient features. First, the diabatic and adiabatic curves are practically the same, on the scale shown they are nearly indistinguishable. This is the ideal consequence of the fact that both approaches utilize the same information. Second, there is remarkable agreement with the EXACT results. Detailed balance is a critically important attributes. Following the figures are tables summarizing the characteristics of the eikonal calculations. Portions describe how good the agreement is with EXACT calculations. Also given are averages representing the computer time involved. The chapter closes with a few remarks on the tables and their contents.

## 6-2. EXACT and SCE/EP Transition Probabilities

While the main impetus for this chapter is to describe the agreement between eikonal and exact calculations, a few additional observations will add to the reader's appreciation of the figures in this section. Figures 6-1 to 6-9 give the EXACT and SCE/EP results (transition probability versus energy) for the NC, CR, and CA potentials.*

As one goes from the NC, to the CR, to the CA potential the oscillation frequency of the probability curves increases. Moreover, in going from NC to CR the maximum for $P_{tr}$ increases as well. Both the rapidity of the oscillations and the maximum of $P_{tr}$ are related to the ratio of the coupling to the separation between the surfaces. The larger the ratio the faster the oscillations and/or the larger the maximum transition probability,

---

* Just a reminder, the values of $\varepsilon$ for the ADIAB calculations are 0.01, 0.01, and 0.001 for the NC, CR, and CA potentials respectively.

$$\left\{ \begin{array}{l} \text{fast oscillations} \\ \text{large maximum } P_{tr} \end{array} \right\} \iff \text{large} \left| \frac{V_{12}^{d}}{(V_{11}^{d}-V_{22}^{d})} \right| .$$

In going from NC to CR the coupling, $V_{12}^{d}$, decreases by a factor of 5, but the CR surfaces cross, the denominator goes through zero, the ratio becomes large, there are faster oscillations and a larger maximum $P_{tr}$. In going from CR to CA both the coupling and surface separation diminish. Apparently, however, the ratio is generally larger for the CA case which oscillates more rapidly.

There is another trend in going from NC to CR to CA. The magnitude of the diabatic coupling decreases. The smaller the coupling the more nearly alike the diabatic and adiabatic equations become. The resemblance between the diabatic and adiabatic curves, even without detailed balance, increases. The figures bear this out. For the NC case agreement between the SCE/EF DIAB (1->2), Figure 6-2, and SCE/EF ADIAB (1->2), Figure 6-3, curves is quite poor. The same curves in the CR case, Figures 6-5 and 6-6, agree very well except at very low energies. The adiabatic curves for the CA case, Figure 6-9, are included here more for the sake of completeness than because of any new information they might contain. They are practically identical to the diabatic ones, Figure 6-8. Numerical values show very small differences at low energies.

It may also be observed that in the high energy limit collisions take place too rapidly for transitions to occur. This is evidenced by decreasing transition probability as energy increases in the high energy regime. This is precisely what is seen in the CR and CA figures. The NC calculation is not taken high enough in energy for this phenomenon to be evident. Presumably one would see the same behavior in this case also.

The reader will notice a peculiarity in the (1->2) calculation for the CA potential, left-hand graphs of Figures 6-8 and 6-9. At about 0.42 Hartree the curve doesn't complete its cycle. It starts to descend, but rises again well before reaching zero. As discussed in the next section, the effective potential for the SCE/EP calculations generally follows the potential surface it starts out on to the turning point and comes out displaced from that surface in proportion to the transition probability. The lower surface for the CA potential has a well. It would appear that when the energy is increased a certain amount the effective potential has a problem following the well. The fact that the (2->1) calculation, right-hand graphs of Figures 6-8 and 6-9, has no peculiarity supports this notion. It examines the same system, but doesn't have to deal with the well. Since all of the (1->2) trajectories do conserve energy the explanation given is not sufficient. As it turns out, this monograph supports the SCE/AEP approach over the

SCE/EP approach. For that reason not much time was spent examining the phenomenon.

The effect of potential wells remains a possibly fertile area for future investigation. It should have something to do with resonances.

Figure 6-1 Exact transition probability versus E.
NC Potential

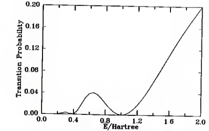
0.20
0.16
0.12
0.06
0.04
0.00
Transition Probability
0.0
0.4
0.8
1.2
1 6
2.0
E/Hartree

Figure 6-2 Diabatic transition probabilities versus E. NC Potential

——————— SCB/EP DIAB (1->2)

– – – – – – – SCB/EP DIAB (2->1)

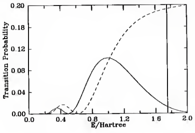
Transition Probability
0.20
0.18
0.12
0.08
0.04
0.00
0.0
0.4
0.8
1.2
1.6
2.0
E/Hartree

Figure 6.3 Adiabatic transition probabilities versus E. NC Potential

———————— SCE/EP ADIAB (1->2)

- - - - - - - SCE/EP ADIAB (2->1)

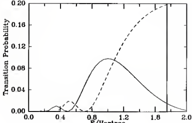
Transition Probability
0.20
0.16
0.12
0.08
0.04
0.00
0.0
0.4
0.8
1.2
1.8
2.0
E/Hartree

Figure 6-4. Exact transition probability versus E. CR Potential.

+ + + + Points taken from an exact calculation tabulated in Currier and Berman (1985)

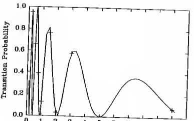
Transition Probability
1.0
0.8
0.6
0.4
0.2
0.0
0
1
2
3
4
5
6
7
8
9
10
11
E/Hartree

Figure 6.5 Diabatic transition probabilities versus E
CR Potential

———————— SCE/EP DIAB (1->2)

- - - - - - - - SCE/EP DIAB (2->1)

⊖ ⊖ ⊖ ⊖ Points taken from an eikonal (1->2) calculation tabulated in Currier and Herman (1985).

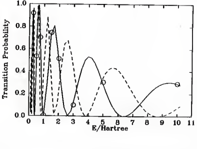
Transition Probability
1.0
0.8
0.6
0.4
0.2
0.0
0
1
2
3
4
5
6
7
8
9
10
11
E/Hartree

Figure 6 6. Adiabatic transition probabilities versus E.
CR Potential.

——————— SCB/EP ADIAB (1->2)

- - - - - - - SCB/EP ADIAB (2->1)

⊖ ⊖ ⊖ ⊖ Points taken from an eikonal (1->2) calculation tabulated in Currier and Herman (1985).

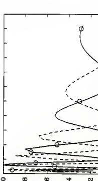
Transition Probability
0.0
0.2
0.4
0.6
0.8
1.0
E/Hartree
0
1
2
3
4
5
6
7
8
9
10
11

Figure 6.7: Exact transition probability versus E.
CA Potential

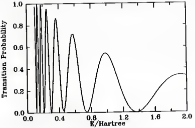
Transition Probability
1.0
0.8
0.6
0.4
0.2
0.0
0.0
0.4
0.8
1.2
1.6
2.0
E/Hartree

Figure 6-8A. Diabatic transition probabilities versus E
CA Potential.

LEFT GRAPH - SCE/EP DIAB (1->2)

RIGHT GRAPH - SCE/EP DIAB (2->1)

Note: These calculations can be carried out at lower energies.

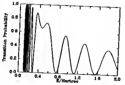
Transition Probability
0.0
0.2
0.4
0.6
0.8
1.0
0.0
0.4
0.8
1.2
1.6
2.0
E/Hartree

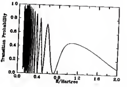
Transition Probability
0.0
0.2
0.4
0.6
0.8
1.0
0.0
0.4
0.8
1.2
1.6
2.0
E/Hartree

Figure 6-8B: Diabatic transition probabilities versus E:
CA Potential.

———————— SCE/EP DIAB (1->2)

— — — — — — — SCE/EP DIAB (2->1)

This figure focuses on the low energy region of the graphs in Figure 6-8A. Note the disagreement between the two curves even in this region.

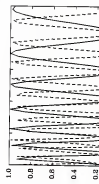
Transition Probability
0.0
0.2
0.4
0.6
0.8
1.0
E/Hartree
0.10
0.12
0.14
0.16
0.18
0.20

Figure 6-9A Adiabatic transition probabilities versus E
CA Potential $\varepsilon = 0.001$

LEFT GRAPH - SCE/EP ADIAB (1->2)

RIGHT GRAPH - SCE/EP ADIAB (2->1)

Note the very strong resemblance to Figure 6-8A. This is attributed to weak diabatic coupling ($V_{12}^{d}=V_{21}^{d}$ is very small )

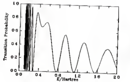
Transition Probability
1 0
0 8
0 6
0 4
0 2
0 0
0 0
0 4
0 8
1 2
1 6
2 0
E/Hartree

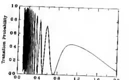
Transition Probability
1 0
0 8
0 6
0 4
0 2
0 0
0 0
0 4
0 8
1 2
1 6
2 0
E/Hartree

Figure 6-9B Adiabatic transition probabilities versus E.
CA Potential.

———————— SCE/EP DIAB (1->2)

— — — — — — — SCE/EP DIAB (2->1)

This figure focuses on the low energy region of the graphs in Figure 6 9A. Note the disagreement between the two curves even in this region. Also note the strong similarity to Fig6-8B.

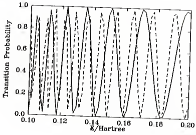
Transition Probability
0.0
0.2
0.4
0.6
0.8
1.0
0.10
0.12
0.14
0.16
0.18
0.20
E/Hartree

## 6-3. The Averaged Effective Potential

While the effective potentials described to this point are (pardon the pun) an effective way of constructing classical trajectories that reflect the average state of the system, an immediate improvement is possible. In an exact calculation the transition probability going from the lower to the upper state precisely equals the probability of going from the upper to the lower state at the same total energy. A graph showing $P_{21}$ (*) versus energy is identical to a graph of $P_{12}$ versus energy. (Equivalently, since $P_{21}+P_{11}=1$ and $P_{12}+P_{22}=1$, a graph of $P_{11}$ versus energy is identical to a graph of $P_{22}$ versus energy.) This results from microscopic reversibility (see Messiah, 1961, vol. II, chap. XIX, sect. 32) telling us that a collision is equally likely to proceed in either the forward or reverse direction. Unfortunately, this is not the result generally obtained from eikonal calculations. The cure is to somehow combine calculations in the 1->2 direction with calculations in the 2->1 direction so they can be run simultaneously. One way to do this is to use an *averaged* effective potential. If $v_1$ is the effective potential constructed using a full set of coefficients for the 1->2

---

(*) P is used as the symbol for momentum and also as the symbol for probability. Whenever it means probability it is followed by a two character subscript, e.g., $P_{11}$, $P_{21}$, or $P_{tr}$, otherwise it refers to momentum.

direction and $v_2$ is the effective potential constructed from 2->1 coefficients, a single trajectory may be calculated from the averaged effective potential,

$$\bar{v} = \frac{v_1+v_2}{2} \quad . \tag{6-1}$$

This trajectory is self-consistently coupled to two complete sets of coefficients that are equivalent to each other except that one starts in the lower state while the other starts in the upper. If the order were reversed, so that the coefficients starting in the upper state started in the lower and the set starting in the lower state started in the upper, the results of the calculation would be unaffected.

Hence we postulate that

"To be successful, the eikonal calculation performed with the averaged effective potential must give results such that $P_{21}=P_{12}$ ($P_{11}=P_{22}$)."

This statement, placed in quotes for emphasis, can be used in connection with two mildly different treatments.

In the *first treatment* one performs the calculation, evaluates $P_{21}$ and $P_{12}$ ($P_{11}$ and $P_{22}$), confirms that they are equal, and states, therefore, that the calculation is successful. This treatment is used with the diabatic eikonal calculation, where the calculation as it has been described is capable of giving meaningful probabilities at all R(t). In fact, the diabatic equations perform beautifully using this approach. Performing the calculation without any additional constraints, each set of coefficients naturally yields probabilities that (to within the numerical error permitted by the program) equal each other at all internuclear separations and all energies,

$$X_{21}^2+Y_{21}^2=X_{12}^2+Y_{12}^2 \quad ,$$

$$P_{21} = P_{12} = P_{tr} \quad . \tag{6-2}$$

where $P_{tr}$ refers to the probability that the state of the system will undergo a transition (tr for short). Figure 6-10 shows $P_{tr}$ versus time.

A *second treatment* has been developed for use with the adiabatic equations. The approach is basically the same except that the calculation is not designed so that $P_{21}=P_{12}$ (or $P_{11}=P_{22}$) at all R(t). Valid probabilities are only obtained at internuclear separations where these equalities hold. Probabilities at these locations are accepted, all others are rejected.

Why does the first treatment work with the diabatic equations and not the adiabatic equations? Notice that the diabatic equations for the coefficients depend only on the coefficients A themselves and $V^d$, Equation (4-15) or (4-18). They are independent of whatever effective potential is used. The adiabatic equations are far more explicit, they depend not only on A and $V^a$, but on terms in P and v as well. This leaves a choice. One could solve for $A_1$ using $v_1$ and $P_1$ $(= [2m(E-v_1)]^{1/2})$, and $A_2$ using $v_2$ and $P_2$ $(= [2m(E-v_2)]^{1/2})$ (see Equations (4-54) and (4-55) ). Notice that $v_1 \neq v_2 \Rightarrow P_1 \neq P_2$. Without going into a great deal of detail (these equations become very tricky), one finds that this kind of approach leads back in the direction of two separate solutions for $P_{21}$ and $P_{12}$ and gives pretty much the same (incorrect) results obtained with the non-averaged effective potentials. There is no choice but to seek an alternative

The alternative is to use $\bar{v}$ and P (from the trajectory equations, the integral of Equation (4-53) ) in all of the adiabatic differential equations for the coefficients. This has the advantage that the sets of differential equations corresponding to the two sets of coefficients are identical in form, a situation that is known to work in the diabatic case. Unfortunately, both sets of equations are now incorrect. They each contain $\bar{v}$, which is an explicit function of both sets of coefficients. Fortunately, this objection is removed when the coefficients in question are equal! One now has valid coefficients that were calculated using a potential that treats collisions starting in the lower and upper states equivalently. For example, at certain locations,

$$X_{21} = X_{12} = X_{tr} \quad ;$$

$$Y_{21} = Y_{12} = Y_{tr} \;;$$

$$X_{21}^2 + Y_{21}^2 = X_{12}^2 + Y_{12}^2 = X_{tr}^2 + Y_{tr}^2 = P_{21} = P_{12} = P_{tr} \; .$$

(6-3)

In fact, $P_{tr}$ is a series of discrete data points corresponding to probabilities at the locations where the coefficients are equal. It is a little easier to visualize $P_{tr}$'s behavior if it is cast in the form of a continuous function whose acceptable values coincide with the discrete data points

Figure 6-11 shows three graphs with a common horizontal axis. The bottom graph shows both $X_{21}$ and $X_{12}$. The middle graph shows $Y_{21}$ and $Y_{12}$. The top graph shows the continuous form of $P_{tr}$. The vertical lines indicate the locations where the coefficients and probability are valid. These lie where the curves for the coefficients intersect. At sufficiently long times (when the outbound trajectory is clearly past the avoided crossing) the consecutive discreet data points of $P_{tr}$ level off to some constant value. This is taken as the post-collision transition probability at the specified total energy If one uses the same treatment to separately calculate the probability that no transition will take place,

$$X_{11} = X_{22} = X_{nt} \;;$$

$$Y_{11} = Y_{22} = Y_{nt} \;;$$

$$X_{11}^2 + Y_{11}^2 = X_{22}^2 + Y_{22}^2 = X_{nt}^2 + Y_{nt}^2 = P_{11} = P_{22} = P_{nt} \; , \tag{6-4}$$

and adds it to the transition probability, one does find

$$P_{nt} + P_{tr} = 1 \tag{6-5}$$

as it should. While this approach was designed to make the adiabatic equations work, there is nothing to prohibit using it with the diabatic equations. Of course this is not preferred, but it is interesting to compare. Figure 6-12 shows the same information as Figure 6-11, but obtained using the diabatic equations. The two figures are very similar. In this particular example the location of the post-collision data points practically coincide. A notable feature is that coefficients from the second set, $X_{12}$ and $Y_{12}$, level off rather than continuing to oscillate. While this was certainly not intended or expected, there is nothing to counter-indicate this behavior.

The most obvious limitation on the treatment just described is its inability to give probabilities that are continuous functions of time (or R(t) ). One may attempt to overcome this deficiency by connecting the peaks in the continuous form of, say, $P_{tr}$ to get at least a partial picture. Figure 6-13 compares the continuous probability from Figure 6-10 to peak-to-peak curves made from Figures 6-11 and 6-12. Starting a little past the turning point, they are all equal. In the turning point region itself, the adiabatic calculation is totally unreliable due to the use of $\varepsilon$. In fact, though Figure 6-13 doesn't show it, the adiabatic peak-to-peak curve may show erratic behavior in this region The diabatic peak-to-peak curve naturally coincides with the continuous diabatic probability of Figure 6-10. Since there is nothing to be gained (and a good deal to be lost) performing diabatic calculations with the second treatment, any diabatic calculation referred to beyond this point has been done with the first approach If all that is required is the post-collision probability the adiabatic equations may be used. If the time evolution of the probability is needed the eikonal method can at present only be applied in the diabatic representation.

Finally, the actual adiabatic calculations were performed using a modification of the averaged effective potential in Equation (6-1). Rather than normalizing the coefficients so that

$$x_{11}'^2 + y_{11}'^2 + x_{21}'^2 + y_{21}'^2 = 1$$

and

$$x_{22}'^2 + y_{22}'^2 + x_{12}'^2 + y_{12}'^2 = 1 \quad ,$$

(see Equations (4-57) and (4-58) ) normalization is carried out so that

$$X_{11}'^2 + Y_{11}'^2 + X_{21}'^2 + Y_{21}'^2 + X_{22}'^2 + Y_{22}'^2 + X_{12}'^2 + Y_{12}'^2 = 1 \quad . \qquad (6\text{-}6)$$

The normalized components, $X'_{mn}$ and $Y'_{mn}$ , are

$$X'_{mn} = X_{mn} \Big/ \left( X_{11}^2+Y_{11}^2+X_{21}^2+Y_{21}^2+X_{22}^2+Y_{22}^2+X_{12}^2+Y_{12}^2 \right)^{1/2} ;$$

$$Y'_{mn} = Y_{mn} \Big/ \left( X_{11}^2+Y_{11}^2+X_{21}^2+Y_{21}^2+X_{22}^2+Y_{22}^2+X_{12}^2+Y_{12}^2 \right)^{1/2} , \qquad (6\text{-}7)$$

where m = 1 or 2 and n = 1 or 2. This has the very practical effect that, during the course of a calculation,

$$X_{1n}'^2 + Y_{1n}'^2 + X_{2n}'^2 + Y_{2n}'^2 = 0.5 \qquad (6\text{-}8)$$

With the coefficients normalized in this manner the averaged effective potential is simply the sum

$$\bar{v} = v_1' + v_2' \qquad (6\text{-}9)$$

Calculations performed using either the averaged effective potential from Equation (6-1) or the averaged effective potential from Equation (6-9) conserve energy superbly (with a maximum error that precisely matches that allowed by the program) over the entire trajectory and pass through the turning point region with the same apparent facility as diabatic calculations. Unfortunately adiabatic calculations performed with the original averaged effective potential, $(v_1 + v_2)/2$, Equation (6-1), only function this way with relatively large $\epsilon$, $5.0 > \epsilon > 0.1$. These calculations behave reasonably in every respect except for the results. In this case the validity of the coefficients is nullified by large $\epsilon$. On the other hand, any small deviation that appears in either of the collectively normalized sets at the turning point region, appears to be simultaneously compensated by an equivalent deviation in the other set, and eventually they self-correct. This allows much smaller values of $\epsilon$ to be used and the coefficients remain valid.

All of the SCE/AEP calculations described in this work were first carried out using the averaged effective potentials described above. Fortunately this is not the whole story. The very fact that microreversibility can be successfully imposed on the calculations can be used to simplify things even more. The averaged effective potential in the diabatic representation is

$$\bar{v} = \sum_{j=1}^{2} w_j v_j \qquad (6\text{-}10)$$

where $w_j$ is a weight factor assigned to each level $j$. In the simple two-state case where each curve is given equal weight (as above) $w_1 = w_2 = 1/2$. In general there might be reasons, such as level degeneracies, to assign the $w_j$ different values.

We have

$$v_j = A_j^{+} V A_j = \left( A_{1j}^{*} \quad A_{2j}^{*} \right) \begin{pmatrix} V_{11} & V_{12} \\ V_{12} & V_{22} \end{pmatrix} \begin{pmatrix} A_{1j} \\ A_{2j} \end{pmatrix}$$

$$= \sum_{kl} A_{kj}^{*} V_{kl} A_{lj} = \sum_{kl} A_{kj}^{*} A_{lj} V_{kl} \, , \qquad (6\text{-}11)$$

where (in the two-state case) k=1,2 and l=1,2. This leads to

$$\sum_{j=1}^{2} v_j = V_{11} + V_{22} \quad , \qquad (6\text{-}12)$$

which is arrived at from the orthonormality relationship

$$\sum_{j} A_{kj}^{*} A_{lj} = \delta_{kl} \quad , \qquad (6\text{-}13)$$

which itself is a consequence of the form of the differential equations for the electronic amplitudes.

In the case being considered

$$\bar{v} = \frac{1}{2} \sum_{j=1}^{2} v_j = \frac{V_{11} + V_{22}}{2} \quad . \qquad (6\text{-}14)$$

This little bit of luck allows the trajectories to be calculated independently of the coefficients. In fact, the same development applies to the adiabatic equations so that, as long as the coefficients are properly normalized, the SCE/AEP calculations can be performed without using ci It is important to realize, however, that when the $w_j$'s are not equal, the averaged effective potential will depend on the coefficients and the more complicated equations must be used.

Before moving on it should be pointed out that the simplified SCE/AEP calculations take just as long as those that use the more general equations. Calculation of the coefficients, not the trajectories, is rate determining.

Figure 6-10. Transition probability versus time
SCE/AB, DIAB, CR, E(total) = 1.5 Hartree.
This is the usual diabatic calculation (first treatment). The curve shows typical behavior. It remains about zero to the turning point region. There is a sharp jump and some oscillation around the turning point. A little past that, just beyond the potential crossing, it levels off to its constant post-collision value

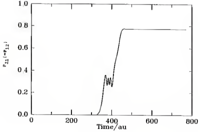
1.0
0.8
0.6
0.4
0.2
0.0
$P_{21}(=P_{12})$
0
200
400
600
800
Time/au

Figure 6-11. Second treatment. SCE/AE ADIAB CR, E(total) = 1.5 hartree, c = 0.01

This is the usual adiabatic calculation (second treatment).

BOTTOM GRAPH – Shows the transition coefficients $X_{21}$ and $X_{12}$. These

are invalid everywhere except at the points where the curves intersect ($X_{21}=X_{12}$).

MIDDLE GRAPH – Shows the transition coefficients $Y_{21}$ and $Y_{12}$. These are invalid

everywhere except at the points where the curves intersect ($Y_{21}=Y_{12}$).

TOP GRAPH – Shows the continuous form of the transition probability. This is invalid everywhere except where the X's and Y's both intersect. Vertical lines indicate these locations.

VERTICAL LINES extending the full height of the figure indicate where the coefficients and probability are valid.

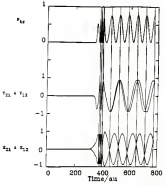
$F_{tr}$
1
0
$Y_{21}$ & $Y_{12}$
1
0
−1
$X_{21}$ & $X_{12}$
1
0
−1
0
200
400
600
800
Time/au

Figure 6-12. Second treatment. SCE/AE DIAB
CR, E(total) = 1.5 Hartree, $\varepsilon = 0.01$

This is the usual adiabatic calculation (second treatment).

BOTTOM GRAPH – Shows the transition coefficients $X_{21}$ and $X_{12}$. These are invalid

everywhere except at the points where the curves intersect ($X_{21}=X_{12}$).

MIDDLE GRAPH – Shows the transition coefficients $Y_{21}$ and $Y_{12}$. These are invalid

everywhere except at the points where the curves intersect ($Y_{21}=Y_{12}$)

TOP GRAPH – Shows the continuous form of the transition probability. This is invalid everywhere except where the X's and Y's both intersect. Vertical lines indicate these locations.

VERTICAL LINES extending the full height of the figure indicate where the coefficients and probability are valid.

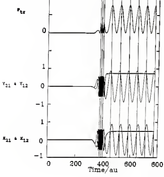

$P_{tr}$
1
0
$Y_{21}$ & $Y_{12}$
1
0
−1
$X_{21}$ & $X_{12}$
1
0
−1
0
200
400
600
Time/au

Figure 6-13. Comparison of transition probabilities versus time. SCE/AE, CR, E(total) = 1.5 hartree

———————— Same as Figure 6-10. The usual diabatic calculation (first treatment)

— — — — — — — Peak-to-peak version of the TOP GRAPH from Figure 6-11
The usual adiabatic calculation (second treatment)

●●●●●●●●●●●●●●● Peak-to-peak version of the TOP GRAPH from Figure 6-12
A unique demonstration of the diabatic calculation performed with the second treatment

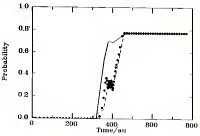
1.0
0.8
0.6
0.4
0.2
0.0
Probability
0
200
400
600
800
Time/au

## 6-4. SCE/AEP Transition Probabilities and Summary

Figure 6-14 shows the SCE/AEP DIAB and ADIAB transition probabilities versus energy for the NC potential. Figures 6-15 and 6-16 show them for the CR and CA potentials respectively. The diabatic and adiabatic curves are nearly identical. The agreement between these curves and the EXACT results, shown here as dashed lines, is remarkably good.

Figure 6-14 Exact and SCE/AEP transition probabilities
NC Potential

- - - - - - - - Exact

———————— SCE/AEP DIAB

———————— SCE/AEP ADIAB

Notice the strong agreement between the SCE/AEP DIAB and SCE/AEP ADIAB.

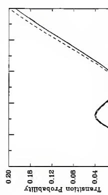
0.20
0.16
0.12
0.08
0.04
0.00
Transition Probability
0.0
0.4
0.8
1.2
1.6
2.0
E/Hartree

Figure 6-15A Exact and SCE/AEP transition probabilities
CR Potential

- - - - - - - Exact

———————— SCE/AEP DIAB

———— ———— SCE/AEP ADIAB

Notice the strong agreement between the SCE/AEP DIAB and SCE/AEP ADIAB.

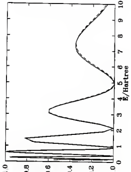
Transition Probability
1.0
0.8
0.6
0.4
0.2
0.0
0
1
2
3
4
5
6
7
8
9
10
E/Hartree

Figure 6.15B Exact and SCE/AEP transition probabilities.
CE Potential.

— — — — — — — Exact

———————— SCE/AEP DIAB

———————— SCE/AEP ADIAB

Notice the strong agreement between the SCE/AEP DIAB and SCE/AEP ADIAB.

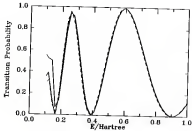
Transition Probability
1.0
0.8
0.6
0.4
0.2
0.0
0.0
0.2
0.4
0.6
0.8
1.0
E/Hartree

Figure 6 16A. Exact and SCE/AEP transition probabilities.
CA Potential.

- - - - - - - Exact

———————— SCE/AEP DIAB

———————— SCE/AEP ADIAB

Notice the strong agreement between the SCE/AEP DIAB and SCE/AEP ADIAB.

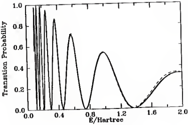
Transition Probability
0.0
0.2
0.4
0.6
0.8
1.0
E/Hartree
0.0
0.4
0.8
1.2
1.6
2.0

Figure 6-16B Exact and SCE/AEP transition probabilities
CA Potential

- - - - - - - Exact

——————— SCE/AEP DIAB

——————— SCE/AEP ADIAB

Notice the agreement extends to the lowest energy shown.
This particular calculation can be taken to lower energies.

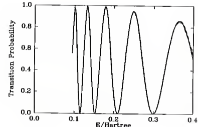
Transition Probability
1.0
0.8
0.8
0.4
0.2
0.0
0.0
0.1
0.2
0.3
0.4
E/Hartree

Table 6-1. Characteristics of Calculations for NC Potential

| Calculation | Agreement** | CPU Time* |
|---|---|---|
| SCE/EP DIAB 1->2 | POOR agreement with EXACT<br>POOR agreement with ADIAB 1->2 | 5.21 s. |
| 2->1 | POOR agreement with ADIAB 2->1 | 5.04 s. |
| ADIAB 1->2 | POOR agreement with EXACT<br>POOR agreement with DIAB 1->2 | 9.51 s. |
| 2->1 | POOR agreement with DIAB 2->1 | 9.42 s |
| SCE/AEP DIAB | VERY GOOD agreement with EXACT<br>MATCHES SCE/AEP ADIAB | 5.76 s. |
| ADIAB | VERY GOOD agreement with EXACT<br>MATCHES SCE/AEP DIAB | 11.64 s. |
| EXACT | ------------------------------ | 48.18 s. |

* CPU Time is in seconds per data point. The programs were run on a Micro-VAX II with VMS Version 5.3. The numbers shown are averages over 10 points in the middle energy range of the calculation. For the NC potential the energy range was about 0-2 Hartree. Ten points were taken around 1 Hartree and averaged.

** Such qualitative terms as GOOD and POOR are admittedly somewhat subjective in nature. The reader who is uncertain of the intent may refer directly to the figures. More quantitative measures of agreement can be deceptive in comparing oscillating curves. A steep curve with a slight horizontal displacement will result in a large unrepresentative vertical error.

Table 6-2. Characteristics of Calculations for CR Potential

| Calculation | Agreement | CPU Time* |
|---|---|---|
| SCE/EP DIAB | POOR agreement with EXACT ** | |
| 1->2 | GOOD agreement with ADIAB 1->2 | 4.81 s. |
| 2->1 | GOOD agreement with ADIAB 2->1 | 4.87 s. |
| ADIAB | POOR agreement with EXACT | |
| 1->2 | GOOD agreement with DIAB 1->2 | 9.54 s. |
| 2->1 | GOOD agreement with DIAB 2->1 | 9.49 s. |
| SCE/AEP DIAB | EXCELLENT agreement with EXACT | |
| | MATCHES SCE/AEP ADIAB | 5.81 s. |
| ADIAB | EXCELLENT agreement with EXACT | |
| | MATCHES SCE/AEP DIAB | 11.64 s. |
| EXACT | --------------------------- | 48.01 s. |

* CPU Time is in seconds per data point.

** Currier and Herman find that there is agreement at low energies (Currier and Herman, 1985). While there is no cause to dispute the fact that agreement is better at low energies, it seems less significant in light of this work.

Table 6-3 Characteristics of Calculations for CA Potential

| Calculation | Agreement | CPU Time* |
|---|---|---|
| SCE/EP DIAB<br>1->2 | POOR agreement with EXACT<br>NEAR MATCH to ADIAB 1->2 | 22.44 s. |
| 2->1 | NEAR MATCH to ADIAB 2->1 | 25.27 s. |
| ADIAB<br>1->2 | POOR agreement with EXACT<br>NEAR MATCH to DIAB 1->2 | 35.34 s. |
| 2->1 | NEAR MATCH to DIAB 2->1 | 39.64 s. |
| SCE/AEP DIAB | EXCELLENT agreement with EXACT<br>MATCHES SCE/AEP ADIAB | 22.37 s. |
| ADIAB | EXCELLENT agreement with EXACT<br>MATCHES SCE/AEP DIAB | 34.20 s. |
| EXACT | ------------------------------ | 69.45 s. |

* CPU Time is in seconds per data point.

A number of secondary trends regarding the agreement characteristics of the SCE/EP results were discussed in Section 6-2. The important overall trends brought out by the tables are these:

there is generally poor agreement between the SCE/EP and EXACT calculations;

there is generally very fine agreement between the SCE/AEP and EXACT calculations;

the SCE/AEP DIAB and ADIAB results match.

The first two trends support the usefulness of the averaged effective potential; the third trend supports the credibility of the adiabatic approach developed in this document. By now there can be little question of either point.

It is nice to know that in the two-state case, where EXACT calculations are possible, the SCE/AEP calculations, which appear to be quite good, are somewhat quicker. This is clearly seen in the right-hand column in the above tables. For the NC and CX potentials there's about an eight-fold savings in time with the DIAB calculation and between a four- and five-fold savings with the ADIAB calculation. In the worst case in this regard, the CA potential*, there's still a three-and-one-half-fold savings with DIAB and two-fold with ADIAB. It is worth knowing that these programs were written solely to develop and perfect the calculations. Even a rudimentary attempt at optimizing the code would result in some greater savings.

The tables reveal two more interesting facets of the AEP calculations. First of all, the SCE/AEP ADIAB calculations invariably take longer than the SCE/AEP DIAB calculations. This adds weight to the previously discussed notion that the adiabatic approach should only be applied when the diabatic approach is unsatisfactory. John Tully suggests that there are certain low energy situations where this might be the case (Tully, 1980).

---

* The CA calculations is slower than the NC and CR because the reduced mass is 30 times heavier. Also the $\epsilon$ used in the ADIAB CA calculation is one-tenth the value used in the other two.

The second facet is a little more curious, the AEP calculations take very little more (and in many cases actually less) computer time than the EP calculations *even though nearly twice as many differential equations are being solved*. The design of DE is such that the calls to and from the various subroutines take proportionately longer compared to the time spent within those routines. This means doubling the number of differential equations will not generally double the computer time. But this doesn't fully explain the diminutive nature of the increases seen, and it doesn't explain the decreases at all! These appear to be brought about by the increased symmetry of the SCE/AEP equations. In fact, in cases where there is a decrease in CPU time, energy conservation is actually several orders of magnitude better than dictated by error tolerance! Energy conservation is obtained from the simple expression

$$\Delta = E - \left(\frac{P^2}{2M} + v\right) \quad , \qquad (6\text{-}18)$$

where E is the initial total energy, $P^2/2M$ is the current kinetic energy, and v is the current potential energy. In the usual case when the error parameters input to DE are set to $10^{-8}$, $\Delta$ will eventually settle to $10^{-8}$ or possibly $10^{-7}$. In cases where the increased number of equations produces a reduction in computer time ε will settle to anywhere from $10^{-11}$ to $10^{-14}$ without any added incentive in the program. DE uses polynomial approximations to predict the behavior of the equations it then solves numerically. Apparently there is some matching of the polynomial predictions when two sets of coefficients are used that makes it easier for DE to handle the whole set of equations.

Overall, the SCE/AEP calculations are more accurate than the SCE/EP calculations by a vast margin. They are also, as indicated in the last paragraph, cost effective in terms of computer time, producing a slight increase in some cases and an actual savings in others. The present work definitely encourages the use of averaged effective potentials.

# CHAPTER VII

# CONCLUSION

After a general introduction to the eikonal method (Micha, 1983), the formalism for previously performed three-dimensional elastic scattering calculations was presented along with a few sample results (Cohen, 1988). Following that was the development of the eikonal formalism for inelastic scattering in one variable. A key part of the effort was aimed at applying the method in both the diabatic and adiabatic representations. The presentation made use of three model two-state potentials selected to cover a range of conditions. There was a non-crossing potential (NC), a potential with curve crossing in the repulsive region (CR), and a potential with crossing in the attractive region (CA). Development of the diabatic equations followed that of Micha and Swaminathan (Micha and Swaminathan, 1986). The adiabatic equations presented in this work were formed by applying a unitary transformation to the diabatic equations. They displayed some very interesting features, both formally and in their computational characteristics.

The most obvious difference in the adiabatic equations is the addition of several terms to Schroedinger's equation for nuclear motion that result from the unitary transformation. When the diabatic equation, already simpler than the adiabatic, is switched to the time dependent form, it can be simplified further yet by an appropriate change in the phase of the eikonal wavefunction. This amounts to a rearrangement so that unwanted expressions become part of the exponential factor, which is then divided out. While the same strategy is used to simplify the adiabatic equation somewhat, it cannot be used to nearly the same extent. A less obvious difference stems from the appearance of a momentum variable, P, in the denominator of the adiabatic equations for the coefficients. This leads to two separate singularities in the vicinity of the turning point, where P goes to zero. These are avoided by the addition of a small imaginary increment, $\varepsilon$, to P. If $\varepsilon$ is too small the calculation will take too long. If $\varepsilon$ is too large the coefficients will not be valid. Tests were made for the appropriate choice of $\varepsilon$.

Other differences concern calculation of the trajectories. Hamilton's equation for the temporal derivative of the momentum requires the spatial derivative of (in this case) the effective potential. It might be expected that, since the effective potential contains the coefficients, this would require the spatial derivatives of the coefficients. In the diabatic case, however, the coefficients can also be arrived at using Hamilton's equations. Because of the symmetric relationships among coefficients formed in this way (see Equation (4-18) ), the spatial derivatives that appear in $\partial U^d/\partial R$ cancel one another (see Equation (4-23) ). In the adiabatic case, on the other hand, the spatial derivatives of the coefficients are needed. Also, the adiabatic effective potential, even after application of the short-wavelength approximation, contains a term in P. This momentum dependant potential requires a little special attention.

Finally, the time-dependant adiabatic equations contain certain non-Hermitian terms. This means that the expression used for probability, $A^+A$, is not automatically conserved. Normalization must be provided to ensure that it is.

All of these oddities and complications certainly make the adiabatic formalism more difficult as well as more troublesome to program, but more importantly, the more demanding equations are less hardy and resilient than the simple symmetric diabatic equations, and most importantly, they take more computer time! Since the same information goes into both the SCE DIAB and ADIAB calculations, ideally, the same results are expected from each. In fact (as something of a triumph) this is true for the calculations presented in this work. Unfortunately however, the adiabatic calculations take longer than the diabatic calculations for every single example. All of the reasons in this paragraph combine to make the adiabatic approach generally less desirable than the diabatic one. One suspects, of course, that, with the infinite variety of chemical systems and potentials to be dealt with, some will be more amenable to the adiabatic treatment.

In any case, the successful development and application of the adiabatic eikonal equations presented in this work adds to the dynamicist's understanding of his subject. This author, at least, envisions the possibility of applying the eikonal method to equations not transformed from diabatic ones. Since, as John Tully points out (John Tully, 1976), curve crossings are only special one-dimensional cases of seams where adiabatic surfaces approach, this might prove very interesting in multidimensional problems. Alternatively, one can always apply the methods of Olson and Micha (Olson and Micha, 1982) to develop an appropriate diabatic potential.

Once the usual eikonal calculations were successfully carried out in both representations, the question of improvements came up. Since the excitation probabilities did not match the de-excitation probabilities, as they do in exact calculations, an averaged effective potential was introduced to impose the condition of microreversibility*. The effective potentials for the excitation and de-excitation processes were calculated simultaneously, along with both sets of coefficients, and trajectories were constructed from their average. The improved agreement with exact calculations was remarkable (see Figures 6-14,

---

* A more rigorous treatment of microreversibility, using variational methods, was developed by Micha and Gazdy (Micha and Gazdy, 1987).

6-15, and 6-16). Calculations that were only qualitatively correct using an effective potential became semi-quantitatively to quantitatively correct using the averaged effective potential. The added cost in computer time of using the averaged effective potential was minimal to nonexistent due to an increase in the symmetry of the equations.

A mildly surprising discovery was that, due to the orthonormality of the electronic functions, the averaged effective potential for the case where the curves are given equal weight is simply the average of the surfaces. In this particular case the coefficients don't appear in the averaged effective potential! Since these trajectories can be calculated independently of the coefficients, the adiabatic calculations for this case no longer require c! Sadly, calculations performed this way take the same computer time as those that include the coefficients in the averaged effective potential. The time is taken up in calculating the coefficients themselves. In the general case reasons might be found to assign the curves different weights, leaving no choice but to use the coefficient dependent potential.

The improved results at little or no extra cost, along with the information from the preceding paragraphs, lead to the conclusion that the method of choice uses the averaged effective potential in the diabatic representation (SCE/AEP DIAB).

The strength of the eikonal method lies not in one-variable calculations, which can be performed exactly, but in multi-variable calculations, which cannot. Clifford Stodden has used the method to treat the photodissociation of methyl iodide (an interesting application in itself) to two variables (Stodden, 1987).

Extending the method is the heart of simplicity. A set of coefficients is added for each new surface. The total probability, $A^{+}A$, is still set to unity and conserved. The sum of the squares for each set of coefficients, $A_i^{+}A_i = X_i^2 + Y_i^2$, represents the probability that the system is on that surface, i. An averaged effective potential might easily be formed from three or more surfaces.

Another simple, at least conceptually, extension of the method would give inelastic scattering information in three dimensions. This would give the scattering angle as well as the state. To accomplish this one would use the vector R in place of the internuclear separation R and the vector P in place of the momentum variable P. Since the initial and final moments would not be equal, there would, unlike the elastic case, be a range of final momenta for each scattering angle. Also the trajectories would not remain in a single plane. Although these complications would add to the complexity and cost, in computer time, of the calculations, the procedure remains eminently practical. A large part of the challenge would lie in constructing appropriate potential surfaces. Central potentials obtained by averaging over scattering experiments might be used for model calculations.

In 1984 Olson and Garrison performed preliminary eikonal calculations for the scattering of Na from W(110) surfaces (Olson and Garrison, 1985). In 1987 more sophisticated model calculations, taking surface motion into account, were applied to collisions of gas atoms with insulator surfaces (Swaminathan, Garrett, and Murthy, 1988). Equations of motion characterizing the surface were formed from a stochastic reduction of the generalized Langevin equation (GLE). For systems studied there was an appreciable loss of gas atom energy to the surface, clearly related to the inelastic transition probability. Possible extensions of the theory include the treatment of photochemical processes on surfaces, and reactions with and on surfaces. In 1988 rotationally electronically inelastic scattering of NO from Ag(111) was treated using the eikonal method and results compared very well to exact calculations (Rice, Garrett, and Swaminathan, 1989).

These calculations seem to be limited only by the availability of potentials along with, as with the GLE, the various other parameters that are used. For the moment at least, that is where things stand. While our handling of it can always be improved, the basic eikonal approach is wholesome and theoretically sound and, as long as correct input is available, useful results will be generated.

## APPENDIX A

## KEY TO PROGRAM NAMES

Key

NC : non-crossing
CR : crossing repulsive
CA : crossing attractive

ADIA : adiabatic
DIAB : diabatic

EXACT : logderiv
SCE/EP : self consistent eikonal, effective potential
SCE/AEP : self consistent eikonal, average effective potential

# APPENDIX B EIKONAL PROGRAM
## SCE/AEP DIAB

```
C*************************************************************
C THIS PROGRAM CALCULATES ELECTRONICALLY INELASTIC
C TRANSITION PROBABILITIES FOR THE RC POTENTIAL (CROSSING
C IN REPULSIVE REGION) USING THE SELF CONSISTENT EIKONAL
C APPROACH IN THE DIABATIC REPRESENTATION WITH AN AVERAGED
C EFFECTIVE POTENTIAL.  IT IS PART OF "COMPUTATIONAL
C STUDIES OF ELECTRONICALLY DIABATIC MOLECULAR COLLISIONS",
C A DOCTORAL DISSERTATION SUBMITTED BY JOEL COHEN TO THE
C UNIVERSITY OF FLORIDA IN OCTOBER 1990.
C SEE CHAPTER II FOR THE GENERAL EIKONAL EQUATIONS, SECTION
C 4-2 FOR THE DIABATIC EIKONAL EQUATIONS, TABLE 4-1 AND
C FIGURE 4-1 FOR THE RC POTENTIAL, AND SECTION 6-3 FOR AN
C EXPLANATION OF THE AVERAGED EFFECTIVE POTENTIAL.
C THE AVERAGED EFFECTIVE POTENTIAL IS ONE HALF
C THE SUM OF THE EXCITATION AND DE-EXCITATION EFFECTIVE
C POTENTIALS.  FUNCTIONS TO BE EVALUATED AT POINTS ALONG THE
C TRAJECTORY ARE STORED IN Y(I). THE INITIAL VALUES ARE
C FOUND IN THE MAIN PROGRAM.  A DIFFERENTIAL EQUATION SOLVER
C (DE) IS CALLED TO SIMULTANEOUSLY GENERATE TRAJECTORIES
C AND TRANSITION AMPLITUDES STARTING AT THE INITIAL
C CONDITIONS LISTED IN MAIN.  DE USES SUBROUTINE FPRIME
C WHICH CONTAINS YP(I), THE ANALYTICAL TEMPORAL DERIVATIVES
C OF Y(I).
C    Y(1) IS THE INTERNUCLEAR SEPARATION.
C    Y(2) IS THE RELATIVE MOMENTUM.
C    Y(3)-Y(6) ARE THE COEFFICIENTS OF EXCITATION.
C    Y(7)-Y(10) ARE THE COEFFICIENTS OF DE-EXCITATION.
C IT IS NOT NECESSARY TO REPRODUCE THE CODE FOR DE,
C THAT IS AVAILABLE FROM OTHER SOURCES.  ONLY ORIGINAL
C MATERIAL REQUIRED BY THE PRESENT WORK IS LISTED BELOW.
C - JOEL COHEN
C   UNIVERSITY OF FLORIDA, 1990
C*************************************************************
CCC    MAIN PROGRAM    CCC
CC INSERT INITIAL CONDITIONS OF FUNCTIONS
CC TO BE EVALUATED BY DE
      IMPLICIT REAL*8 (A-H,O-Z)
      DIMENSION Y(10)
      COMMON/ABC/NNN,RTES,NEND
      EXTERNAL FPRIME
C
C  DATA FOR RC MODEL POTENTIAL

      DATA A11/3./,A22/3./,B22/1./,ALPHA11/3./,ALPHA22/3./,
     XBETA22/2./,V20/.1/,A12/0.01/,ALPHA12/2./,R12/2./
```

```
C   CM = REDUCED MASS IN AU = PROTON MASS/ ELECTRON MASS
     CM=(1.67265E-27/9.10953E-31)
C    RI IS INITIAL INTERNUCLEAR SEPARATION
C    Y(1) HOLDS R
C    RTES IS THE CUTOFF VALUE OF R FOR THE CALCULATION
       RI=15.1
      Y(1)=RI
       RTES=RI-.01
C    EVALUATE THE POTENTIAL AT RI
      H11=A11*DEXP(-ALPHA11*(RI))
       H221=A22*DEXP(-ALPHA22*(RI))
       H222=-B22*DEXP(-BETA22*(RI))
      H22=H221+H222+V20
       TANA=TANH(ALPHA12*(RI-R12))
      H12=A12*(1.-TANA)
C VEFFI IS THE INTIAL VALUE
C OF THE AVERAGED EFFECTIVE POTENTIAL
      VEFFI=(H11+H22)/2.
C
C     Y(3)-Y(10) ARE THE INITIAL VALUES OF THE COEFFICIENTS
C
C  THE FIRST SET STARTS IN THE LOWER STATE
C     Y(3)=X1=1 Y(4)=X2=0
C     Y(5)=Y1=0 Y(6)=Y2=0
C
C  THE SECOND SET STARTS IN THE UPPER STATE
C     Y(7)=X1S=0 Y(8)=X2S=1
C     Y(9)=Y1S=0 Y(10)=Y2S=0
C
C  (THE S, AS IN X1S, IS USED TO INDICATE THE SECOND SET)
C
      Y(3)=1.
      Y(4)=0.
      Y(5)=0.
      Y(6)=0.
      Y(7)=0.
      Y(8)=1.
      Y(9)=0.
      Y(10)=0.
C  LOOP OVER THE TOTAL ENERGY, EE
C  NT IS THE TRAJECTORY NUMBER
C  NTMAX IS THE MAXIMUM TRAJECTORY NUMBER
C  CRI IS THE INITIAL MOMENTUM
C  Y(2) HOLDS THE MOMENTUM
C  NEQN IS THE NUMBER OF DIFFERENTIAL EQUATIONS
C    TO BE SOLVED BY DE
C  NEND IS A FLAG USED TO INDICATE THAT THE CUTOFF POINT
C    HAS BEEN REACHED
       NTMAX=81
      DO 1 NT=1,NTMAX
       EE=.1+(REAL(NT-1)/40.0)*.9
       CRI=-SQRT(2.*CM*(EE-VEFFI))
      Y(2)=CRI
       NEQN=10
       NEND=0
```

```
C  T IS THE TIME IN A.U.
C  NNN COUNTS THE CALLS TO FPRIME
C  RELERR IS THE MAXIMUM ALLOWABLE RELATIVE ERROR
C  ABSERR IS THE MAXIMUM ALLOWABLE ABSOLUTE ERROR
C  TOUT IS THE MAXIMUM ALLOWABLE TIME FOR A TRAJECTORY
C  IFLAG IS USED BY DE TO INDICATE
C     THE STATUS OF THE CALCULATION
         T=0.D0
         NNN=0
         RELERR=1.E-8
         ABSERR=1.E-8
         TOUT=10000
         IFLAG=1
        CALL DE(F,NEQN,Y,T,TOUT,RELERR,ABSERR,IFLAG)
        PRINT*,'NT,IFLAG,NEQN,TOUT,Y',NT,IFLAG,NEQN,TOUT,Y
          Y35=((Y(3)**2+Y(5)**2))
          Y46=((Y(4)**2+Y(6)**2))
          Y79=((Y(7)**2+Y(9)**2))
          Y80=((Y(8)**2+Y(10)**2))
          XAV=(Y(4)+Y(7))/2.
          YAV=(Y(6)+Y(9))/2.
          PAV=XAV**2+YAV**2

 1        CONTINUE


C         OUTPUT GOES HERE   PRINT TO FILES, TABLES,
C         DRAW GRAPHS, ETC


       STOP
       END


       SUBROUTINE FPRIME(T,Y,YP)
CC  CONTAINS DERIVATIVES OF FUNCTIONS CCC
CC  TO BE EVALUATED BY DE             CCC
       IMPLICIT REAL*8 (A-H,O-Z)
       DIMENSION Y(10),YP(10)
       COMMON/ABC/NNN,RTES,NEND
       DATA A11/3./,A22/3./,B22/1./,ALPHA11/3./,ALPHA22/3./,
      XBETA22/2./,V20/.1/,A12/.01/,ALPHA12/2./,R12/2./
C  R IS THE INTERNUCLEAR SEPARATION
        R=Y(1)
C  COUNT THE CALLS TO FPRIME
        NNN=NNN+1
C  STOP THE CALCULATION AT R=RTES
              IF(NNN.GT.150.and.R.GE.RTES)THEN
                PRINT* 'R-FINAL',R
                NEND=1
                RETURN
                ENDIF
```

```
C  EVALUATE THE POTENTIAL AND ITS FIRST DERIVATIVE AT R
      H11=A11*DEXP(-ALPHA11*(R))
        DH11DR=-ALPHA11*H11
       H221=A22*DEXP(-ALPHA22*(R))
       H222=-B22*DEXP(-BETA22*(R))
      H22=H221+H222+V20
        DH22DR=-ALPHA22*H221-BETA22*H222
        TANA=TANH(ALPHA12*(R-R12))
      H12=A12*(1.-TANA)
        DH12DR=-A12*ALPHA12*(1.-(TANA**2))

C   ATHA/ATA IS THE EFFECTIVE POTENTIAL FOR EXCITATION

       X1=Y(3)
       X2=Y(4)
       Y1=Y(5)
       Y2=Y(6)
      Y35=(X1**2+Y1**2)
      Y46=(X2**2+Y2**2)
      Y3456=(X1*X2+Y1*Y2)
     ATA=Y35+Y46
     ATHA=H11*Y35+H22*Y46+2.*H12*(Y3456)

C   ATHAS/ATAS IS THE EFFECTIVE POTENTIAL FOR DE-EXCITATION

       X1S=Y(7)
       X2S=Y(8)
       Y1S=Y(9)
       Y2S=Y(10)
      Y79=(X1S**2+Y1S**2)
      Y80=(X2S**2+Y2S**2)
      Y7980=(X2S*X1S+Y2S*Y1S)
     ATAS=Y79+Y80
     ATHAS=H11*Y79+H22*Y80+2.*H12*(Y7980)

C   VEFF IS THE AVERAGED EFFECTIVE POTENTIAL

      VEFF=(ATHA/ATA)+(ATHAS/ATAS))/2.

      W11=H11-VEFF
      W22=H22-VEFF
      W12=H12

C YP(3)-YP(10) ARE THE TEMPORAL
C DERIVATIVES OF THE COEFFICIENTS

        YP(3)=(W11*Y1+W12*Y2)
        YP(4)=(W12*Y1+W22*Y2)
        YP(5)=(-W11*X1-W12*X2)
        YP(6)=(-W12*X1-W22*X2)

        YP(7)=(W11*Y1S+W12*Y2S)
        YP(8)=(W12*Y1S+W22*Y2S)
        YP(9)=(-W11*X1S-W12*X2S)
        YP(10)=(-W12*X1S-W22*X2S)
```

```
C  DATHADR IS THE SPATIAL DERIVATIVE
C  OF THE EFFECTIVE POTENTIAL

          DATHADR=(DH11DR*Y35+DH22DR*Y46+2.*DH12DR*Y3456
     1     +DH11DR*Y79+DH22DR*Y80+2.*DH12DR*Y7890)/2.

C NOTE:
C IN THE SPECIAL CASE WHERE THE SURFACES ARE WEIGHTED
C EQUALLY, VEFF = (H11 + H22)/2,
C AND DHDR = (DH11DR + DH22DR)/2
C MAY BE USED IN PLACE OF DATHADR.

C  YP(1) IS EDOT ; YP(2) IS PDOT

      YP(1)=Y(2)/CM
      YP(2)=-DATHADR
C
      RETURN
      END

C
      SUBROUTINE DE(F,NEQN,Y,T,TOUT,RELERR,ABSERR,IFLAG)
      IMPLICIT REAL*8 (A-H,O-Z)
C.....................................................................
C  SUBROUTINE DE INTEGRATES A SYSTEM OF UP TO 200 FIRST
C  ORDER ORDINARY DIFFERENTIAL EQUATIONS OF THE FORM
C             DY(I)/DT = F(T,Y(1),Y(2),...Y(NEQN))
C             Y(I) GIVEN AT T
C  THE SUBROUTINE INTEGRATES FROM T TO TOUT.  ON RETURN THE
C  PARAMETERS IN THE CALL LIST ARE INITIALIZED FOR
C  CONTINUING THE INTEGRATION.  THE USER HAS ONLY TO DEFINE
C  A NEW VALUE TOUT AND CALL DE AGAIN.
C  THIS CODE IS COMPLETELY EXPLAINED AND DOCUMENTED IN THE
C  TEXT, "COMPUTER SOLUTION OF ORDINARY DIFFERENTIAL
C  EQUATIONS: THE INITIAL VALUE PROBLEM", BY L. F. SHAMPINE
C  AND M. K. G  GORDON.
C  THE PARAMETERS FOR DE ARE:
C     F --SUBROUTINE F(T,Y,YP) TO EVALUATE DERIVATIVES
C          YP(I)=DY(I)/DT
C     NEQN -- NUMBER OF EQUATIONS TO BE INTEGRATED
C     Y(*) -- SOLUTION VECTOR AT T
C     T -- INDEPENDENT VARIABLE
C     TOUT -- POINT AT WHICH SOLUTION IS DESIRED
C     RELERR,ABSERR -- RELATIVE AND ABSOLUTE ERROR
C                      TOLERANCES FOR LOCAL
C                      ERROR TEST.
C     IFLAG -- INDICATES STATUS OF INTEGRATION
C     THE USER MUST SUPPLY THE SUBROUTINE FPRIME(T,Y,YP) TO
C     EVALUATE DY(I)/DT =YP(I)= F(T,Y(I),Y(2),...,Y(NEQN)),
C     AND INITIALIZE THE PARAMETERS.
CCCCCCCCCCCCCCCCCCCCCCCCCCCCCCCCCCCCCCCCCCCCCCCCCCCCCCCCCCCCCC
```

```
      DIMENSION Y(10),PSI(12),RC(500)
C***************************************************************
COMMON/ARC/NNN,RTES,NEND
C  THIS ROUTINE WAS SENSITIZED TO THE CUTOFF POINT, RTES
      RETURN
      END
C
C

SUBROUTINE STEP(X,Y,F,NEQN,H,EPS,WT,START,HOLD,
     XK,KOLD,CRASH,PHI,P,YP,PSI)
C***************************************************************
COMMON/AC/NT,NTMAX,DREH,VTI,NOSTEP,HBAR,PI,TMAIN0
C**************************************************************

C  THIS ROUTINE WAS SENSITIZED TO THE CUTOFF POINT, RTES
      RETURN
      END
```

# BIBLIOGRAPHY

Abramowitz, M., and Stegun, I.A. The Handbook of Mathematical Functions. New York: Dover Publications, 1972.

Bernstein, Richard. "Quantum mechanical (phase shift) analysis of differential elastic scattering of molecular beams." J. Chem. Phys. 33 (1960): 795-804.

---. Chemical Dynamics via Molecular Beam and Laser Techniques. New York: Oxford University Press, 1982.

Bunker, D.L. "Classical trajectory methods." Methods in Computational Physics 10 (1971): 287-325.

Child, M.S. Molecular Collision Theory. New York: Academic Press, 1974.

--- "Electronic excitations: nonadiabatic transitions" Atom-Molecule Collision Theory--A Guide for the Experimentalist. Ed. Richard B. Bernstein. New York: Plenum Press, 1979. 427-465.

Cohen, Joel. Computer Studies of Molecular Collisions. Master's Thesis, University of Florida, 1988.

Cross, R.J. "Semiclassical methods in inelastic scattering." J. Chem. Phys. 51 (1969): 5163-5170.

Currier, R., and Herman, M.F. "Numerical comparison of generalized surface hopping, classical analog and self-consistent eikonal approximations for nonadiabatic scattering." J. Chem. Phys. 82 (1985): 4509+.

DCSEVU. Computer software. Houston: IMSL, revised 1981. IBM/Double Precision.

Delos, J.B., "Semiclassical calculation of quantum mechanical wavefunctions." Advances in Chemical Physics 65 (1986): 161+.

Evans, S.A., Cohen, J.S., and Lane, N.F. "Quantum mechanical calculation of cross-sections for inelastic atom-atom collisions." Physical Review A 4 (1971): 2235-2248 & 2248-2253.

Feynmann, R.P., and Hibbs, A.R. Quantum Mechanics and Path Integrals. New York: McGraw-Hill Book Company, 1965.

Ford, Kenneth W., and Wheeler, John A. "Semiclassical description of scattering." Annals of Physics 7 (1959): 259+.

Herman, Michael F. "Generalization of the optical series approach for nonadiabatic scattering problems." J. Chem. Phys. 76 (1982): 2949-2958.

ICSEVU. Computer software. Houston: IMSL, revised 1987. IBM/Double Precision.

Johnson, B.R. "The multichannel log-derivative method for scattering calculations." J. Comput. Phys. 13 (1973): 445-449.

Knudson, S.K., Delos, J.B., and Bloom, B. "Semiclassical calculation of quantum mechanical wave functions for a two-dimensional scattering system." J. Chem. Phys. 83 (1985): 5703-5711.

Levine, Ira. Quantum Chemistry. Boston: Allyn and Bacon, 1983.

McCarroll, Ronald. "Charge Exchange and Ionization in Ion Atom Collisions." Atomic and Molecular Collision Theory. Ed. F.A. Gianturco. New York: Plenum Press, 1980, N. pag.

Messiah, Albert. Quantum Mechanics. 2 vols. New York: John Wiley and Sons, 1961.

Micha, D.A. "Quantum theory of reactive molecular collisions." Adv. Chem. Phys. 30 (1975): 221-260.

---. "A self-consistent eikonal treatment of electronic transitions in molecular collisions." J. Chem. Phys. 78 (1983): 7138-7145.

---, and Gazdy, Bela. "Phase-invariant variational methods for transition amplitudes of atomic collisions." Phys. Rev. A 36 (1987): 539-545.

---, and Swaminathan, P.K. Photodissociation of Polyatomics by Visible and UV Radiation: the Selfconsistent Eikonal Approximation. QTP Report 788. Gainesville: University of Florida, 1986. Unpublished.

Miller, W. H., and George, T. F. "Semiclassical Theory of electronic transitions in low energy atomic and molecular collisions involving several degrees of freedom." *J. Chem. Phys.* 56 (1972): 5637-5652.

Olson, John, and Micha, D.A. "Electronic state representation at molecular potential pseudocrossings." *Intl. J. Quant. Chem.* 22 (1982): 971-988.

---, and Garrison B.G. "Theory of nonadiabatic gas-surface reactions." *J. Chem. Phys.* 83 (1985): 1392-1403

Pauly, H. "Elastic scattering cross sections I: Spherical Potentials" *Atom-Molecule Collision Theory.* Ed. Richard B. Bernstein. New York: Plenum Press, 1979. 111-199.

Relyea, Lawrence R. *OPTIK.* Computer software. The exact quantum mechanical calculation of elastic scattering angles. Quantum Theory Project. Gainesville: University of Florida, 1975.

---. *LOGDERIV.* Computer software. The log-derivative method applied to multi-channel scattering. Quantum Theory Project. Gainesville: University of Florida, 1977

---. *Theory of Ionizing Atomic Collisions at Thermal Energies.* Doctoral Dissertation, University of Florida, 1980

Rice, Betsy M., Garrett, Bruce C., and Swaminatan, P.K. "A semiclassical treatment of rotationally electronically inelastic scattering of NO from Ag(111)." *J. Chem. Phys.* 90 (1989): 575-586

Sawada, Shin-ichi, and Metiu, Horia. "A Gaussian wave packet method for studying time dependent quantum mechanics in a curve crossing system. Low energy motion, tunneling, and thermal dissipation." *J. Chem. Phys.* 84 (1986): 6293-6311.

Shampine, L.F., and Gordon, M.K. *Computer Solutions of Ordinary Differential Equations: The Initial Value Problem.* San Francisco: W. H. Freeman, 1975.

Smith, F.T. "Diabatic and adiabatic representations for collision problems." *Phys. Rev.* 179 (1969): 111-123.

Stodden, Clifford D. *Photodissociation of Polyatomic Molecules: State-to-State Cross Sections from the Self-Consistent Eikonal Method.* Doctoral Dissertation, University of Florida, 1987.

Stodden, Clifford D., and Micha, D.A. "Generating wave functions from classical trajectory calculations: the divergence of streamlines." *Int. J. Quantum Chem. Symp.* 21 (1987). 238-244.

Swaminathan, P.K., Garrett, Bruce C., and Murthy, C.S. "Electronical excitation of atoms at insulator surfaces." *J. Chem. Phys.* 88 (1988). 2822-2830.

---, Stodden, C.D., and Micha, D.A. "The eikonal approximation to molecular photodissociation. Application to $CH_3I$." *J. Chem. Phys.* 90 (1989). 5501-5509.

Tully, J.C. "Nonadiabatic processes in molecular collisions." *Dynamics of Molecular Collisions, Part B*, ed. W.H. Miller. New York: Plenum Press, 1976. 217-267.

Zygelman, B., Dalgarno, A., Kimura, M., and Lane, N.F. "Radiative and non-radiative charge transfer in He+ + H collisions at low energy." *Phys. Rev. A* 40 (1989). 2340-2345.

## BIOGRAPHICAL SKETCH

Mr. Joel Cohen was born in Brooklyn, New York, on August 3, 1945, just as the second war was ending. He left the city just in time to experience an old country schoolhouse in the mountainous upstate region. From there he moved to a coeducational boarding school outside Stamford, Connecticut. With being snowed in, not much else to do, and only about a hundred students, he managed to go from grade school to high school without the preliminaries. In spite of various other setbacks, he hung onto that advantage and graduated high school in New Orleans, Louisiana, two years ahead of his classmates. By that time health and personal problems forced him to drop out of university in the first year. Determined to become an intellectual luminary of some sort he read voraciously, was always writing something, attended and gave poetry recitals and lectures, kept up with the latest in art, music, psychology, philosophy, . . . whatever. The sixties were ideal for that kind of growth. At some time, however, he realized that even if he succeeded at what he was doing it would not constitute, in his own mind, a genuine accomplishment. He became more and more interested in science as his way to make a real contribution. He resumed his formal education in earnest in 1977 at a branch of Florida Junior College in

Jacksonville. By July of 1979 he earned an A.A. degree, appearing on the Dean's List several times. From there he went on to the University of North Florida, receiving a Bachelor of Arts degree in May, 1982. In December, 1988 he completed an M.S. at the University of Florida and now, two years later, a Ph.D. He looks forward, with great anticipation, to his new career.

I certify that I have read this study and in my opinion it conforms to acceptable standards of scholarly presentation and is fully adequate, in scope and quality, as a thesis for the degree of Doctor of Philosophy.

David Micha, Chairman
Professor of Chemistry and Physics

I certify that I have read this study and in my opinion it conforms to acceptable standards of scholarly presentation and is fully adequate, in scope and quality, as a dissertation for the degree of Doctor of Philosophy.

Robert J. Hanrahan
Professor of Chemistry

I certify that I have read this study and in my opinion it conforms to acceptable standards of scholarly presentation and is fully adequate, in scope and quality, as a dissertation for the degree of Doctor of Philosophy.

Jack Sabin
Professor of Physics

I certify that I have read this study and in my opinion it conforms to acceptable standards of scholarly presentation and is fully adequate, in scope and quality, as a dissertation for the degree of Doctor of Philosophy.

Charles Reid
Professor of Chemistry

I certify that I have read this study and in my opinion it conforms to acceptable standards of scholarly presentation and is fully adequate, in scope and quality, as a dissertation for the degree of Doctor of Philosophy.

Philip Brucat
Professor of Chemistry

This dissertation was submitted to the Graduate Faculty of the Department of Chemistry in the College of Liberal Arts and Sciences and to the Graduate School and was accepted as partial fulfillment of the requirements for the degree of Doctor of Philosophy.

December 1990

Dean, Graduate School